Instability of Fluid Flows, Including Boundary Slip

Mark Webber

A thesis presented for the degree of
Doctor of Philosophy

Numerical Analysis
Department of Mathematical Sciences
University of Durham
England

June 2007

Dedicated to

Mum and Dad.

Instability of Fluid Flows, Including Boundary Slip

Mark Webber

Submitted for the degree of Doctor of Philosophy
June 2007

Abstract

We investigate the onset of instability in a variety of fluid models, and present results and details of their computation in each case. The fluid models we consider are: convection in the setting of the Navier-Stokes equations with boundary slip; Poiseuille-type solutions of the Navier-Stokes equations, again with boundary slip; Poiseuille-type solutions of the Green-Naghdi and dipolar fluid equations.

In Chapter two we examine the onset of thermal convection in a thin fluid layer, with slip boundary conditions at the top and bottom surfaces of the layer. We show that non-zero boundary conditions do not affect the classical steady state solution, and the principle of exchange of stabilities still applies. It is seen that boundary slip reduces the critical Rayleigh number at which convection begins, below that found in the setting of no-slip boundary conditions.

The next two chapters concern the transition to turbulence of pressure driven flow in a microchannel, at the boundaries of which the fluid obeys slip boundary conditions. In Chapter three we perform linear and nonlinear stability analyses for this flow, and show that we do not have exchange of stabilities for such flows. In Chapter four we perform a linear stability analysis for channel flow in the case when the fluid viscosity is a function of temperature. We show that for pressure driven flow in the plane, boundary slip stabilizes the flow.

In Chapter five we develop a model of thread-annular flow, in which we believe boundary slip to be an important part. As well as our development of the model, we present previously unpublished results on the linear stability of thread-annular

flow to non-axisymmetric disturbances. Some surprising behaviour is observed in the neutral curves, including behaviour missed by the computations of previous authors.

Finally, we use Chapter six to discuss two alternative fluid models: the Green-Naghdi equations and the dipolar equations. We find Poiseuille flow type solutions in both of these settings, and perform linear stability analyses. These fluid models are systems of fourth order differential equations, and we show that the fourth order derivative terms dominate the stability of the flow.

Declaration

The work in this thesis is based on research carried out at the Numerical Analysis Group, the Department of Mathematical Sciences, University of Durham, England. No part of this thesis has been submitted elsewhere for any other degree or qualification and it is all my own work with the exception of Chapter three, which contains work published in collaboration with Prof. B. Straughan, University of Durham, United Kingdom [68]. The contents of Chapter two are published in [67].

Acknowledgements

I would like to thank my supervisor, Prof. Brian Straughan, for all the support he has given me over the past three years, and for helping to make my postgraduate studies both enjoyable and rewarding.

My thanks go to everyone in the Department of Mathematical Sciences, in particular the Numerical Analysis Group, for all their help and support. Thanks also to Imran M for preparing the LaTeX template used for this thesis.

Finally, I would like to acknowledge the Engineering and Physical Sciences Research Council, whose financial support made this work possible.

Contents

List of Figures

List of Tables

Chapter 1

Introduction

A large number of hydrodynamic stability problems are concerned with a Newtonian fluid obeying the Navier-Stokes equations for incompressible flow,

$$\rho\left(\mathbf{u}_{,t} + (\mathbf{u}\cdot\nabla)\,\mathbf{u}\right) = -\nabla p + \mu\Delta\mathbf{u} + \mathbf{F}, \tag{1.1}$$

$$\nabla\cdot\mathbf{u} = 0, \tag{1.2}$$

for velocity field $\mathbf{u}$, pressure p, density ρ, dynamic viscosity μ, and where $\mathbf{F}$ is the body force term. Typically, these equations are satisfied on some given domain $\Omega \subset \mathbb{R}^3$ bounded by a surface $\partial\Omega$, where often the geometry of Ω defines the problem to be solved.

Alongside equations (1.1) and (1.2) we must prescribe boundary conditions on the fluid at $\partial\Omega$. The classical approach is to state that fluid molecules adjacent to a solid surface are at rest, with respect to that surface. This is called the no-slip boundary condition, and despite its historical prevalence in the fluid mechanics literature, it is an assumption that cannot be derived from first principles, see [39,71].

Boundary slip (that is, motion of a fluid with respect to a solid surface) in gases was predicted by Maxwell [41], and experiments have shown that gas flow in geometries with dimensions of the order of the mean free path of the gas can show significant slip at a boundary, see [44]. However, the measurement of boundary slip of Newtonian liquids has been the subject of much more recent research, see [4,5,9,11,12,15,34,46,49,61,70]. In particular, there is growing evidence that fluid

velocity at the boundary is dependent upon the shear strain, see for example Craig *et al* [15,46] and Zhu & Granick [70].

Navier [45] proposed a linear boundary condition relating $\mathbf{u}$ to the shear rate, which has become standard in the study of boundary slip problems. Letting the surface $\partial\Omega$ have unit normal $\hat{\mathbf{n}}(\mathbf{x})$ directed out of the fluid, and $\hat{\mathbf{t}}(\mathbf{x})$ be either of the vectors tangent to $\partial\Omega$ at $\mathbf{x} \in \partial\Omega$, this boundary condition can be expressed as

$$u_i \hat{n}_i|_{\partial\Omega} = U_i \hat{n}_i, |_{\partial\Omega} \tag{1.3}$$

$$u_i \hat{t}_i|_{\partial\Omega} = (U_i - \lambda \epsilon_{ij} \hat{n}_j)\, \hat{t}_i|_{\partial\Omega}. \tag{1.4}$$

Here, $\epsilon = \epsilon(\mathbf{u})$ is the shear strain tensor, and $U_i = U_i(\partial\Omega)$ is the ith component of the local surface velocity. The model is essentially to set the component of $\mathbf{u}$ normal to $\partial\Omega$ to be zero, thus imposing a condition of zero flux across the surface, while setting the two tangential components of $\mathbf{u}$ proportional to the corresponding components of shear stress. We denote the constant of proportionality $\lambda \geq 0$, which has the dimension of length, and it can be seen that $\lambda = 0$ in (1.3) and (1.4) recovers the no-slip boundary condition. Clearly, if we wish to perform any numerical work on the system (1.1)-(1.4) we must have a value for λ at hand.

We now describe a simple type of fluid motion known as Couette flow, which illustrates how the value of λ affects a fluid. Let $\mathbf{x} = (x, y, z)^T$ denote the Cartesian coordinates of a point in the domain $\Omega = (-\infty, \infty) \times [-h, h] \times (-\infty, \infty)$, on which equations (1.1)-(1.4) describe a fluid. Then, Ω is a channel in the (x, z) plane of width $2h$, bounded above by the surface $\partial\Omega_h = \{\mathbf{x} = (x, y, z) | y = h\}$ and below by $\partial\Omega_{-h} = \{\mathbf{x} = (x, y, z) | y = -h\}$. The upper surface moves with constant velocity $(U, 0, 0)^T$ where $U > 0$, while the lower surface moves with velocity $-(U, 0, 0)^T$ (see Figure 1.1), thus the fluid is sheared and motion is induced along the $x-$axis. We assume that the body force $\mathbf{F} = \mathbf{0}$.

We shall assume a solution of the form $\mathbf{u} = (u(y), 0, 0)^T$, $\nabla p = \mathbf{0}$. In this coordinate system the shear strain tensor takes the form,

$$\epsilon_{ij} = u_{i,j} + u_{j,i}, \tag{1.5}$$

and we note that $\hat{\mathbf{n}} = (0, \pm 1, 0)^T$ while $\hat{\mathbf{t}} \in \{(1, 0, 0)^T, (0, 0, 1)^T\}$. Therefore, substi-

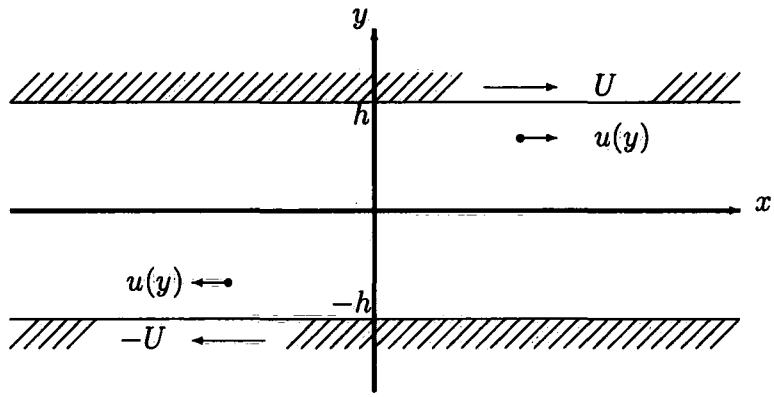

Figure 1.1: Diagram illustrating Couette flow. The two surfaces $y = \pm h$ move in opposite directions, shearing the fluid held between.

tuting our forms for $\mathbf{u}$ and p into (1.1)-(1.4) leaves us with the ordinary differential equation,

$$u'' = 0, \tag{1.6}$$

$$u|_{y=h} = U - \lambda u'|_{y=h}, \tag{1.7}$$

$$u|_{y=-h} = -U + \lambda u'|_{y=-h}, \tag{1.8}$$

from which we easily obtain the solution,

$$u(y) = \left(\frac{U}{h+\lambda}\right) y. \tag{1.9}$$

We arrive at the standard no-slip solution by setting $\lambda = 0$. However, we note that our velocity $u(y)$ appears to satisfy a no-slip boundary condition a distance λ outside the domain Ω, see Figure 1.2. For this reason, λ is commonly known as the *slip length*. In general, the velocity profile of a fluid obeying slip boundary conditions will extrapolate to the no-slip boundary condition a distance of the order λ normal to a solid surface.

The larger λ is relative to the characteristic length of the domain Ω, the more the velocity profile will differ from that calculated with the no-slip boundary condition, and so we might expect boundary slip to play an important role for sufficiently

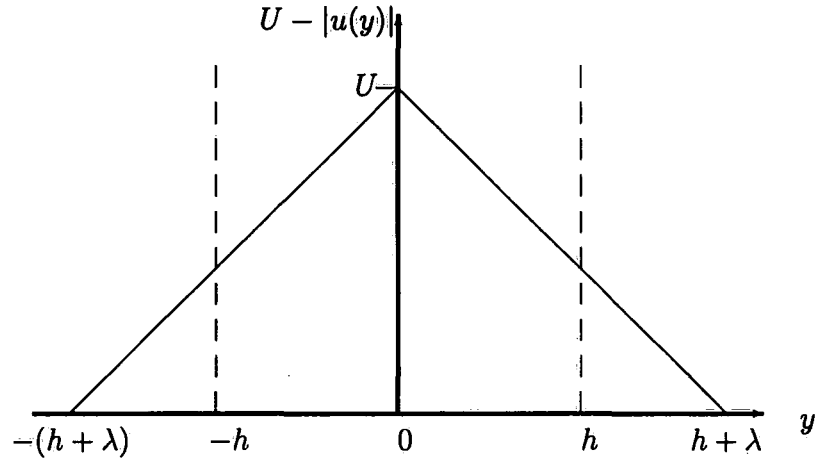

Figure 1.2: Graph of $U - |u(y)|$, where $u(y)$ is the Couette flow solution given in (1.9) and U is the constant shearing velocity. The no-slip boundary condition is seen to be satisfied a distance λ outside the domain Ω.

large slip lengths. Therefore, slip-boundary conditions are particularly applicable in the study of problems where fluids interact with solids of small length scales, which includes flows in porous media, microfluidics, and biological fluids.

One of the aims of this thesis is to investigate the impact of boundary slip on the classical problem of hydrodynamic stability. We begin in Chapter two with the problem of the onset of Bénard convection in a thin fluid layer, before moving on to the problem of the stability of Poiseuille flow in a channel in chapters three and four.

In Chapter five we turn our attention to a modern surgical technique known as thread injection, which we model as a fluid stability problem. We argue for the applicability of slip boundary conditions in this model, as well as developing the current model of thread-annular flow to include rotation.

In Chapter six we consider two fluid models where the fluid particle obeys equations of motion different from (1.1). These alternative equations of motion contain fourth order derivatives, and we can recover the Navier-Stokes equations from them as various parameters approach zero. The first of these models is known as the

Green-Naghdi equations, developed by Green & Naghdi [25], while the second model describes a dipolar fluid [3]. We find Poiseuille-type flows in both these settings, and perform linear stability analyses.

Throughout this thesis, including above in this chapter, we use bold type to denote vector quantities, and we make use of the Einstein index summation convention. For example, for $\mathbf{u}(\mathbf{x}) = (u_1, u_2, u_3)^T$ with $\mathbf{x} = (x_1, x_2, x_3)^T$, then

$$u_i u_i = u_1^2 + u_2^2 + u_3^2, \quad u_j u_{i,j} = \left(u_1 \frac{\partial u_i}{\partial x_1} + u_2 \frac{\partial u_i}{\partial x_2} + u_3 \frac{\partial u_i}{\partial x_3} \right). \tag{1.10}$$

Chapter 2

The influence of boundary slip on convective instability

We begin our investigation into the effects of slip boundary conditions, by applying them to the classical problem of the convective instability of a thin horizontal layer of stationary fluid, heated from below.

In most cases, the adverse temperature gradient will cause the fluid at the bottom of the layer to expand. For a sufficiently large temperature gradient the buoyancy of this lower region overcomes the stabilizing effects of viscosity and thermal conductivity, and the fluid becomes potentially unstable. Moreover, the resulting convective motion arranges itself into a tessellating, regular structure of convective cells separated by vertical walls, with the fluid rising at the centre of a cell and falling towards the edges. This is called Bénard convection after the experiments of Bénard [2].

The theory behind such convective instability is due to Rayleigh [52], who identified a non-dimensional number R given by

$$R = \sqrt{\frac{\alpha\beta g h^4}{\kappa\nu}}, \tag{2.1}$$

where α is the thermal expansion coefficient, β is the magnitude of the temperature difference between the upper and lower surfaces, g is the acceleration due to gravity, ν is the kinematic viscosity, κ is the thermometric conductivity, and h is the depth of the fluid layer. Thus R represents the competing effects of buoyancy, viscosity and thermal conductivity, and so the stability of the fluid is dependent upon the

value of R. We call $Ra = R^2$ the Rayleigh number, and aim to find $Ra = Ra_{\text{crit}}$ such that thermal instability occurs for $Ra > Ra_{\text{crit}}$, but the fluid remains at rest for $Ra < Ra_{\text{crit}}$.

Rayleigh [52] showed that, in the case of free boundary conditions, we may obtain the analytical result $Ra_{\text{crit}} = \rho_1 = 27\pi^4/4 \sim 657.5$ (see also Chandrasekhar [8] and Drazin & Reid [18]), whereas for no-slip boundary conditions (i.e. rigid surfaces above and below the layer with classical boundary conditions) we have $Ra_{\text{crit}} = \rho_2 \sim 1708$ (see for example, Harris & Reid [27], Jeffreys [30]).

In applying slip boundary conditions, we are interested in the thermal stability of very thin layers where the fluid depth and slip length are comparable. We show that boundary slip allows a critical Rayleigh number in the interval (ρ_1, ρ_2). Therefore, with respect to the standard no-slip result, boundary slip is shown to be a destabilizing factor in Bénard convection.

2.1 Equations of motion

Let $\mathbf{x} = (x, y, z)$ denote the Cartesian coordinates of a point in $\mathbb{R}^3$. We consider a fluid contained in the region $\Omega \subset \mathbb{R}^3$, which is the infinite layer defined by $\Omega = (-\infty, \infty) \times (-\infty, \infty) \times [0, h]$. We define $\mathbf{u}(\mathbf{x}; t)$, $T(\mathbf{x}; t)$, $p(\mathbf{x}; t)$ to be, respectively, the velocity, temperature and pressure of the fluid at the point $\mathbf{x} \in \Omega$ and time $t \in [0, \infty)$, and label the components of velocity $\mathbf{u} = (u, v, w) = (u_1, u_2, u_3)$.

Ω is bounded above by the surface $\partial\Omega_h = \{\mathbf{x} = (x, y, z) | z = h\}$ and below by $\partial\Omega_0 = \{\mathbf{x} = (x, y, z) | z = 0\}$. The temperature at the upper and lower surfaces is kept constant,

$$T|_{z=0} = T_0, \quad T|_{z=h} = T_h, \tag{2.2}$$

for constants $T_0 > T_h$, and thus the layer is heated from below.

The behaviour of this fluid is described by the Boussinesq equations (2.3)-(2.5), which comprise the Navier-Stokes equations (where the fluid buoyancy is accounted for in the body force term, see Boussinesq [6]), and an energy balance equation.

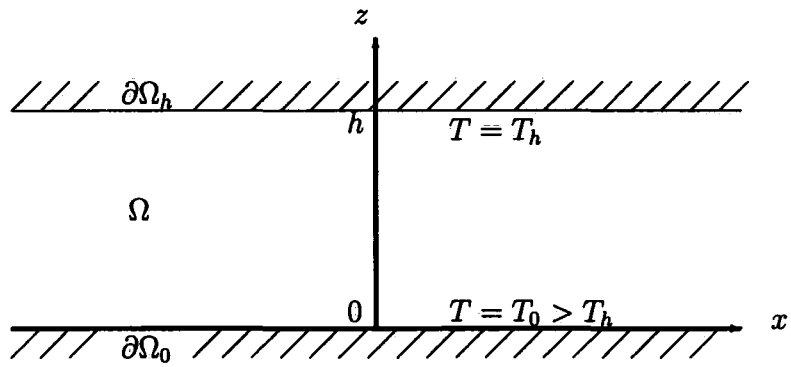

Figure 2.1: Diagram illustrating Bénard's experiment. A constant temperature difference is applied across a thin horizontal layer of stationary fluid.

A detailed derivation can be found in the books by Chandrasekhar [8], Drazin & Reid [18] and Straughan [59].

$$\rho_m \left(u_{i,t} + u_j u_{i,j}\right) = -p_{,i} + \mu \Delta u_i - \hat{k}_i g \rho_m \left[1 - \alpha (T - T_m)\right], \tag{2.3}$$

$$u_{i,i} = 0, \tag{2.4}$$

$$T_{,t} + u_i T_{,i} = \kappa \Delta T. \tag{2.5}$$

The constants α and κ in (2.3)-(2.4) are as previously defined; μ is the dynamic viscosity; ρ_m is the density at some appropriate reference temperature T_m (for example we could choose T_0 or T_h); $\hat{k}_i$ is the ith component of the vector $\hat{\mathbf{k}} = (0, 0, 1)^T$. We define the temperature gradient $\beta = (T_0 - T_h)/h$.

We now apply the boundary conditions (1.3)-(1.4) to the Boussinesq model. Since the fluid is confined to Ω, from (1.3) we impose,

$$w|_{z=0,h} = 0, \tag{2.6}$$

and we note that since there is no variation of w in the surfaces $\partial\Omega_0$ and $\partial\Omega_h$, we must have

$$w_{,x}|_{z=0,h} = w_{,y}|_{z=0,h} = 0. \tag{2.7}$$

Let λ_0 be the slip length associated with the fluid-solid interface at $\partial\Omega_0$, and define λ_h similarly. Then, from (1.4) we have

$$u|_{z=0} = \lambda_0 u_{,z}|_{z=0}, \quad v|_{z=0} = \lambda_0 v_{,z}|_{z=0}, \tag{2.8}$$

$$u|_{z=h} = -\lambda_h u_{,z}|_{z=h}, \quad v|_{z=h} = -\lambda_h v_{,z}|_{z=h}. \tag{2.9}$$

We note that these boundary conditions allow the zero solution $\mathbf{u} = \mathbf{0}$, which represents a fluid at rest. Then, letting $\bar{T} = T(z)$ only, equation (2.5) simplifies to $T''(z) = 0$, which is easily solved as a linear function in z using (2.2). We can then solve for the pressure, and in choosing a pressure scale such that $p|_{z=0} = 0$ we obtain the classic steady-state solution $\bar{\mathbf{u}}$, $\bar{T}$, $\bar{p}$ given by

$$\bar{\mathbf{u}} = \mathbf{0}, \quad \bar{T} = -\beta z + T_0, \quad \bar{p} = -\rho_m g\left[1 + \alpha\left(T_m - T_0\right)\right] z - \frac{1}{2}\rho_m g \alpha \beta z^2, \tag{2.10}$$

therefore slip boundary conditions have no effect on the steady-state solution already reported in the literature (see for example [59]).

This solution represents the fluid undergoing thermal conduction, and our aim is to find necessary and sufficient conditions for cellular, convective motion to begin. We do this by investigating the stability of the steady-state (2.10) to three-dimensional disturbances which we shall assume to be periodic in the x and y directions, and in this way identify the onset of convection with the bifurcation from stability to instability.

We begin by nondimensionalizing equations (2.3)-(2.5) via the scalings

$$t = \frac{h^2\rho_m}{\mu}t^*, \quad \mathbf{x} = h\mathbf{x}^*, \quad \mathbf{u} = \frac{\mu}{\rho_m h}\mathbf{u}^*, \quad T = \frac{\rho_m \mu}{h}\sqrt{\frac{\beta\mu}{\kappa\alpha\rho_m g}}T^*, \quad p = \frac{\mu^2}{\rho_m h^2}p^*,$$

where the '*' notation denotes a non-dimensional quantity. We also introduce the non-dimensional parameters

$$\lambda_0^* = \frac{\lambda_0}{h}, \quad \lambda_1^* = \frac{\lambda_h}{h}, \quad R^* = \sqrt{\frac{\alpha\beta g\rho_m h^4}{\kappa\mu}}, \quad Pr^* = \frac{\mu}{\rho_m \kappa}, \quad Q^* = \frac{h^3\rho_m^2 g}{\mu^2},$$

where Pr is the Prandtl number for the system, and $Ra = R^2$ the Rayleigh number. Dropping the '*' notation, we obtain from (2.3)-(2.5) the non-dimensional equations

of motion

$$u_{i,t} + u_j u_{i,j} = -p_{,i} + \Delta u_i - \hat{k}_i \left[Q - R\left(T - T_m\right)\right], \tag{2.11}$$

$$u_{i,i} = 0, \tag{2.12}$$

$$Pr\left(T_{,t} + u_i T_{,i}\right) = \Delta T, \tag{2.13}$$

at all points $\mathbf{x} \in \Lambda = (-\infty, \infty) \times (-\infty, \infty) \times [0, 1]$ and time $t \in [0, \infty)$, and subject to the boundary conditions

$$u|_{z=0} = \lambda_0 u_{,z}|_{z=0}, \quad v|_{z=0} = \lambda_0 v_{,z}|_{z=0}, \quad w|_{z=0} = 0, \quad T|_{z=0} = T_0, \tag{2.14}$$

$$u|_{z=1} = -\lambda_1 u_{,z}|_{z=1}, \quad v|_{z=1} = -\lambda_1 v_{,z}|_{z=1}, \quad w|_{z=1} = 0, \quad T|_{z=1} = T_1, \tag{2.15}$$

where T_0 and T_1 are understood to be non-dimensional. Similarly, after nondimensionalizing, our steady-state (2.10) becomes

$$\bar{\mathbf{u}} = \mathbf{0}, \quad \bar{T} = -\frac{R}{Pr} z + T_0, \quad \bar{p} = -\left[Q + R\left(T_m - T_0\right)\right] z - \frac{1}{2}\frac{R^2}{Pr} z^2, \tag{2.16}$$

where the constant T_m is also understood to have been non-dimensionalized.

We shall suppose there is some minimal shape $\partial\Gamma_0 \subset \mathbb{R}^2$ that tessellates the (x, y) plane, such that for $\Gamma = \partial\Gamma_0 \times [0, 1] \subset \Lambda$ then at the onset of convection the fluid motion is periodic modulo Γ. In this way Γ is a typical convective cell, and we restrict ourselves to investigating the stability of solution (2.16) for $\mathbf{x} \in \Gamma$. We denote by $\partial\Gamma_1$ the projection of $\partial\Gamma_0$ on the surface $z = 1$, and by $\partial\Gamma$ the total boundary of Γ.

With this definition of Γ, and for volume element $dV = dxdydz$, let $< .. >$ be the inner product with associated norm $\|.\|$ defined by

$$< fg >= \int_\Omega fg dV, \quad \|f\| = \sqrt{< ff >}.$$

Now let $H^1(\Gamma)$ be the complex Hilbert space of measurable functions defined on Γ such that for $f \in H^1(\Gamma)$ we have

$$\|f\| + \|f'\| < \infty.$$

Finally, let $\mathcal{H}$ be the set of all pairs of vector functions $\mathbf{u}(\mathbf{x};t) \in [H^1(\Gamma)]^3$ and scalar functions $T(\mathbf{x};t) \in H^1(\Gamma)$, such that for $\mathbf{u} = (u,v,w)$

$$\nabla \cdot \mathbf{u} = 0, \tag{2.17}$$

$$u|_{z=0} = \lambda_0 u_{,z}|_{z=0}, \quad v|_{z=0} = \lambda_0 v_{,z}|_{z=0}, \quad w|_{z=0} = 0, \quad T|_{z=0} = 0, \tag{2.18}$$

$$u|_{z=1} = -\lambda_1 u_{,z}|_{z=1}, \quad v|_{z=1} = -\lambda_1 v_{,z}|_{z=1}, \quad w|_{z=1} = 0, \quad T|_{z=1} = 0, \tag{2.19}$$

and $\mathbf{u}$ and T are periodic modulo Γ (and therefore $\mathbf{u}$ satisfies periodic boundary conditions on $\partial\Gamma \setminus \{\partial\Gamma_0 \cup \partial\Gamma_1\}$).

We let the steady-state be subject to a disturbance modelled by velocity $\mathbf{v}(\mathbf{x};t) = (u,v,w)^T$, temperature $\theta(\mathbf{x};t)$ and pressure $q(\mathbf{x};t)$, where $(\mathbf{v},\theta) \in \mathcal{H}$, i.e. we perturb the steady state by

$$\bar{\mathbf{u}} \mapsto \bar{\mathbf{u}} + \mathbf{v}, \quad \bar{T} \mapsto \bar{T} + \theta, \quad \bar{p} \mapsto \bar{p} + q,$$

where q also has periodic (x,y) dependence. We assume that the temperature at Γ_0 and Γ_1 is kept constant, and therefore we choose the temperature perturbation to be zero there. Substituting for our perturbed forms in equations (2.11)-(2.13) we obtain the perturbation equations

$$v_{i,t} + v_j v_{i,j} = -q_{,i} + \Delta v_i + \hat{k}_i R\theta, \tag{2.20}$$

$$v_{i,i} = 0, \tag{2.21}$$

$$Pr\,(\theta_{,t} + v_i\theta_{,i}) = Rw + \Delta\theta, \tag{2.22}$$

for $\mathbf{x} \in \Gamma$, $t \in [0,\infty)$ and $(\mathbf{v},\theta) \in \mathcal{H}$, and where $w = v_3$. Finally, we assume that the perturbations satisfy the initial data

$$\mathbf{v}|_{t=0} = \mathbf{v}_0, \quad \theta|_{t=0} = \theta_0,$$

for functions $\mathbf{v}_0(\mathbf{x})$ and $\theta_0(\mathbf{x})$.

We note that although Pr is a property of the fluid substance, it is not a property of the fluid flow, and therefore Pr is not a factor in determining the stability of the zero solution. R, however, is a measure of the flow, and therefore we move on to study the behaviour of solutions to (2.20)-(2.22) with respect to the value of R.

2.2 Coincidence of linear and non-linear stability bounds

We have reduced the problem of finding conditions for the onset of convection in our fluid layer to that of investigating the stability of the zero solution (2.16) with respect to perturbations $\mathbf{v}$, θ, q as defined above. In this way we aim to find, for fixed λ_0 and λ_1, the critical Rayleigh number $R^2_{\text{crit}}(\lambda_0, \lambda_1)$ such that solutions to (2.20)-(2.22) decay over time for $R < R_{\text{crit}}$ and grow for $R > R_{\text{crit}}$, regardless of the initial data $\mathbf{v}_0$, θ_0.

We do this by showing that there exists R_L such that thermal instability will occur for $R > R_L$, and R_E such that $R < R_E$ guarantees stability of the zero solution, before showing that in fact $R_E = R_L = R_{\text{crit}}$. Though this has been done for no-slip boundary conditions (see Joseph [31,32]) we show that this also holds in our case of slip boundary conditions.

2.2.1 Conditions guaranteeing instability

Removal of the non-linear terms of (2.20)-(2.22) results in the equations

$$v_{i,t} = -q_{,i} + \Delta v_i + \hat{k}_i R\theta, \tag{2.23}$$

$$v_{i,i} = 0, \tag{2.24}$$

$$Pr\theta_{,t} = Rw + \Delta\theta, \tag{2.25}$$

with boundary conditions as prescribed for $(\mathbf{v}, \theta) \in \mathcal{H}$. We suppose that we can expand the solutions $\mathbf{v}$, θ, q to (2.23)-(2.25) as series of Fourier modes

$$\mathbf{v}(\mathbf{x};t) = \sum_{n=1}^{\infty} \mathbf{v}_n(\mathbf{x})e^{\sigma_n t}, \quad \theta = \sum_{n=1}^{\infty} \theta_n(\mathbf{x})e^{\sigma_n t}, \quad q(\mathbf{x};t) = \sum_{n=1}^{\infty} q_n(\mathbf{x})e^{\sigma_n t}, \tag{2.26}$$

where in general $\sigma_n \in \mathbb{C}$. It follows that in finding conditions for instability of the linearized system it is sufficient to consider just one mode of this expansion (since if a single mode grows unboundedly with time, so too does the whole solution), and therefore we look for solutions of the form $\mathbf{v}(\mathbf{x};t) = \mathbf{v}(\mathbf{x})e^{\sigma t}$, $\theta(\mathbf{x};t) = \theta(\mathbf{x})e^{\sigma t}$,

$q(\mathbf{x};t) = q(\mathbf{x})e^{\sigma t}$. Upon substitution and removal of exponential parts we obtain

$$\sigma v_i = -q_{,i} + \Delta v_i + \hat{k}_i R\theta, \tag{2.27}$$

$$v_{i,i} = 0, \tag{2.28}$$

$$\sigma P_r \theta = Rw + \Delta\theta. \tag{2.29}$$

We now show that $\sigma \in \mathbb{R}$, and therefore the principle of 'exchange of stabilities' applies to the linearized system, an expression formalized by Poincaré [50] and Jeffreys [29]. Let v_i^* be the complex conjugate of v_i, and define θ^* similarly. Then multiplying (2.27) by v_i^* and (2.29) by θ^*, taking the volume integral of these two expressions over Γ and adding, leads us to the equality

$$\begin{aligned}\sigma\left(< v_i v_i^* > + P_r < \theta\theta^* >\right) &= - < v_i^* q_{,i} > + < v_i^* v_{i,jj} > + < \theta^* \theta_{,jj} > \\ &\quad + R\left(< w^*\theta > + < w\theta^* >\right).\end{aligned}$$

Letting dS be a surface element on $\partial\Gamma$, we obtain

$$\begin{aligned}\sigma\left(< v_i v_i^* > + P_r < \theta\theta^* >\right) &= - < (v_i^* q)_{,i} > + < v_{i,i}^* q > + < (v_i^* v_{i,j})_{,j} > - < v_{i,j}^* v_{i,j} > \\ &\quad + < (\theta^*\theta_{,j})_{,j} > - < \theta_{,j}^* \theta_{,j} > + R\left(< w^*\theta > + < w\theta^* >\right), \\ &= - \int_{\partial\Gamma} v_i^* q \hat{n}_i dS + \int_{\partial\Gamma} v_i^* v_{i,j} \hat{n}_j dS + \int_{\partial\Gamma} \theta^* \theta_{,j} \hat{n}_j dS \\ &\quad - < v_{i,j}^* v_{i,j} > - < \theta_{,j}^* \theta_{,j} > + R\left(< w^*\theta > + < w^*\theta >^*\right),\end{aligned}$$

where we have used integration by parts, and (2.28). Upon applying the boundary conditions on $\mathbf{v}$ on the surface $\partial\Gamma \setminus \{\partial\Gamma_0 \cup \partial\Gamma_1\}$, and the boundary conditions on θ on $\partial\Gamma$, we arrive at the expression

$$\begin{aligned}\sigma\left(< v_i v_i^* > + P_r < \theta\theta^* >\right) &= -\frac{1}{\lambda_0} \int_{\partial\Gamma_0} v_i^* v_i dS - \frac{1}{\lambda_1} \int_{\partial\Gamma_1} v_i^* v_i dS \\ &\quad - < u_{i,j}^* u_{i,j} > - < \theta_{,j}^* \theta_{,j} > + R\left(< w^*\theta > + < w^*\theta >^*\right),\end{aligned}$$

and clearly, for this to hold, we must have that the imaginary part of σ is zero, i.e. $\sigma \in \mathbb{R}$. Therefore, we have the simple case whereby solutions of (2.27)-(2.29) decay for $\sigma < 0$ and grow for $\sigma > 0$, and so $\sigma = 0$ represents a stability boundary. We are therefore interested in the case $\sigma = 0$, and so removing parts multiplied by σ in

(2.27)-(2.29) leaves us with

$$\Delta v_i + \hat{k}_i R\theta = q_{,i}, \tag{2.30}$$

$$v_{i,i} = 0, \tag{2.31}$$

$$\Delta\theta + Rw = 0, \tag{2.32}$$

which is an eigenvalue problem in R. We select R_L as the smallest value of R in the spectrum of (2.30)-(2.32), since this is the lowest value of R for which neutral stability exists. Instability in the linearized case is sufficient to ensure instability of the non-linear system (see for example, Sattinger [56]). Thus, R_L represents a stability boundary such that for $R > R_L$, solutions to (2.20)-(2.22) do not decay over time, and so we have convective motion.

2.2.2 Conditions guaranteeing stability

We now use an energy type method to find conditions that will ensure stability of the conductive solution. Define the non-negative quantity $E(t)$ by

$$E(t) = \frac{1}{2} < v_i v_i > + \frac{1}{2} Pr < \theta^2 >,$$

so that differentiating with respect to time and substituting for $v_{i,t}$ and $\theta_{,t}$ from (2.20) and (2.22) leaves us the equality

$$\begin{aligned}
\frac{dE}{dt} &= < v_i v_{i,t} > + Pr < \theta\theta_{,t} >, \\
&= < v_i \left(-q_{,i} + v_{i,jj} + \hat{k}_i R\theta - v_j v_{i,j} \right) > + Pr < \theta \left(\frac{Rw + \theta_{,jj}}{Pr} - v_i \theta_{,i} \right) >, \\
&= - < v_i q_{,i} > + < v_i v_{i,jj} > - \frac{1}{2} < (v_i v_i)_{,j} v_j > + 2R < w\theta > + < \theta\theta_{,jj} > \\
&\quad - \frac{1}{2} Pr < v_i (\theta^2)_{,i} >, \\
&= - < (v_i q)_{,i} > + < v_{i,i} q > + < v_i v_{i,jj} > - \frac{1}{2} < (v_i v_i v_j)_{,j} > + \frac{1}{2} < v_i v_i v_{j,j} > \\
&\quad + 2R < w\theta > + < (\theta\theta_{,j})_{,j} > - < \theta_{,j}\theta_{,j} > - \frac{1}{2} Pr < (v_i \theta^2)_{,i} > + \frac{1}{2} Pr < v_{i,i} \theta^2 > .
\end{aligned}$$

We have expanded dE/dt in this way, since by noting that $\nabla \cdot \mathbf{v} = 0$ we can cancel out many of the above terms. Then, upon integrating by parts we arrive at

$$\begin{aligned}
\frac{dE}{dt} &= - \int_{\partial\Gamma} v_i q \hat{n}_i dS - \frac{1}{2} \int_{\partial\Gamma} v_i v_i v_j \hat{n}_j dS + \int_{\partial\Gamma} \theta\theta_{,j} \hat{n}_j dS - \frac{1}{2} P_r \int_{\partial\Gamma} v_i \theta^2 \hat{n}_i dS, \\
&\quad + < v_i v_{i,jj} > + 2R < w\theta > - < \theta_{,j}\theta_{,j} > .
\end{aligned}$$

Referring to the boundary conditions on $(\mathbf{v}, \theta) \in \mathcal{H}$, we see that all the above surface integrals vanish, such that we are left with

$$\frac{dE}{dt} = R\mathcal{I} - \mathcal{D}, \tag{2.33}$$

where $\mathcal{I}$ and $\mathcal{D}$ are given by

$$\begin{aligned}
\mathcal{I}(\mathbf{v}, \theta) &= 2 < w\theta >, \\
\mathcal{D}(\mathbf{v}, \theta) &= - < v_i v_{i,jj} > + < \theta_{,i}\theta_{,i} >, \\
&= \frac{1}{\lambda_0}\int_{\partial\Gamma_0} v_i v_i dS + \frac{1}{\lambda_1}\int_{\partial\Gamma_1} v_i v_i dS + < v_{i,j} v_{i,j} > + < \theta_{,i}\theta_{,i} > \geq 0.
\end{aligned}$$

We now define the quantity R_E by

$$\frac{1}{R_E} = \max_{(\mathbf{v},\theta)\in\mathcal{H}} \frac{\mathcal{I}}{\mathcal{D}}, \tag{2.34}$$

assuming that a bounded maximum exists. This leads us to the inequality

$$\frac{dE}{dt} = \mathcal{D}\left(R\frac{\mathcal{I}}{\mathcal{D}} - 1\right) \leq \mathcal{D}\left(\frac{R - R_E}{R_E}\right). \tag{2.35}$$

We now require to show that provided $R < R_E$, then $E(t)$ decays to zero for all $E(0)$ (i.e. the perturbations $\mathbf{v}$, θ will decay for all initial data $\mathbf{v}_0$, θ_0). If we let $c_1 = \min\{\lambda_0^{-1}, \lambda_1^{-1}, 1\}$ and $c_2 = (R_E - R)/R_E$, then from (2.35) we have the inequality

$$\frac{dE}{dt} \leq -c_1 c_2 \left(\int_{\partial\Gamma_0\cup\partial\Gamma_1} v_i v_i dS + \int_\Gamma v_{i,j} v_{i,j} dV + \int_\Gamma \theta_{,i}\theta_{,i} dV\right). \tag{2.36}$$

We now make use of the following Poincaré inequalities. For some $(\eta_v, \eta_\theta) \in [0, \infty) \times [0, \infty)$ it holds that

$$\eta_\theta \int_\Gamma \theta^2 dV \leq \int_\Gamma \theta_{,i}\theta_{,i} dV, \tag{2.37}$$

$$\eta_v \int_\Gamma v_i v_i dV \leq \int_\Gamma v_{i,j} v_{i,j} dV + \int_{\partial\Gamma_0\cup\partial\Gamma_1} v_i v_i dS. \tag{2.38}$$

Applying (2.37) and (2.38) to (2.36), and letting $c_3 = \min\{\eta_v, \eta_\theta\}$, we obtain

$$\frac{dE}{dt} \leq -c_1 c_2 c_3 \left(< v_i v_i > + < \theta^2 >\right). \tag{2.39}$$

Finally, setting $c_4 = \min\{1, Pr^{-1}\}$ we obtain from (2.35)

$$\frac{dE}{dt} \leq -2c_1 c_2 c_3 c_4 \left(< v_i v_i > + Pr < \theta^2 >\right) = -cE(t),$$

where $c = 2c_1c_2c_3c_4 > 0$, provided $R < R_E$. We can integrate this with respect to time

$$\begin{aligned} \frac{dE}{dt} + cE(t) \leq 0 \Longrightarrow \frac{d}{dt}\left(E(t)e^{ct}\right) &\leq 0, \\ \Longrightarrow E(t)e^{ct} - E(0) &\leq 0, \\ \Longrightarrow E(t) \leq e^{-ct}E(0). & \end{aligned}$$

Therefore the condition $R < R_E$ is sufficient to ensure that all perturbations in $\mathcal{H}$ decay at least exponentially as time evolves.

It is left for us to perform the maximization necessary to find R_E, as defined in (2.34). If the quotient $\mathcal{I}(\mathbf{v},\theta)/\mathcal{D}(\mathbf{v},\theta)$ is at a maximum, i.e. $\mathbf{v}$ and θ have been optimally chosen in $\mathcal{H}$, then for all $(\mathbf{h},\psi) \in \mathcal{H}$ we have that

$$\frac{d}{d\epsilon}\left(\frac{\mathcal{I}(\mathbf{v}+\epsilon\mathbf{h},\theta+\epsilon\psi)}{\mathcal{D}(\mathbf{v}+\epsilon\mathbf{h},\theta+\epsilon\psi)}\right)\Bigg|_{\epsilon=0} = 0. \tag{2.40}$$

Using the quotient rule, and assuming $\mathcal{I}/\mathcal{D}$ is at a maximum, we obtain

$$\begin{aligned} \frac{d}{d\epsilon}\left(\frac{\mathcal{I}(\mathbf{v}+\epsilon\mathbf{h},\theta+\epsilon\psi)}{\mathcal{D}(\mathbf{v}+\epsilon\mathbf{h},\theta+\epsilon\psi)}\right)\Bigg|_{\epsilon=0} &= \frac{1}{\mathcal{D}(\mathbf{v},\theta)}\left(\frac{d}{d\epsilon}\mathcal{I}(\mathbf{v}+\epsilon\mathbf{h},\theta+\epsilon\psi)|_{\epsilon=0} - \frac{\mathcal{I}(\mathbf{v},\theta)}{\mathcal{D}(\mathbf{v},\theta)}\frac{d}{d\epsilon}\mathcal{D}(\mathbf{v}+\epsilon\mathbf{h},\theta+\epsilon\psi)|_{\epsilon=0}\right), \\ &= \frac{1}{\mathcal{D}(\mathbf{v},\theta)}\left(\frac{d}{d\epsilon}\mathcal{I}(\mathbf{v}+\epsilon\mathbf{h},\theta+\epsilon\psi)|_{\epsilon=0} - \frac{1}{R_E}\frac{d}{d\epsilon}\mathcal{D}(\mathbf{v}+\epsilon\mathbf{h},\theta+\epsilon\psi)|_{\epsilon=0}\right), \end{aligned}$$

and so $\mathcal{I}/\mathcal{D}$ is at a maximum provided that

$$R_E\frac{d}{d\epsilon}\mathcal{I}(\mathbf{v}+\epsilon\mathbf{h},\theta+\epsilon\psi)|_{\epsilon=0} - \frac{d}{d\epsilon}\mathcal{D}(\mathbf{v}+\epsilon\mathbf{h},\theta+\epsilon\psi)|_{\epsilon=0}. \tag{2.41}$$

Calculating the above derivatives,

$$\begin{aligned} \frac{d}{d\epsilon}\mathcal{I}(\mathbf{v}+\epsilon\mathbf{h},\theta+\epsilon\psi)|_{\epsilon=0} &= 2\frac{d}{d\epsilon} < (w+\epsilon h_3)(\theta+\epsilon\psi) > |_{\epsilon=0}, \\ &= 2 < h_3\theta > +2 < w\psi >, \end{aligned}$$

$$\begin{aligned}
\frac{d}{d\epsilon}\mathcal{D}(\mathbf{v}+\epsilon\mathbf{h},\theta+\epsilon\psi)|_{\epsilon=0} &= -\frac{d}{d\epsilon}<(v_i+\epsilon h_i)(v_{i,jj}+\epsilon h_{i,jj})>|_{\epsilon=0} \\
&\quad +\frac{d}{d\epsilon}<(\theta_{,i}+\epsilon\psi_{,i})(\theta_{,i}+\epsilon\psi_{,i})>|_{\epsilon=0}, \\
&= -<h_i v_{i,jj}> -<v_i h_{i,jj}> +2<\psi_{,i}\theta_{,i}>, \\
&= -<h_i v_{i,jj}> -<(v_i h_{i,j})_{,j}> +<v_{i,j}h_{i,j}> \\
&\quad +2<(\psi\theta_{,i})_{,i}> -2<\psi\theta_{,ii}>, \\
&= -2<h_i v_{i,jj}> -2<\psi\theta_{,ii}> \\
&\quad +<(v_{i,j}h_i)_{,j}> -<(v_i h_{i,j})_{,j}> +2<(\psi\theta_{,i})_{,i}>, \\
&= -2<h_i v_{i,jj}> -2<\psi\theta_{,ii}> \\
&\quad +\int_{\partial\Gamma} v_{i,j}h_i\hat{n}_j dS - \int_{\partial\Gamma} v_i h_{i,j}\hat{n}_j dS + 2\int_{\partial\Gamma}\psi\theta_{,i}\hat{n}_i dS.
\end{aligned}$$

Once more, the surface integrals vanish on $\partial\bar{\Gamma}\backslash\{\partial\Gamma_0\cup\partial\Gamma_1\}$, owing to the periodicity of $\mathbf{h}$ and ψ, while the surface integral of $\psi\theta_{,i}$ vanishes altogether. Therefore, applying the boundary conditions on $\mathbf{v}$ and $\mathbf{h}$ at $\partial\Gamma_0$ and $\partial\Gamma_1$,

$$\begin{aligned}
\int_{\partial\Gamma} v_{i,j}h_i\hat{n}_j dS - \int_{\partial\Gamma} v_i h_{i,j}\hat{n}_j dS &= \int_{\partial\Gamma_0}(v_{i,j}h_i - v_i h_{i,j})\hat{n}_j dS + \int_{\partial\Gamma_1}(v_{i,j}h_i - v_i h_{i,j})\hat{n}_j dS, \\
&= -\int_{\partial\Gamma_0}\left(\frac{1}{\lambda_0}v_i h_i - \frac{1}{\lambda_0}v_i h_i\right)\hat{n}_j dS \\
&\quad +\int_{\partial\Gamma_1}\left(-\frac{1}{\lambda_1}v_i h_i + \frac{1}{\lambda_1}v_i h_i\right)\hat{n}_j dS, \\
&= 0.
\end{aligned}$$

We include the conditions $h_{i,i}=0$ by way of a Lagrange multiplier $2\phi(\mathbf{x})$,

$$\begin{aligned}
2<h_{i,i}\phi> &= 2<(h_i\phi)_{,i}> -2<h_i\phi_{,i}>, \\
&= 2\int_{\partial\Gamma} h_i\hat{n}_i dS - 2<h_i\phi_{,i}>, \\
&= -2<h_i\phi_{,i}>.
\end{aligned}$$

Finally, grouping all our terms in h_i and ψ, we obtain for equation (2.41)

$$<h_i\left(R_E\hat{k}_i\theta + v_{i,jj} - \phi_{,i}\right)> + <\psi\left(R_E w + \theta_{,jj}\right)>=0. \tag{2.42}$$

The functions $\mathbf{h}$ and ψ were chosen arbitrarily from $\mathcal{H}$. Therefore, in general, we

must have

$$\Delta v_i + R_E \hat{k}_i \theta = \phi_{,i}, \tag{2.43}$$

$$v_{i,i} = 0, \tag{2.44}$$

$$\Delta\theta + R_E w = 0. \tag{2.45}$$

Identifying ϕ with q, we see that in deriving equations (2.43)-(2.45) we have recovered system (2.30)-(2.32). That is, we have shown that the stability threshold of system (2.43)-(2.45) coincides with that for the linear system, and so we conclude that $R_E = R_L = R_{\text{crit}}$. Moreover, we can solve the system with solutions of the form of single Fourier modes.

2.3 Solution of linear stability equations

To solve system (2.30)-(2.32) we begin by removing the pressure gradient $q_{,i}$ by performing $\nabla \times \nabla \times$(2.30). We find

$$\begin{aligned}
\{\nabla \times (\nabla \times \mathbf{v})\}_i &= -\Delta v_i, \\
\{\nabla \times (\nabla \times \Delta \mathbf{v})\}_i &= -\Delta^2 v_i, \\
\{\nabla \times (\nabla \times \nabla q)\}_i &= 0, \\
\{\nabla \times \left(\nabla \times \hat{\mathbf{k}}\theta\right)\}_i &= \theta_{,i3} - \hat{k}_i \Delta\theta,
\end{aligned}$$

and so upon choosing $i = 3$, we obtain

$$\Delta^2 w - R\Delta^* \theta = 0, \tag{2.46}$$

$$\Delta\theta + Rw = 0, \tag{2.47}$$

where $\Delta^* = (\partial^2/\partial x^2) + (\partial^2/\partial y^2)$, the Laplacian operator in $\mathbb{R}^2$. We now turn our attention to the boundary conditions on w. Since the fluid is incompressible we have that $w_{,z} = -(u_{,x} + v_{,y})$. Therefore $w_{,zz} = -(u_{,xz} + v_{,yz})$, and from the boundary conditions on u and v we see that w satisfies

$$w = 0, \quad w_{,z} = \lambda_0 w_{,zz} \quad \text{at } z = 0, \tag{2.48}$$

$$w = 0, \quad w_{,z} = -\lambda_1 w_{,zz} \quad \text{at } z = 1, \tag{2.49}$$

while we remind the reader that θ vanishes at $z = 0$ and $z = 1$.

Since $\mathbf{v}$ and θ have the same periodic (x, y) dependence, we let our single mode solution to (2.30)-(2.32) be of the form

$$w = w(z)f(x, y), \quad \theta = \theta(z)f(x, y).$$

Then, from (2.47) we have that

$$\theta(z)(f(x,y)_{,xx} + f(x,y)_{,yy}) + \theta''(z)f(x,y) + Rw(z)f(x,y) = 0,$$
$$\Longrightarrow \frac{\Delta^* f(x,y)}{f(x,y)} = -\frac{Rw(z) + \theta''(z)}{\theta(z)} = \xi,$$

for separation constant ξ. Therefore $\Delta^* f = \xi f$.

Since we require periodic solutions, we set $\xi = -a^2 < 0$, and thus our solutions w and θ are consistent with a wave number a such that $\Delta^* w = -a^2 w$, and $\Delta^* \theta = -a^2\theta$. Then, substituting our modes into equations (2.46) and (2.47), and removing the (x, y) dependent parts, we have

$$\left(\frac{d^2}{dz^2} - a^2\right)^2 w - Ra^2\theta = 0, \tag{2.50}$$
$$\left(\frac{d^2}{dz^2} - a^2\right)\theta + Rw = 0, \tag{2.51}$$

for $z \in [0, 1]$ and $w = w(z)$, $\theta = \theta(z)$, subject to the boundary conditions

$$w(0) = w(1) = 0, \quad \lambda_0 w''(0) - w'(0) = 0, \quad \lambda_1 w''(1) + w'(1) = 0, \quad \theta(0) = \theta(1) = 0. \tag{2.52}$$

Equations (2.50) and (2.51) are the classic stability equations for the Bénard problem. We note that in the limit $\lambda_1 \to 0$ we obtain from (2.52) the no-slip boundary condition at $z = 1$, while for $\lambda_1 \to \infty$ we recover the free boundary condition (and similarly for λ_0 at $z = 0$).

2.4 Numerical solution of instability equations

2.4.1 Chebyshev tau method

We refer the reader to Appendix A for a thorough description of the Chebyshev tau method, and use this Section to explain its implementation in the problem discussed

in this chapter. The Chebyshev tau method exploits the orthogonality of Chebyshev polynomials over the interval $[-1,1]$, and so we begin by transforming the domain of equations (2.50) and (2.51) from $z \in [0,1]$ to $r \in [-1,1]$ via $r = 2z - 1$.

Equation (2.50) has a fourth order derivative. Dongarra, Straughan & Walker [17] show that high order differentiation matrices, for instance in this case the D^4 matrix, can introduce significant round off errors. Therefore we use what is described in the literature as a D^2 method, and make the substitution

$$\psi = \left(4\frac{d^2}{dr^2} - a^2\right) w, \tag{2.53}$$

where we now consider w, ψ, θ to be functions of the variable r. We assume that our solutions can be expanded as series of Chebyshev polynomials, specifically

$$w(r) = \sum_{n=0}^{\infty} w_n T_n(r), \quad \psi(r) = \sum_{n=0}^{\infty} \psi_n T_n(r), \quad \theta(r) = \sum_{n=0}^{\infty} \theta_n T_n(r),$$

where T_n is the Chebyshev polynomial of degree n. In this way, we aim to approximate w, ψ and θ by the finite dimensional functions W, Ψ, Θ given by

$$W(r) = \sum_{n=0}^{N} W_n T_n(r), \quad \Psi(r) = \sum_{n=0}^{N} \Psi_n T_n(r), \quad \Theta(r) = \sum_{n=0}^{N} \Theta_n T_n(r),$$

for some integer N. Rewriting equations (2.50) and (2.51) in terms of the new variable r, we require to solve

$$L_1(W,\Psi) = \left(4\frac{d^2}{dz^2} - a^2\right) W - \Psi = \tau_1 T_{N-1} + \tau_2 T_N, \tag{2.54}$$

$$L_2(\Psi,\Theta) = \left(4\frac{d^2}{dz^2} - a^2\right) \Psi - a^2 R\Theta = \tau_3 T_{N-1} + \tau_4 T_N, \tag{2.55}$$

$$L_3(W,\Theta) = RW + \left(4\frac{d^2}{dz^2} - a^2\right) \Theta = \tau_5 T_{N-1} + \tau_6 T_N, \tag{2.56}$$

where the constants τ_i are a measure of the error in our approximation. Taking the weighted Chebyshev inner-products (A.1.4) of L_i with T_k where $i = 1,2,3$ and $k = 0,1,2,...,N-2$, we remove the τ's and obtain $3N-3$ equations in the $3N+3$ unknowns W_n, Ψ_n and Θ_n,

$$< L_i, T_k >= 0.$$

We close the system with the six boundary conditions (2.52), using the identities $T_n(\pm 1) = (\pm 1)^n$, and $T_n'(\pm 1) = n^2(\pm 1)^{n+1}$. Thus with our expansions for W, Ψ

and Θ we obtain

$$W(1) = \sum_{n=0}^{N} W_n = 0, \quad W(-1) = \sum_{n=0}^{N} (-1)^n W_n = 0,$$

$$\Theta(1) = \sum_{n=0}^{N} \Theta_n = 0, \quad \Theta(-1) = \sum_{n=0}^{N} (-1)^n \Theta_n = 0.$$

The mixed boundary conditions are accounted for by

$$\begin{aligned} 2\lambda_1 W''(1) + W'(1) &= 2\lambda_1(\Psi(1) + a^2 W(1)) + W'(1), \\ &= 2\lambda_1 \Psi(1) + W'(1), \\ &= 2\lambda_1 \sum_{n=0}^{N} \Psi_n + \sum_{n=0}^{N} n^2 W_n = 0, \end{aligned}$$

$$\begin{aligned} 2\lambda_0 W''(-1) - W'(-1) &= 2\lambda_0(\Psi(-1) + a^2 W(-1)) - W'(-1), \\ &= 2\lambda_0 \Psi(-1) - W'(-1), \\ &= 2\lambda_0 \sum_{n=0}^{N} (-1)^n \Psi_n - \sum_{n=0}^{N} n^2 (-1)^{n+1} W_n = 0. \end{aligned}$$

Letting $\mathbf{x} = (W_0, ..., W_N, \Psi_0, ..., \Psi_N, \Theta_0, ..., \Theta_N)^T$ the vector of unknown coefficients, I be the $(N-1) \times (N-1)$ identity matrix, and D^2 the $(N-1) \times (N-1)$ Chebyshev differentiation matrix for d^2/dr^2, we obtain the generalised eigenvalue problem

$$\begin{pmatrix} 4D^2 - a^2 I & -I & 0 \\ BC1 & 0...0 & 0...0 \\ BC2 & 0...0 & 0...0 \\ 0 & 4D^2 - a^2 I & 0 \\ BC3 & BC3 & 0...0 \\ BC4 & BC4 & 0...0 \\ 0 & 0 & 4D^2 - a^2 I \\ 0...0 & 0...0 & BC5 \\ 0...0 & 0...0 & BC6 \end{pmatrix} \mathbf{x} = R \begin{pmatrix} 0 & 0 & 0 \\ 0...0 & 0...0 & 0...0 \\ 0...0 & 0...0 & 0...0 \\ 0 & 0 & a^2 I \\ 0...0 & 0...0 & 0...0 \\ 0...0 & 0...0 & 0...0 \\ -I & 0 & 0 \\ 0...0 & 0...0 & 0...0 \\ 0...0 & 0...0 & 0...0 \end{pmatrix},$$

where the rows BC1-BC6 are our boundary condition equations.

We solve this eigenvalue for a given pair of slip length (λ_0, λ_1), by passing the above matrices to the NAG routine F02GJF (which utilises the QZ method of Moler

& Stewart [42]). For an initial value of the wave number a, we obtain a spectrum of eigenvalues where the positive part of the spectrum is $\{R_1, R_2, R_3, ...\}$, ordered according to $R_i < R_{i+1}$. We select R_1 as the smallest eigenvalue such that the fluid is stable for all $R < R_1$. We then repeat for other values of a, so that we may build the *neutral curve* of $Ra = R_1^2$ against a, along which the fluid is neutrally stable. By iterating over a we are thus able to obtain the critical Rayleigh number Ra_{crit} as the minimum value on this curve, which occurs at wave number a_{crit}.

2.4.2 Compound matrix method

We refer the reader to Appendix B for an introduction to the compound matrix method, and use this Section to present a compound matrix formulation for the solution of (2.50)-(2.51). We convert the boundary value problem into a system of initial value problems, using the boundary conditions at $z = 0$ as the initial data. We then integrate forwards to $z = 1$, while iterating on the value of R until the boundary conditions at $z = 1$ are satisfied. The problem is to formulate the problem in variables that are zero at $z = 0$, taking into account the linear slip boundary condition on w. We propose the following compound matrix method.

Alongside w and θ we introduce the variable χ_α given by

$$\chi_\alpha(z) = \lambda_0^{\alpha+1} w''(z) - \lambda_0^\alpha w'(z), \tag{2.57}$$

for some $\alpha \in \mathbb{R}$, and in this way $w(0) = \chi_\alpha(0) = \theta(0)$, i.e. each of the boundary conditions at $z = 0$ are represented by a single variable. The dependence of χ_α on α is present to allow for the many variations on how such a variable might be defined.

Rewriting system (2.50)-(2.51) in terms of w, χ_α, and θ gives us

$$\begin{aligned} \chi_\alpha'' &= (2a^2 - \lambda_0^{-2})(\chi_\alpha + \lambda_0^\alpha w') - \lambda_0^{-1}\chi_\alpha' - a^4\lambda_0^{\alpha+1} w + a^2 R\lambda_0^{\alpha+1}\theta, \\ \theta'' &= a^2\theta - Rw. \end{aligned}$$

We let $\mathbf{v}(z) = (w, w', \chi_\alpha, \chi_\alpha', \theta, \theta')^T$ be a 'solution vector' to the above system, and decompose it into the linear form $\mathbf{v} = c_1\mathbf{v}_1 + c_2\mathbf{v}_2 + c_3\mathbf{v}_3$, for

$$\mathbf{v}_i(z) = (w_i, w_i', \chi_{\alpha i}, \chi_{\alpha i}', \theta_i, \theta_i')^T.$$

Letting $M(z) = (\mathbf{v}_1\mathbf{v}_2\mathbf{v}_3)$ be the matrix of these solution vectors, we prescribe the initial data

$$M(0) = \begin{pmatrix} 0 & 0 & 0 \\ 1 & 0 & 0 \\ 0 & 0 & 0 \\ 0 & 1 & 0 \\ 0 & 0 & 0 \\ 0 & 0 & 1 \end{pmatrix},$$

such that our solution is composed of three linearly independent parts, and satisfies the prescribed boundary conditions at $z = 0$. We then calculate the variables $y_i(z)$, $i = 1, ..., 20$ where y_i is the ith minor of $M(z)$

$$\begin{aligned}
y_1 &= w_1 w_2' \chi_{\alpha 3} + ... & y_8 &= w_1 \chi_{\alpha 2}' \theta_3 + ... & y_{15} &= w_1' \chi_{\alpha 2}' \theta_3' + ... \\
y_2 &= w_1 w_2' \chi_{\alpha 3}' + ... & y_9 &= w_1 \chi_{\alpha 2}' \theta_3' + ... & y_{16} &= w_1' \theta_2 \theta_3' + ... \\
y_3 &= w_1 w_2' \theta_3 + ... & y_{10} &= w_1 \theta_2 \theta_3' + ... & y_{17} &= \chi_{\alpha 1} \chi_{\alpha 2}' \theta_3 + ... \\
y_4 &= w_1 w_2' \theta_3' + ... & y_{11} &= w_1' \chi_{\alpha 2} \chi_{\alpha 3}' + ... & y_{18} &= \chi_{\alpha 1} \chi_{\alpha 2}' \theta_3' + ... \\
y_5 &= w_1 \chi_{\alpha 2} \chi_{\alpha 3}' + ... & y_{12} &= w_1' \chi_{\alpha 2} \theta_3 + ... & y_{19} &= \chi_{\alpha 1} \theta_2 \theta_3' + ... \\
y_6 &= w_1 \chi_{\alpha 2} \theta_3 + ... & y_{13} &= w_1' \chi_{\alpha 2} \theta_3' + ... & y_{20} &= \chi_{\alpha 1}' \theta_2 \theta_3' + ... \\
y_7 &= w_1 \chi_{\alpha 2} \theta_3' + ... & y_{14} &= w_1' \chi_{\alpha 2}' \theta_3 + ...
\end{aligned}$$

Differentiating each y_i with respect to z gives us a system of twenty ordinary differential equations $\mathbf{y} = \mathbf{f}(y_1, ..., y_{20})$ with initial condition derived from the $z = 0$ boundary conditions

$$y_{15}(0) = 1, \quad y_{i \neq 15}(0) = 0. \tag{2.58}$$

For a given R and wave number a, and pair of slip lengths (λ_0, λ_1) we integrate this system forward, and then test for the condition

$$\lambda_0^{-(\alpha+1)} y_6(1) + (\lambda_0^{-1} + \lambda_1^{-1}) y_3(1) = 0, \tag{2.59}$$

and repeat, iterating on R using NAG routine C05ADF (a combined linear interpolation, extrapolation and bisection method) until (2.59) is satisfied to within a given tolerance, all the while iterating over a until the minimum point $(a_{\text{crit}}, R_{\text{crit}})$ is found, using NAG routine E04ABF (which uses the method of quadratic interpolation).

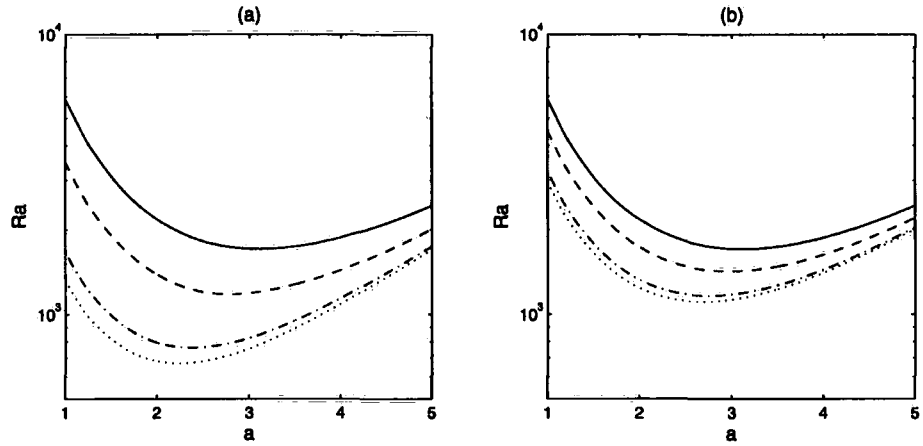

Figure 2.2: Effect of slip length on neutral curve. Graph (a) shows the case $\lambda_0 = \lambda_1 = \lambda$, where: $\lambda = 0$, '–'; $\lambda = 10^{-1}$, '- -'; $\lambda = 10^{0}$, '-·'; $\lambda = 10^{1}$, '··'. Graph (b) shows the case when $\lambda_0 = 0$, and: $\lambda_1 = 0$, '–'; $\lambda_1 = 10^{-1}$, '- -'; $\lambda_1 = 10^{0}$, '-·'; $\lambda_1 = 10^{1}$, '··'.

2.5 Results

In the case of symmetric slip $\lambda_0 = \lambda_1 = \lambda$, with $\lambda_0 = 0$ we obtain no-slip conditions at the upper and lower surfaces, and in the limit $\lambda \to \infty$ we have the free boundary case. Thus from the literature we already have the results $Ra_{\text{crit}}(\lambda = 0) = 1707.7$ and $Ra_{\text{crit}}(\lambda^{-1} = 0) = 657.5$, see [8, 18, 27, 30, 52]. However, the behaviour of $Ra_{\text{crit}}(0 < \lambda < \infty)$ represents a new contribution to this hydrodynamic stability problem.

Using the Chebyshev tau method we calculated neutral curves (see Figure 2.2) and Ra_{crit} for symmetric slip lengths in the range $10^{-5} < \lambda < 10^{5}$, see Figure 2.3 (a) and (b). We see that increasing the slip length has a strongly destabilizing effect on the critical Rayleigh number at which convection begins, and that for all values of λ for which we ran our calculations, Ra_{crit} was observed to be a strictly decreasing function of λ.

Next, we performed calculations for the case of no-slip boundary conditions at the surface $z = 0$, and slip boundary conditions at the surface $z = 1$. Therefore, for

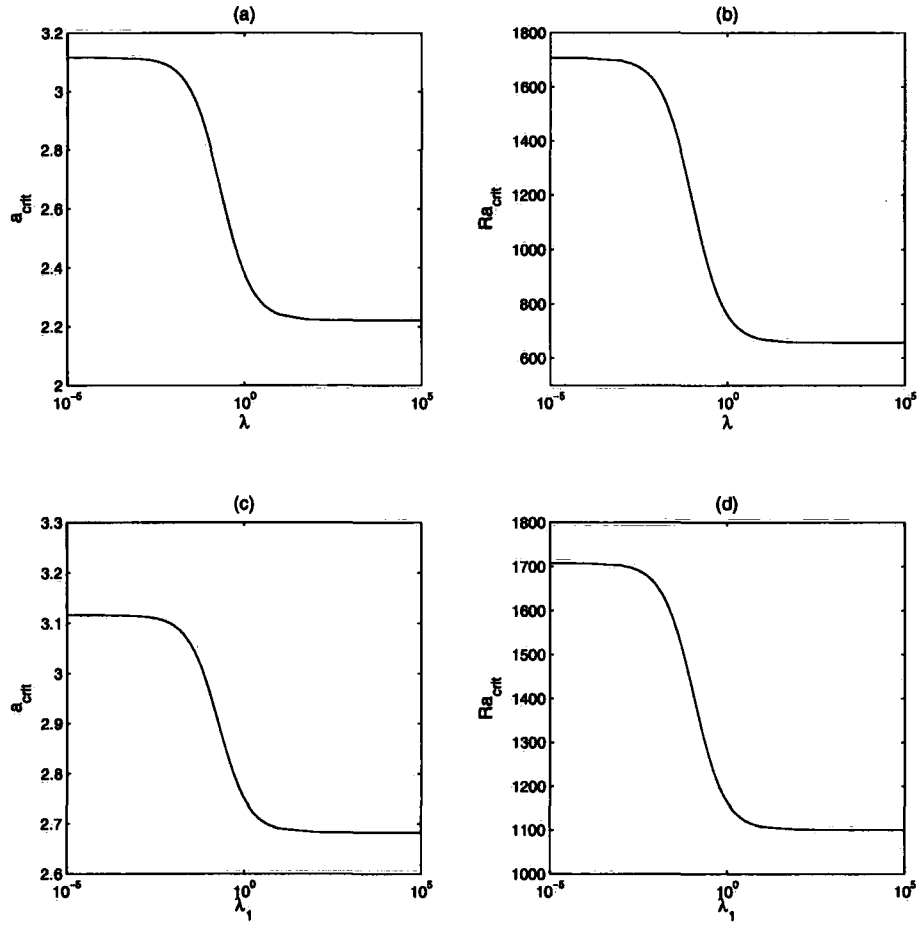

Figure 2.3: Graphs (a) and (b): the variation of the critical point $(a_{\text{crit}}, Ra_{\text{crit}})$ as a function of λ in the case of symmetric slip. Graphs (c) and (d): the variation of the critical point $(a_{\text{crit}}, Ra_{\text{crit}})$ as a function of λ_1 in the case of no-slip boundary conditions at $z = 0$, slip boundary conditions at $z = 1$.

$\lambda_1 = 0$ we have the no-slip case $Ra_{\text{crit}} = 1707.7$, while in the limit $\lambda_1 \to \infty$ (i.e. a free boundary at $z = 1$, no-slip boundary at $z = 0$) we have $Ra_{\text{crit}} = 1100.6$, see [18]. Once more, we show numerically that Ra_{crit} is a strictly decreasing function of the slip length, see Figure 2.3 (c) and (d).

When exchange of stabilities can be shown, the compound matrix method has proved to be the standard numerical method employed in the literature. However, in the previous section we showed that a special formulation of the compound matrix method was needed in order to incorporate the slip boundary conditions. In performing our calculations using this formulation, we were able verify some of the results generated by the Chebyshev tau method, but for slip lengths much smaller than or much larger than $\lambda \sim O(10^0)$ the numerical integration of system $\mathbf{y}' = \mathbf{f}(y_1, .., y_{20})$ suffered severely from round off errors.

The exact form of the system of twenty ODEs is given by

$$
\begin{aligned}
y_1' &= \lambda_0^{-1} y_1 + y_2, \\
y_2' &= (2a^2 - \lambda_0^{-2}) y_1 + a^2 R \lambda_0^{\alpha+1} y_3 + \lambda_0^{-(\alpha+1)} y_5, \\
y_3' &= \lambda_0^{-1} y_3 + y_4 + \lambda_0^{-(\alpha+1)} y_6, \\
y_4' &= a^2 y_3 + \lambda_0^{-1} y_4 + \lambda_0^{-(\alpha+1)} y_7, \\
y_5' &= -\lambda_0^{\alpha}(2a^2 - \lambda_0^{-2}) y_{10} + \lambda_0^{-1} y_5 + a^2 R \lambda_0^{\alpha+1} y_6 + y_{11}, \\
y_6' &= y_7 + y_8 + y_{12}, \\
y_7' &= a^2 y_6 + y_9 + y_{13}, \\
y_8' &= (2a^2 - \lambda_0^{-2})(\lambda_0^{\alpha} y_3 + y_6) - \lambda_0^{-1} y_8 + y_9 + y_{14}, \\
y_9' &= (2a^2 - \lambda_0^{-2})(\lambda_0^{\alpha} y_4 + y_7) + a^2 y_8 - \lambda_0^{-1} y_9 + a^2 R \lambda_0^{\alpha+1} y_{10} + y_{15}, \\
y_{10}' &= y_{16}, \\
y_{11}' &= -a^4 \lambda_0^{\alpha+1} y_1 + a^2 R \lambda_0^{\alpha+1} y_{12}, \\
y_{12}' &= \lambda_0^{-1} y_{12} + y_{13} + y_{14},
\end{aligned}
$$

$$
\begin{aligned}
y'_{13} &= -Ry_1 + a^2 y_{12} + \lambda_0^{-1} y_{13} + y_{15}, \\
y'_{14} &= a^4 \lambda_0^{\alpha+1} y_3 + (2a^2 - \lambda_0^{-2}) y_{12} + y_{15} + \lambda_0^{-(\alpha+1)} y_{17}, \\
y'_{15} &= -Ry_2 + a^4 \lambda_0^{\alpha+1} y_4 + (2a^2 - \lambda_0^{-2}) y_{13} + a^2 y_{14} + a^2 R \lambda_0^{\alpha+1} y_{16} + \lambda_0^{-(\alpha+1)} y_{18}, \\
y'_{16} &= -Ry_3 + \lambda_0^{-1} y_{16} + \lambda_0^{-(\alpha+1)} y_{19}, \\
y'_{17} &= a^4 \lambda_0^{\alpha+1} y_6 - \lambda_0^{\alpha} (2a^2 - \lambda_0^{-2}) y_{12} - \lambda_0^{-1} y_{17} + y_{18}, \\
y'_{18} &= -Ry_5 + a^4 \lambda_0^{\alpha+1} y_7 - \lambda_0^{\alpha} (2a^2 - \lambda_0^{-2}) y_{13} + a^2 y_{17} - \lambda_0^{-1} y_{18} + a^2 R \lambda_0^{\alpha+1} y_{19}, \\
y'_{19} &= -Ry_6 + y_{20}, \\
y'_{20} &= -Ry_8 - a^4 \lambda_0^{\alpha+1} y_{10} + (2a^2 - \lambda_0^{-2})(\lambda_0^{\alpha} y_{16} + y_{19}) - \lambda_0^{-1} y_{20}.
\end{aligned}
$$

Since none of the y'_i depend on z, we have in effect to solve the system of first order differential equations

$$\mathbf{y}' = A\mathbf{y}, \quad y_{15}(0) = 1, \quad y_{i \neq 15}(0) = 0, \tag{2.60}$$

for the constant 20×20 matrix A. We integrated this using the NAG routine D02EJF, a variable step method for stiff systems of first order ODEs using the Backwards Differentiation Formula, see [26].

Our expressions for each of the y_i show us that many of the coefficients of A are scaled like $\lambda_0^{-(\alpha+1)}$, $\lambda_0^{\alpha-2}$, λ_0^{α}, $\lambda_0^{\alpha+1}$, i.e. their magnitude depends both on our choice of α in defining χ_α, and on the slip length we impose at $z = 0$. Then, we see that for large $|\alpha|$, or large λ_0 (or λ_0^{-1}), the coefficients of A will be correspondingly large. The effect of this is seen in the norm of the solution $|\mathbf{y}(z)| = \sqrt{\sum_{i=1}^{20} (y_i(z))^2}$, which increases dramatically as we integrate from $z = 0$ to $z = 1$. Thus, both the numerical integration, and the checking of condition (2.59) at $z = 1$, suffer from rounding error.

We see in Figure 2.4 that large values of λ, λ^{-1} and $|\alpha|$ all lead to an increase in $|\mathbf{y}|$. The optimum choice for α is seen to be close to $\alpha = 0$, while we see that computations using slip lengths of a different order than $\lambda \sim O(10^0)$ also increased the size of $|\mathbf{y}|$. In the special case $\lambda = 10^0$ (and so $\lambda = \lambda^{-1}$) the function $|\mathbf{y}(z)|$ was not observed to vary with α. This can easily be verified by via the role of λ in our definition (2.57).

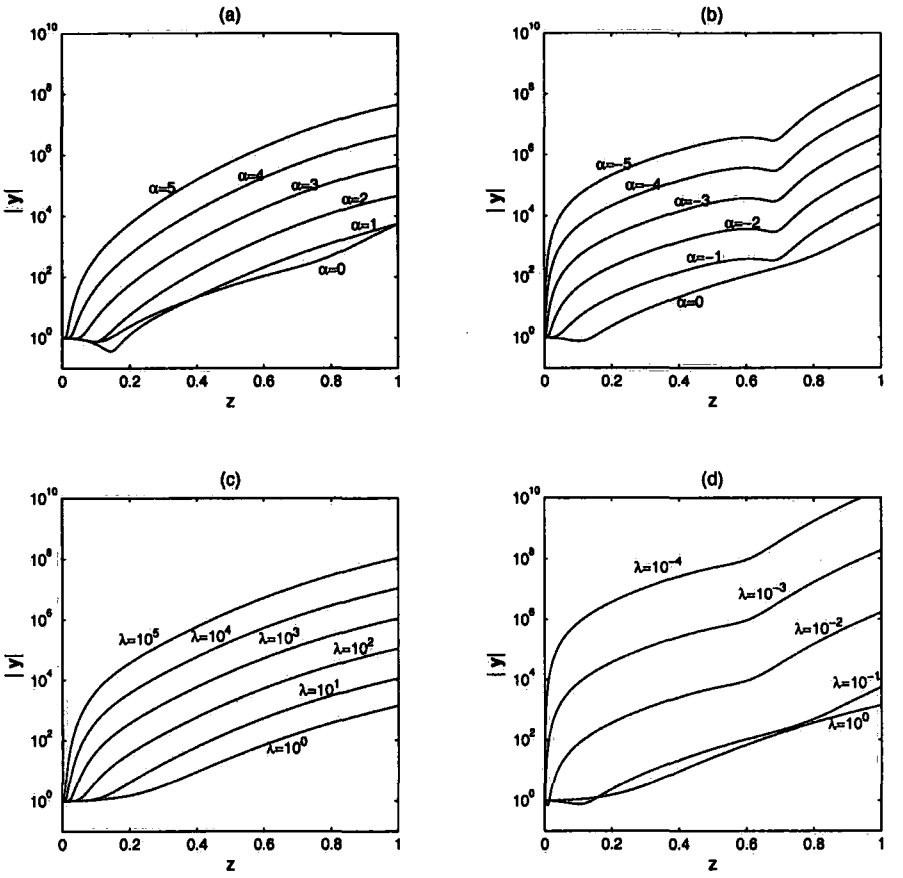

Figure 2.4: Graphs (a) and (b): the variation of $|\mathbf{y}|$ with z for various compound matrix formulations (i.e. choices of α) when $\lambda = 10^{-1}$, and $a = a_{\text{crit}}$, $Ra = Ra_{\text{crit}}$. Graphs (b) and (c): the variation of $|\mathbf{y}|$ with z for various values of λ, with $\alpha = 0$ and $a = a_{\text{crit}}$, $Ra = Ra_{\text{crit}}$.

Chapter 3

Poiseuille flow with slip boundary conditions

We now turn from the problem of convection to that of parallel flows, specifically Poiseuille flow. This consists of an incompressible fluid under isothermal conditions, contained in an infinite channel, along which there is a constant pressure gradient. The fluid moves along this pressure gradient in a laminar way, producing a parabolic velocity profile independently of time. Therefore, a crucial difference with the work of the previous chapter is that the steady-state solution is non-zero.

The problem of instability of pressure driven flow has a long history, starting with the experiments of Reynolds [54] on the transition to turbulence of a liquid flowing through a circular pipe. The instability of such laminar flows is governed by the Orr-Sommerfeld equation [47], an eigenvalue problem with the Reynolds number Re as a parameter, from which we aim to obtain Re_L, the smallest Reynolds number such that the flow is unstable for $Re > Re_L$. However, the linear analyses of pressure driven flow along a pipe fail as the flow has been shown to be linearly stable, see Drazin & Reid [18] for a discussion.

More successful have been the investigations into the related problem of instability of pressure driven flow in a channel. An accurate solution of the Orr-Sommerfeld equation in this setting was not calculated until the paper of Orszag [48], who found the figure $Re_L = 5772$ using the Chebyshev tau method. However, the experiments

of Davies & White [16] suggest that transition to turbulence occurs for Reynolds numbers closer to $Re \sim 1000$, and this discrepancy between the predictions of linear theory and experimental observations is widely reported in the literature, though the rectangular channel used by Davies & White was far from the idealised infinite channel studied here. Having observed boundary slip to have a destabilizing effect on the steady-state solution calculated in the Beńard problem, it is interesting to turn to the problem of advective instability, since if boundary slip has the same effect it could solve the problem of the large experimental discrepancy.

There has been some recent work published on the solution of the Orr-Sommerfeld problem for plane Poiseuille flow with slip boundary conditions, which is in disagreement over the fundamental question of how the slip length affects the stability of the steady-state. The papers of Spille, Rauh & Bühring [57] and Lauga & Cossu [38] report increasing slip length to have a stabilizing effect, increasing the critical Reynolds number guaranteeing instability. However, the papers of A. Chu [13] and W. Chu [14] report the opposite to be true.

With the aim of presenting a clear analysis of the Orr-Sommerfeld problem, and so end the disagreement over the effect of the slip length, this chapter begins with our work on the instability of Poiseuille flow in the plane with slip boundary conditions. We then move on to discuss a nonlinear stability analysis of the problem. We include our computational results in both cases.

3.1 Perturbation equations

We let $\mathbf{x} = (x, y, z)$ denote the Cartesian coordinates of a point in $\mathbb{R}^3$, and consider a fluid contained in the region $\Omega = (-\infty, \infty) \times [-h, h] \times (-\infty, \infty) \subset \mathbb{R}^3$. We use the standard notation of letting $\mathbf{u}(\mathbf{x}; t)$, $p(\mathbf{x}; t)$ denote the fluid velocity and pressure fields at the point $\mathbf{x} \in \Omega$ and time $t \in [0, \infty)$, and label the components of velocity $\mathbf{u} = (u, v, w) = (u_1, u_2, u_3)$.

Denoting the constant density ρ and constant dynamic viscosity μ, the fluid obeys the incompressible Navier-Stokes equations (1.1) and (1.2) with $\mathbf{F} = \mathbf{0}$. We

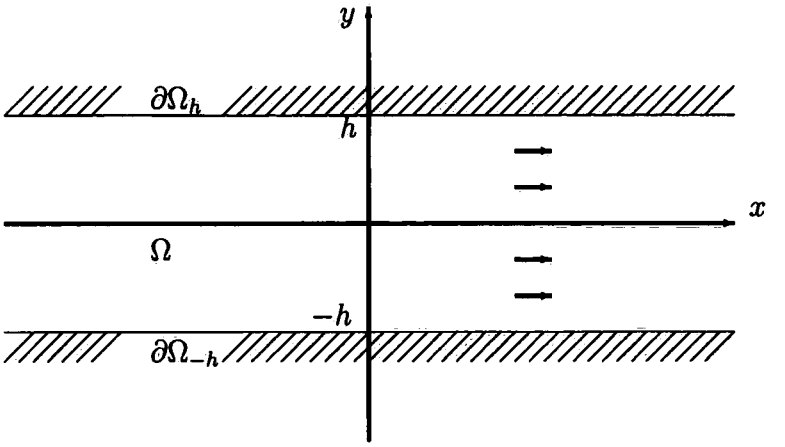

Figure 3.1: Diagram of Poiseuille flow in the plane. A constant pressure gradient $\partial p/\partial x = -g < 0$ drives parallel flow in the $x-$ direction.

define $\partial\Omega_{-h} = \{\mathbf{x} = (x, y, z) | y = -h\}$ and $\partial\Omega_h = \{\mathbf{x} = (x, y, z) | y = h\}$ to be the upper and lower surfaces bounding the channel Ω, at which the fluid satisfies the slip boundary condition (1.3), (1.4). Specifically, these are

$$u|_{y=-h} = \lambda_{-h} u_{,y}|_{y=-h}, \quad v|_{y=-h} = 0, \quad w|_{y=-h} = \lambda_{-h} w_{,y}|_{y=-h}, \tag{3.1}$$

$$u|_{y=h} = -\lambda_h u_{,y}|_{y=h}, \quad v|_{y=h} = 0, \quad w|_{y=h} = -\lambda_h w_{,y}|_{y=h}, \tag{3.2}$$

where λ_h is the slip length at $\partial\Omega_h$, and λ_{-h} is defined similarly.

We consider a steady-state solution to (1.1)-(1.2) of the form $\bar{p}_{,x} = -g < 0$, $\bar{\mathbf{u}} = (\bar{u}(y), 0, 0)$, $\mathbf{F} = \mathbf{0}$. That is, parallel flow in the $x-$direction driven by a constant pressure gradient g, and no body force term. Substitution of these assumed forms into the Navier-Stokes equations leaves us the system,

$$\begin{aligned} 0 &= g + \mu \bar{u}''(y), \\ 0 &= \bar{p}_{,y}, \\ 0 &= \bar{p}_{,z}, \end{aligned}$$

while clearly $\nabla \cdot \bar{\mathbf{u}} = 0$ already. It is seen that $\bar{p}$ is a linear function of x only, while $\bar{u}$ is a quadratic function of y. Applying the boundary conditions we eventually arrive

at

$$\bar{u}(y) = \frac{g}{2\mu}\left(h^2 + h\sigma - \frac{h\delta^2}{2h+\sigma} + \frac{2h\delta}{2h+\sigma}y - y^2\right), \quad \bar{p}(x) = p_0 - gx, \tag{3.3}$$

where, for algebraic neatness, we have let $\sigma = \lambda_h + \lambda_{-h}$ and $\delta = \lambda_h - \lambda_{-h}$.

It is convenient to nondimensionalize the equations of motion via the scalings

$$\mathbf{x} = h\mathbf{x}^*, \quad t = \frac{h}{\bar{u}_{\max}}t^*, \quad \mathbf{u} = \bar{u}_{\max}\mathbf{u}^*, \quad p = \rho\bar{u}_{\max}^2 p^*,$$

where $\bar{u}_{\max} = \bar{u}(0)$ (i.e. the maximum value of $\bar{u}$ when $\lambda_h = \lambda_{-h} = \lambda$), and introduce the nondimensional numbers

$$Re = \frac{\rho h\bar{u}_{\max}}{\mu}, \quad \lambda_1 = \frac{\lambda_h}{h}, \quad \lambda_{-1} = \frac{\lambda_{-h}}{h},$$

where Re is the Reynolds number, based on the half-channel depth h. Then, dropping the '*' notation, the nondimensional equations of motion are

$$u_{i,t} + u_j u_{i,j} = -p_{,i} + \frac{1}{R}\Delta u_i, \tag{3.4}$$

$$u_{i,i} = 0, \tag{3.5}$$

for $\mathbf{x} \in \Gamma = (-\infty, \infty) \times [-1, 1] \times (-\infty, \infty)$ and $t \in [0, \infty)$. Our flow profile nondimensionalizes to give the steady-state

$$\bar{u}(y) = \frac{(2+\sigma)^2(1+\sigma-y^2) - \delta(2+\sigma)(\delta-2y)}{(1+\sigma)[(2+\sigma)^2 - \delta^2]}, \tag{3.6}$$

where the parameters σ and δ are understood to have been nondimensionalized. We note that for $\sigma = \delta = 0$ we recover the no-slip boundary conditions, and the no-slip base solution $\bar{u} = 1 - y^2$ (see, e.g. Drazin & Reid [18]).

We require to investigate the stability of the flow (3.6) to disturbances which we assume to be periodic in the x and z directions. Therefore we perturb the velocity and pressure by

$$\bar{\mathbf{u}}(y) \mapsto \bar{\mathbf{u}}(y) + \mathbf{v}(\mathbf{x}; t), \quad \bar{p}(x) \mapsto \bar{p} + q(\mathbf{x}; t),$$

where $\mathbf{v}(\mathbf{x}; t) = (u, v, w) = (v_1, v_2, v_3)$, and assume that there is some domain $\Lambda = [x_1, x_2] \times [-1, 1] \times [z_1, z_2]$ that tiles the microchannel Γ, such that both $\mathbf{v}$ and q are

periodic modulo Λ. Substituting the perturbed forms into equations (3.4) and (3.5) we obtain the perturbation equations

$$v_{i,t} + u_j v_{i,j} + v_j u_{i,j} + v_j v_{i,j} = -q_{,i} + \frac{1}{Re}\Delta v_i, \tag{3.7}$$

$$v_{i,i} = 0, \tag{3.8}$$

for $\mathbf{x} \in \Lambda$, $t \in [0, \infty)$ and assume initial data $\mathbf{v}_0(\mathbf{x})$ such that $\mathbf{v}|_{t=0} = \mathbf{v}_0$. Since $\bar{\mathbf{u}} + \mathbf{v}$ must satisfy the slip boundary conditions, we have for the components of $\mathbf{v}$

$$u|_{y=-1} = \lambda_{-1} u_{,y}|_{y=-1}, \quad v|_{y=-1} = 0, \quad w|_{y=-1} = \lambda_{-1} w_{,y}|_{y=-1}, \tag{3.9}$$

$$u|_{y=1} = -\lambda_1 u_{,y}|_{y=1}, \quad v|_{y=1} = 0, \quad w|_{y=1} = -\lambda_1 w_{,y}|_{y=1}. \tag{3.10}$$

Finally, we denote by $\partial\Lambda_{-1} = \{\mathbf{x} = (x, y, z) | y = -1\}$ the lower surface of Λ, with $\partial\Lambda_1$ similarly defined.

3.2 Linear theory

We remove the nonlinear terms of (3.7)-(3.8), and look for sufficient conditions for instability of the solution to the linearized equations,

$$v_{i,t} + u_j v_{i,j} + v_j u_{i,j} = -q_{,i} + \frac{1}{Re}\Delta v_i, \tag{3.11}$$

$$v_{i,i} = 0. \tag{3.12}$$

We assume that we can expand our solutions to the linearized system as

$$\mathbf{v} = \sum_{n=0}^{\infty} \mathbf{v}_n(y) e^{i(\alpha_n x + \beta_n z - \alpha c_n t)}, \quad q = \sum_{n=0}^{\infty} q_n(y) e^{i(\alpha_n x + \beta_n z - \alpha c_n t)},$$

where $(\alpha_n, \beta_n) \in \mathbb{R}^2$ and $c_n \in \mathbb{C}$, and since we only require a single mode to be unstable for instability of the whole solution, we consider a solution of the form

$$\mathbf{v} = \mathbf{v}(y) e^{i(\alpha x + \beta z - \alpha c t)}, \quad q = q(y) e^{i(\alpha x + \beta z - \alpha c t)}. \tag{3.13}$$

Substitution of (3.13) together with (3.6) into the linearized perturbation equations and removal of the exponential parts gives us

$$i\alpha(\bar{u}-c)u+\bar{u}'v = -i\alpha q+\frac{1}{Re}\left(\frac{d^2}{dy^2}-(\alpha^2+\beta^2)\right)u, \tag{3.14}$$

$$i\alpha(\bar{u}-c)v = -Dq+\frac{1}{Re}\left(\frac{d^2}{dy^2}-(\alpha^2+\beta^2)\right)v, \tag{3.15}$$

$$i\alpha(\bar{u}-c)w = -i\beta q+\frac{1}{Re}\left(\frac{d^2}{dy^2}-(\alpha^2+\beta^2)\right)w, \tag{3.16}$$

$$i\alpha u+\frac{d}{dy}v+i\beta w = 0. \tag{3.17}$$

However, if we add $\alpha\times$(3.14) to $\beta\times$(3.16), and define a 'Squire transform' by

$$a=\sqrt{\alpha^2+\beta^2},\quad a\hat{u}=\alpha u+\beta w,\quad \hat{v}=v,\quad a\hat{Re}=\alpha Re,\quad aq=\alpha\hat{q},$$

we obtain the system

$$ia(\bar{u}-c)\hat{u}+\bar{u}'\hat{v} = -ia\hat{q}+\frac{1}{\hat{Re}}\left(\frac{d^2}{dy^2}-a^2\right)\hat{u}, \tag{3.18}$$

$$ia(\bar{u}-c)\hat{v} = -\frac{d}{dy}\hat{q}+\frac{1}{\hat{Re}}\left(\frac{d^2}{dy^2}-a^2\right)\hat{v}, \tag{3.19}$$

$$ia\hat{u}+\frac{d}{dy}\hat{v} = 0. \tag{3.20}$$

This is exactly as we would have, had we considered a solution of the form

$$\mathbf{v}=(u(y),v(y),w(y))e^{ia(x-ct)},\quad q=q(y)e^{ia(x-ct)},$$

i.e. a perturbation dependent on (x,y) only, since in setting $\beta=0$ in (3.14)-(3.16) the w equation decouples, and is solved by $w=0$.

Moreover, since solutions to (3.18)-(3.20) will resemble solutions to (3.14)-(3.17), the fact that $\hat{Re}<Re$ means that for every unstable (x,y,z) dependent solution to the linearized equations, there is a $z-$ independent solution that is unstable for a lower Reynolds number. It follows that in looking for instability we need only consider solutions to (3.18)-(3.20).

Removal of the pressure terms by performing $(d/dy)\times$(3.18)-$ia\times$(3.19) results in the Orr-Sommerfeld equation

$$iaR\left[(\bar{u}-c)\left(\frac{d^2}{dy^2}-a^2\right)-\bar{u}''\right]v=\left(\frac{d^2}{dy^2}-a^2\right)^2 v, \tag{3.21}$$

which, upon transferring the boundary conditions from u onto v using (3.20), we must solve subject to

$$v(\pm 1) = 0, \quad \lambda_1 v''(1) + v'(1) = 0, \quad \lambda_{-1} v''(-1) - v'(-1) = 0. \tag{3.22}$$

We solve (3.21) using the Chebyshev tau method (see Orszag [48]), and so we suppose that v can be expressed as the infinite series $v(y) = \sum_{n=0}^{\infty} v_n T_n(y)$. We also suppose that there exists the function $\psi(y) = v''(y) - a^2 v(y)$ where ψ has the similar expansion $\psi(y) = \sum_{n=0}^{\infty} \psi_n T_n(y)$.

We then substitute these series into (3.21), and truncate the series at the $n = N$th term, so that we in effect approximate v and ψ by $V = \sum_{n=0}^{N} V_n T_n(y)$, $\Psi = \sum_{n=0}^{N} \Psi_n T_n(y)$, and due to the error in this series truncation we have

$$\begin{aligned} L_1(V,\Psi) &= V'' - a^2 V - \Psi = \tau_1 T_{N-1} + \tau_2 T_N, \\ L_2(V,\Psi) &= iaRe\left[(\bar{u} - c)\,\Psi - \bar{u}'' V\right] - \left(\frac{d^2}{dy^2} - a^2\right)\Psi = \tau_3 T_{N-1} + \tau_4 T_N. \end{aligned}$$

The τ coefficients are then eliminated in the usual way by taking the Chebyshev weighted inner products $< L_1, T_i >$ and $< L_2, T_i >$, for $i = 0, 1, ..., N-2$. This leaves us with $2N-2$ linear equations in $2N+2$ unknowns V_i, Ψ_i. Upon including the four boundary conditions, we arrive at the generalized eigenvalue problem $(A_r + iA_i)\mathbf{x} = c(B_r + iB_r)\mathbf{x}$ for $\mathbf{x}^T = (V_0, ..., V_N, \Psi_0, ..., \Psi_N)$ and $(2N+2)\times(2N+2)$ square matrices Ar, A_i, B_r and B_i, explicitly

$$\begin{pmatrix} D^2 - a^2 I & -I \\ BC1 & 0...0 \\ BC2 & 0...0 \\ 0 & -D^2 + a^2 I \\ BC3 & BC3 \\ BC4 & BC4 \end{pmatrix} + i \begin{pmatrix} 0 & 0 \\ 0...0 & 0...0 \\ 0...0 & 0...0 \\ -aR\gamma & aRe\bar{U} \\ 0...0 & 0...0 \\ 0...0 & 0...0 \end{pmatrix} = c \left[\begin{pmatrix} 0 & 0 \\ 0...0 & 0...0 \\ 0...0 & 0...0 \\ 0 & 0 \\ 0...0 & 0...0 \\ 0...0 & 0...0 \end{pmatrix} + i \begin{pmatrix} 0 & 0 \\ 0...0 & 0...0 \\ 0...0 & 0...0 \\ 0 & aRe I \\ 0...0 & 0...0 \\ 0...0 & 0...0 \end{pmatrix} \right], \tag{3.23}$$

where D and D^2 are the first and second order Chebyshev differentiation matrices, $\bar{U}$ is the Chebyshev representation matrix of the function $\bar{u}$, and the constant $\gamma(\lambda_{-1}, \lambda_1) = \bar{u}''$. The rows BC1 to BC4 are the boundary conditions,

$$\sum_{n=0}^{N} V_n = 0, \quad \sum_{n=0}^{N} (-1)^n V_n = 0,$$

$$\sum_{n=0}^{N} \left(n^2 V_n + \lambda_1 \Psi_n\right) = 0, \quad \sum_{n=0}^{N} \left(n^2 (-1)^{n+1} V_n - \lambda_{-1} (-1)^n \Psi_n\right) = 0,$$

where we have used the identities $T(\pm 1) = (\pm 1)^n$, $T_n'(\pm 1) = n^2 (\pm 1)^{n+1}$, and the boundary conditions in (3.22).

For a given wave number a, Reynolds number Re, and pair of slip lengths $(\lambda_{-1}, \lambda_1)$ we solve the above generalized eigenvalue problem using NAG routine F02GJF, obtaining the spectrum $\{c_1, c_2, ...\}$ ordered such that $\Im m\{c_1\} \geq \Im m\{c_2\}$. We iterate over Re using NAG routine C05ADF until we have $\Im m\{c_1\} = 0$ (and therefore neutral stability), and then repeat, iterating over a with via NAG routine E04ABF until we have the minimum point (a_L, Re_L) such that the system is linearly stable for all $Re < Re_L$.

3.3 Nonlinear theory

We use the energy method of the previous chapter to find sufficient conditions to ensure stability of the base flow. That is, we aim to find Re_E such that the steady-state (3.6) is stable for Reynolds numbers $Re < Re_E$. Again, we let $< .. >$ denote the $L^2(\Lambda)$ inner-product with associated norm $\|.\|$, given by

$$< fg >= \int_\Lambda fg dV, \quad \|f\| = \sqrt{< ff >} \quad \forall f, g \in L^2(\Lambda),$$

for volume element $dV = dxdydz$, and let $H^1(\Lambda)$ be the complex Hilbert space of measurable functions defined on Λ such that for $f \in H^1(\Lambda)$ we have

$$\|f\| + \|f'\| < \infty.$$

Then, we can define the subspace $\mathcal{H} \subset [H^1(\Lambda)]^3$ such that for $\mathbf{v} = (u, v, w) \in \mathcal{H}$ then $\nabla \cdot \mathbf{v} = 0$, the components of $\mathbf{v}$ satisfy (3.9) and (3.10), and $\mathbf{v}$ is periodic modulo Λ.

Assuming $\mathbf{v} \in \mathcal{H}$, we let $E(t)$ be the non-negative quantity defined by

$$E(t) = \frac{1}{2}\|\mathbf{v}\|^2.$$

Differentiating E with respect to times and substituting from (3.7) we have

$$\begin{aligned} \frac{dE}{dt} &= < v_i \left(-q_{,i} + \frac{1}{Re} v_{i,jj} - u_j v_{i,j} = v_j u_{i,j} - v_j v_{i,j} \right) >, \\ &= - < v_i q_{,i} > + \frac{1}{Re} < v_i v_{i,jj} > - < v_i u_j v_{i,j} > - < v_i v_j u_{i,j} > - < v_i v_j v_{i,j} > . \end{aligned}$$

We now look at each of these terms, and simplify by integrating by parts and

applying (3.9) and (3.10), and the incompressibility condition $v_{i,i} = 0$.

$$\begin{aligned} < v_i q_{,i} > &= < (v_i q_i)_{,i} > - < v_{i,i} q >, \\ &= \int_{\partial\Lambda} v_i q \hat{n}_i dS = 0, \end{aligned}$$

$$\begin{aligned} < v_i v_{i,jj} > &= < (v_i v_{i,j})_{,j} > - < v_{i,j} v_{i,j} >, \\ &= \int_{\partial\Lambda} v_i v_{i,j} \hat{n}_j dS - < v_{i,j} v_{i,j} >, \\ &= -\frac{1}{\lambda_{-1}} \int_{\partial\Lambda_{-1}} v_i v_i dS - \frac{1}{\lambda_1} \int_{\partial\Lambda_1} v_i v_i dS - < v_{i,j} v_{i,j} > \leq 0, \end{aligned}$$

$$\begin{aligned} < v_i v_j v_{i,j} > &= < (v_i v_j v_i)_{,j} > - < v_i v_{j,j} v_i > - < v_{i,j} v_j v_i >, \\ &= \int_{\partial\Lambda} v_i v_j v_i \hat{n}_j dS - < v_{i,j} v_j v_i >, \\ &= - < v_i v_j v_{i,j} > = 0, \end{aligned}$$

$$\begin{aligned} < v_i u_j v_{i,j} > &= < (v_i u_j v_i)_{,j} > - < v_i u_{j,j} v_i > - < v_{i,j} u_j v_i >, \\ &= \int_{\partial\Lambda} v_i u_j v_i \hat{n}_j dS - < v_{i,j} u_j v_i >, \\ &= - < v_{i,j} u_j v_i > = 0, \end{aligned}$$

$$< v_i v_j u_{i,j} > = - < v_i v_j F_{ij} >,$$

for surface element dS, and where we have let $F_{ij} = \frac{1}{2}(u_{i,j} + u_{j,i})$. Therefore, the energy gradient reduces to

$$\frac{dE}{dt} = \mathcal{I} - \frac{1}{Re}\mathcal{D},$$

where the functionals $\mathcal{I}$ and $\mathcal{D}$ are given by

$$\begin{aligned} \mathcal{I}(\mathbf{v}) &= - < v_i v_j F_{ij} >, \\ \mathcal{D}(\mathbf{v}) &= - < v_i v_{i,jj} > \geq 0, \end{aligned}$$

If we define Re_E by

$$\frac{1}{Re_E} = \max_{\mathbf{v} \in \mathcal{H}} \frac{\mathcal{I}}{\mathcal{D}},$$

then provided $Re < Re_E$ we have

$$\frac{dE}{dt} \leq - \left(\frac{Re_E - Re}{Re Re_E} \right) \mathcal{D} \leq 0,$$

and we now aim to use $\mathcal{D}$ to provide a useful bound for dE/dt. Letting $c_1 = \min\{\lambda_{-1}^{-1}, \lambda_1^{-1}, 1\}$ we can use Poincaré's inequality as follows.

$$\begin{aligned} -\mathcal{D} &= -\frac{1}{\lambda_{-1}} \int_{\partial\Lambda_{-1}} v_i v_i dS - \lambda_1 \int_{\partial\Lambda_1} v_i v_i dS - < v_{i,j} v_{i,j} >, \\ &\leq -c_1 \left(\int_{\partial\Lambda_{-1} \cup \partial\Lambda_1} v_i v_i dS + < v_{i,j} v_{i,j} > \right), \\ &\leq -c_1 c_2 < v_i v_i >, \\ &= -2 c_1 c_2 E, \end{aligned}$$

where $c_2 > 0$ is the constant from Poincaré's inequality, see previous chapter. Therefore

$$\frac{dE}{dt} \leq -2 c_1 c_2 \left(\frac{Re_E - Re}{Re Re_E} \right) E(t) \Longrightarrow E(t) \leq e^{-c_3 t} E(0),$$

where $c_3 = 2 c_1 c_2 (Re_E - Re)/Re Re_E > 0$. Hence, all perturbations in $\mathcal{H}$ to the base solution will decay at least exponentially fast, regardless of the initial data $\mathbf{v}_0$, provided that we have $Re < Re_E$.

We now derive the Euler-Lagrange equations to obtain conditions necessary for $\mathcal{I}/\mathcal{D}$ to be at a maximum. For an arbitrary function $\mathbf{h}(\mathbf{v}) \in \mathcal{H}$, $\mathcal{I}/\mathcal{D}$ is at an extremum provided that

$$\begin{aligned} \frac{d}{d\epsilon} \frac{\mathcal{I}(\mathbf{v} + \epsilon \mathbf{h})}{\mathcal{D}(\mathbf{v} + \epsilon \mathbf{h})}\bigg|_{\epsilon=0} &= \frac{1}{\mathcal{D}(\mathbf{v})} \left(\frac{d}{d\epsilon} \mathcal{I}(\mathbf{v} + \epsilon \mathbf{h})|_{\epsilon=0} - \frac{1}{Re_E} \frac{d}{d\epsilon} \mathcal{D}(\mathbf{v} + \epsilon \mathbf{h})|_{\epsilon=0} \right), \\ &= 0. \end{aligned}$$

We now differentiate the $\mathcal{I}$ and $\mathcal{D}$ terms.

$$\begin{aligned} \frac{d}{d\epsilon} \mathcal{I}(\mathbf{v} + \epsilon \mathbf{h})|_{\epsilon=0} &= -\frac{d}{d\epsilon} < (v_i + \epsilon h_i)(v_j + \epsilon h_j) F_{ij} >|_{\epsilon=0}, \\ &= - < h_i v_j F_{ij} > - < v_i h_j F_{ij} >, \\ &= -2 < h_i v_j F_{ij} >, \end{aligned}$$

since F_{ij} is symmetric.

$$\begin{aligned}
\frac{d}{d\epsilon}\mathcal{D}(\mathbf{v}+\epsilon\mathbf{h})|_{\epsilon=0} &= \frac{d}{d\epsilon} < (v_i+\epsilon h_i)(v_{i,jj}+\epsilon h_{i,jj}) >|_{\epsilon=0}, \\
&= < v_i h_{i,jj} > + < h_i v_{i,jj} >, \\
&= < (v_i h_{i,j})_{,j} > - < (v_{i,j} h_i)_{,j} > + 2 < h_i v_{i,jj} >, \\
&= \int_{\partial\Lambda} v_i h_{i,j} \hat{n}_j dS - \int_{\partial\Lambda} v_{i,j} h_i \hat{n}_j dS + 2 < h_i v_{i,jj} >, \\
&= -\frac{1}{\lambda_{-1}} \int_{\partial\Lambda_{-1}} (v_i h_i - h_i v_i) dS - \frac{1}{\lambda_1} \int_{\partial\Lambda_1} (v_i h_i - h_i v_i) dS \\
&\quad + 2 < h_i v_{i,jj} >, \\
&= 2 < h_i v_{i,jj} > .
\end{aligned}$$

We include the restriction $h_{i,i} = 0$ via a Lagrange multiplier $2\phi(\mathbf{x})$,

$$\begin{aligned}
2 < h_{i,i}\phi > &= 2 < (h_i\phi)_{,i} > -2 < h_i\phi_{,i} >, \\
&= \int_{\partial\Lambda} h_i \phi \hat{n}_i dS - 2 < h_i \phi_{,i} >, \\
&= -2 < h_i \phi_{,i} > .
\end{aligned}$$

Collecting together all terms in h_i, $\mathcal{I}/\mathcal{D}$ is at an extremum provided that

$$< h_i(v_{i,jj} - Re_E v_j F_{ij} + \phi_{,i}) >= 0. \tag{3.24}$$

Since $\mathbf{h}$ was chosen arbitrarily, and if we identify ϕ with the pressure field q, we obtain the Euler-Lagrange equations

$$\Delta v_i - Re_E v_j F_{ij} = -q_{,i}, \tag{3.25}$$

$$v_{i,i} = 0. \tag{3.26}$$

We therefore aim to solve the above Euler-Lagrange equations, which are an eigenvalue problem in Re_E, and select the smallest Reynolds number in the spectrum as our critical Reynolds number Re_E.

If we substitute $\bar{\mathbf{u}} = (\bar{u}(y), 0, 0)$ into (3.25) and (3.26), then we see that the

system we must solve is

$$\Delta u - \frac{1}{2}Re\bar{u}'v = -q_{,x}, \tag{3.27}$$

$$\Delta v - \frac{1}{2}Re\bar{u}'u = -q_{,y}, \tag{3.28}$$

$$\Delta w = -q_{,z}, \tag{3.29}$$

$$u_{,x} + v_{,y} + w_{,z} = 0. \tag{3.30}$$

We note that there can be no analogue of the Squire transform we performed on equations (3.14)-(3.16), since linearly combining the spanwise components u and w fails owing to the u term in (3.28). Therefore, we consider in turn (x, y) dependent solutions, and (y, z) dependent solutions.

3.4 Stability with respect to a $z-$ independent perturbation

If we let $\mathbf{v} = \mathbf{v}(x, y; t)$, then (3.27)-(3.30) reduce to

$$\Delta u - \frac{1}{2}Re\bar{u}'v = -q_{,x}, \tag{3.31}$$

$$\Delta v - \frac{1}{2}Re\bar{u}'u = -q_{,y}, \tag{3.32}$$

$$\Delta w = 0, \tag{3.33}$$

$$u_{,x} + v_{,y} = 0, \tag{3.34}$$

where u, v and w satisfy (3.9)-(3.10), and $\Delta = (\partial^2/\partial x^2) + (\partial^2/\partial y^2)$. We see that the w equation uncouples and is solved by $w = 0$. Therefore we can eliminate q by performing $(\partial/\partial y)\times$(3.31)-$(\partial/\partial x)\times$(3.32)

$$\Delta(u_{,y} - v_{,x}) - \frac{1}{2}Re\bar{u}'(v_{,y} - u_{,x}) - \frac{1}{2}Re\bar{u}''v = 0. \tag{3.35}$$

Differentiating this equality with respect to x, and using (3.34) to substitute $u_{,yx} = -v_{,yy}$ and $u_{,xx} = -v_{,yx}$, we arrive at the eigenvalue problem

$$\Delta^2 v + Re\bar{u}'v_{,xy} + \frac{1}{2}Re\bar{u}''v_{,x} = 0, \tag{3.36}$$

and we are left to transfer the boundary conditions from u onto v.

$$\begin{aligned} u|_{y=\pm 1} &= \mp\lambda_{\pm 1} u_{,y}|_{y=\pm 1}, \\ \Longrightarrow u_{,x}|_{y=\pm 1} &= \mp\lambda_{\pm 1} u_{,xy}|_{y=\pm 1}, \\ \Longrightarrow v_{,y}|_{y=\pm 1} &= \mp\lambda_{\pm 1} v_{,yy}|_{y=\pm 1}, \end{aligned}$$

where we have used (3.34). Therefore v must satisfy

$$v|_{y=\pm 1} = 0, \quad \lambda_{-1} v_{,yy}|_{y=-1} - v_{,y}|_{y=-1} = 0, \quad \lambda_1 v_{,yy}|_{y=1} + v_{,y}|_{y=1} = 0. \tag{3.37}$$

We suppose that we can expand v as the infinite series $v = \sum_{n=0}^{\infty} v_n(y) e^{ia_n(x-c_n t)}$. Orr [47] and later Joseph & Carmi [33] and Busse [7] helped establish the precedent of using a single Fourier mode of this series to solve equation (3.36). However, a complete nonlinear analysis should deal with the full series, as is done in the recent work of Kaiser & Mulone [35] and Kaiser & Schmitt [36], who provide estimates on the Reynolds number providing conditional nonlinear stability.

In order for our work to be consistent with the classic results of [7,33] we consider solutions to equation (3.36) of the form $v(y)e^{iax}$. Substituting this form into (3.36) and removing exponential parts results in the equation

$$\left(\frac{d^2}{dy^2} - a^2\right)^2 v + iaRe\left(\bar{u}'v' + \frac{1}{2}\bar{u}''v\right) = 0. \tag{3.38}$$

We now describe a D^2 Chebyshev tau formulation of (3.38), as detailed in Appendix A. We begin by making the substitution

$$\left(\frac{d^2}{dy^2} - a^2\right) v - \psi = 0,$$

i.e. we define a function $\psi = \Delta v$. Then, we suppose that the functions $v(y)$ and $\psi(y)$ can be expressed as

$$v(y) = \sum_{n=0}^{\infty} v_n T_n(y), \quad \psi(y) = \sum_{n=0}^{\infty} \psi_n T_n(y).$$

Then, we truncate these series at the $n = N$th term, and aim to solve

$$\begin{aligned} L_1(v,\psi) &= \left(\frac{d^2}{dy^2} - a^2\right) v - \psi = \tau_1 T_{N-1} + \tau_2 T_N, \\ L_2(v,\psi) &= \left(\frac{d^2}{dy^2} - a^2\right) \psi + iaRe\left(\bar{u}'v + \frac{1}{2}\bar{u}''v\right) = \tau_3 T_{N-1} + \tau_4 T_N, \end{aligned}$$

where the τ's are a measure of the error in our series truncation. Then, taking the inner-product (A.1.4) of $< L_i, T_j >$ for $i = 1, 2$ and $j = 0, 1, ..., N-2$ removes the τ's and, upon letting D^2 be the second order Chebyshev differentiation matrix, $\bar{U}'$ be the Chebyshev representation matrix of the function $\bar{u}'$ (see Appendix A.4), and the constant $\gamma(\lambda_{-1}, \lambda_1) = \bar{u}''$, we obtain the linear system

$$\left\{\begin{pmatrix} D^2 - a^2 I & -I \\ BC1 & 0...0 \\ BC2 & 0...0 \\ 0 & D^2 - a^2 I \\ BC3 & BC3 \\ BC4 & BC4 \end{pmatrix} + i \begin{pmatrix} 0 & 0 \\ 0...0 & 0...0 \\ 0...0 & 0...0 \\ 0 & 0 \\ 0...0 & 0...0 \\ 0...0 & 0...0 \end{pmatrix}\right\} \mathbf{x} = Re \left\{\begin{pmatrix} 0 & 0 \\ 0...0 & 0...0 \\ 0...0 & 0...0 \\ 0 & 0 \\ 0...0 & 0...0 \\ 0...0 & 0...0 \end{pmatrix} + i \begin{pmatrix} 0 & 0 \\ 0...0 & 0...0 \\ 0...0 & 0...0 \\ a(\bar{U}' + \frac{1}{2}\gamma I) & 0 \\ 0...0 & 0...0 \\ 0...0 & 0...0 \end{pmatrix}\right\} \mathbf{x},$$

for solution vector $\mathbf{x}^T = (v_0, ..., v_N, \psi_0, ..., \psi_N)$.

The rows $BC1$ to $BC4$ are our boundary conditions, which (referring to (3.37)) and using the identities $T_n(\pm 1) = (\pm 1)^n$ and $T_n'(\pm 1) = n^2(\pm 1)^{n+1}$, are

$$\sum_{n=0}^{N} v_N = 0, \quad \sum_{n=0}^{N} (-1)^n v_n = 0,$$

$$\sum_{n=0}^{N} (\lambda_1 \psi_n + n^2 v_n) = 0, \quad \sum_{n=0}^{N} (\lambda_{-1}(-1)^n \psi_n - n^2(-1)^{n+1} v_n) = 0.$$

For a given pair of slip lengths λ_{-1} and λ_1, we choose a value for our wave number a and solve the above generalized eigenvalue problem with NAG routine F02GJF (which uses the QZ algorithm of Moler & Stewart [42]), and then proceed to iterate over choices of a, tracking the smallest positive eigenvalue in the spectrum until we have found the critical Reynolds number which we denote by Re_E. The iteration methods are as described in Chapter two.

3.5 Stability with respect to an $x-$ independent perturbation

For the case $\mathbf{v}_{,x} = \mathbf{0}$, $q_{,x} = 0$ and letting $\Delta = (\partial^2/\partial y^2) + (\partial^2/\partial z^2)$, (3.27)-(3.30) become

$$\Delta u - \frac{1}{2} Re \bar{u}' v = 0, \tag{3.39}$$

$$\Delta v - \frac{1}{2} Re \bar{u}' u = -q_{,y}, \tag{3.40}$$

$$\Delta w = -q_{,z}, \tag{3.41}$$

$$v_{,y} + w_{,z} = 0, \tag{3.42}$$

and we note that the solution (u, v, w) does not simplify as in the $z-$independent case. We can eliminate q by performing taking derivatives of equations (3.40) and (3.41), and use the continuity equation (3.42) to remove w,

$$\begin{aligned}\frac{\partial}{\partial z}\left(\frac{\partial}{\partial z}\{\text{equation (3.40)}\} - \frac{\partial}{\partial y}\{\text{equation (3.41)}\}\right) &= \frac{\partial}{\partial z}\left(\Delta(v_{,z} - w_{,y}) - \frac{1}{2}Re\bar{u}'u_{,z}\right), \\ &= \Delta(v_{,zz} - w_{,yz}) - \frac{1}{2}Re\bar{u}'u_{,zz}, \\ &= \Delta^2 v - \frac{1}{2}Re\bar{u}'u_{,zz}, \qquad (3.43) \\ &= 0. \qquad (3.44)\end{aligned}$$

Taking the Laplacian of this,

$$\begin{aligned}\Delta^3 v &= \frac{1}{2}Re\Delta\left(\bar{u}'u_{,zz}\right), \\ &= Re\bar{u}''u_{,zzy} + \frac{1}{2}Re\bar{u}'\Delta u_{,zz} \quad \text{since } \bar{u}''' \equiv 0, \\ &= Re\bar{u}''u_{,zzy} + \frac{1}{4}(Re)^2(\bar{u}')^2 v_{,zz} \quad \text{using equation (3.39).}\end{aligned}$$

We then use equation (3.43) to eliminate the $u_{,yzz}$ term, so that we eventually arrive at the sixth order eigenvalue problem in $(Re)^2$

$$(\bar{u}')^2\Delta^3 v = \frac{1}{4}(Re)^2(\bar{u}')^4 v_{,zz} + 2\bar{u}'\bar{u}''\Delta^2 v_{,y} - 2(\bar{u}'')^2\Delta^2 v. \qquad (3.45)$$

To close the system we need to transfer both the boundary conditions on u and w onto v.

$$\begin{aligned} w|_{y=\pm 1} &= \mp\lambda_{\pm 1} w_{,y}|_{y=\pm 1}, \\ \Longrightarrow w_{,z}|_{y=\pm 1} &= \mp\lambda_{\pm 1} w_{,yz}|_{y=\pm 1}, \\ \Longrightarrow v_{,y}|_{y=\pm 1} &= \mp\lambda_{\pm 1} v_{,yy}|_{y=\pm 1} \quad \text{using equation (3.42),}\end{aligned}$$

$$\begin{aligned} u|_{y=\pm 1} &= \mp\lambda_{\pm 1} u_{,y}|_{y=\pm 1}, \\ \Longrightarrow u_{,zz}|_{y=\pm 1} &= \mp\lambda_{\pm 1} u_{,yzz}|_{y=\pm 1}, \\ \Longrightarrow (\bar{u}' \mp \lambda_{\pm 1}\bar{u}'')\Delta^2 v|_{y=\pm 1} &= \mp\lambda_{\pm 1}\bar{u}'\Delta^2 v_{,y}|_{y=\pm 1} \quad \text{using equation (3.43).}\end{aligned}$$

Again, we suppose solutions have the form of a single Fourier mode, in this case $v = v(y)e^{iaz}$, and in anticipation of applying a D^2 Chebyshev tau formulation we introduce the functions ψ and ϕ such that

$$\psi = \left(\frac{d^2}{dy^2} - a^2\right) v, \quad \phi = \left(\frac{d^2}{dy^2} - a^2\right) \psi.$$

Upon substituting these forms into (3.45), removing exponential parts, and supposing Chebyshev expansions $v(y) = \sum_{n=0}^{\infty} v_n T_n(y)$, $\psi(y) = \sum_{n=0}^{\infty} \psi_n T_n(y)$, $\phi(y) = \sum_{n=0}^{\infty} \phi_n T_n(y)$, we truncate these series at the $n = N$th term and aim to solve

$$\begin{aligned} L_1(v,\psi) &= \left(\frac{d^2}{dy^2} - a^2\right) v - \psi = \tau_1 T_{N-1} + \tau_2 T_N, \\ L_2(\psi,\phi) &= \left(\frac{d^2}{dy^2} - a^2\right) \psi - \phi = \tau_3 T_{N-1} + \tau_4 T_N, \\ L_3(v,\psi,\phi) &= (\bar{u}')^2 \left(\frac{d^2}{dy^2} - a^2\right) \phi + \frac{a^2}{4}(Re)^2 (\bar{u}')^4 v - 2\bar{u}'\bar{u}''\phi' + 2(\bar{u}'')^2 \phi = \tau_5 T_{N-1} + \tau_N T_N. \end{aligned}$$

We take the inner product (A.1.4) of $< L_i, T_j >$ for $i = 1, 2, 3$, $j = 0, 1, ..., N-2$ which removes the τ's due to orthogonality. Then, once more letting $\bar{U}'$ be the Chebyshev representation matrix of the function $\bar{u}'$, the constant $\gamma(\lambda_{-1}, \lambda_1) = \bar{u}''$, and D, D^2 denote the first and second order Chebyshev differentiation matrices, then we obtain the linear system

$$\begin{pmatrix} D^2 - a^2 I & -I & 0 \\ BC1 & 0...0 & 0...0 \\ BC2 & 0...0 & 0...0 \\ 0 & D^2 - a^2 I & -I \\ BC3 & BC3 & 0...0 \\ BC4 & BC4 & 0...0 \\ 0 & 0 & (\bar{U}')^2 D^2 - a^2 (\bar{U}')^2 - 2\gamma \bar{U}' D + 2\gamma^2 I \\ 0...0 & 0...0 & BC5 \\ 0...0 & 0...0 & BC6 \end{pmatrix} \mathbf{x} = (Re)^2 \begin{pmatrix} 0 & 0 & 0 \\ 0...0 & 0...0 & 0...0 \\ 0...0 & 0...0 & 0...0 \\ 0 & 0 & 0 \\ 0...0 & 0...0 & 0...0 \\ 0...0 & 0...0 & 0...0 \\ -\frac{a^2}{4}(\bar{U}')^4 0...0 & 0...0 & 0...0 \\ 0...0 & 0...0 & 0...0 \end{pmatrix} \mathbf{x},$$

where $\mathbf{x}^T = (v_0, ..., v_N, \psi_0, ..., \psi_N, \phi_0, ..., \phi_N)$. Our search algorithm for the critical Reynolds number Re_E is similar to that of the previous Section.

3.6 Results

We present results for the case of symmetric slip, where $\lambda_{-1} = \lambda_1 = \lambda$. Figure 3.3 shows that the critical Reynolds number Re_L, above which instability is assured, is a rapidly increasing function of slip length λ. Therefore, our results are in agreement with the conclusions of Lauga & Cossu [38] and Spille *et al* [57]. While contradicting the results of A. Chu and W. Chu [13, 14].

While the work in [13, 14] performs a linear analysis using the Orr-Sommerfeld equation (3.21) with a base solution $\bar{u}$ which satisfies slip boundary conditions, the pertubation $\mathbf{v} = (u, v, w)$ satisfies homogeneous boundary conditions at $y = \pm 1$. We believe this to be in error, since the function $\bar{\mathbf{u}} + \mathbf{v}$ must satisfy the linear slip boundary conditions prescribed for $\mathbf{u}$, i.e. the components of $\mathbf{v}$ must also satisfy

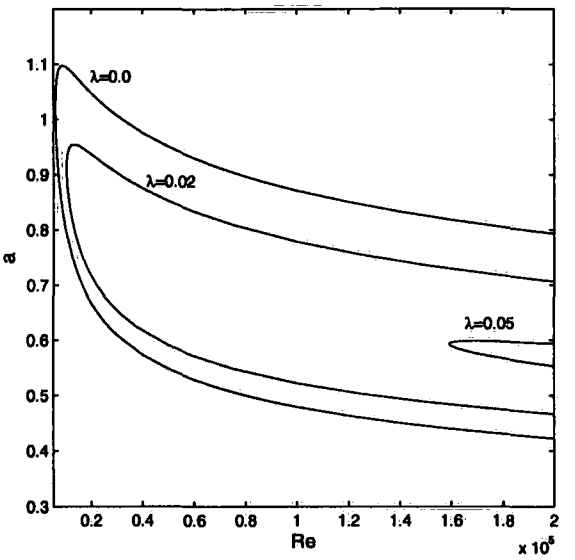

Figure 3.2: Neutral curves from linear analysis, along which the system is neutrally linearly stable.

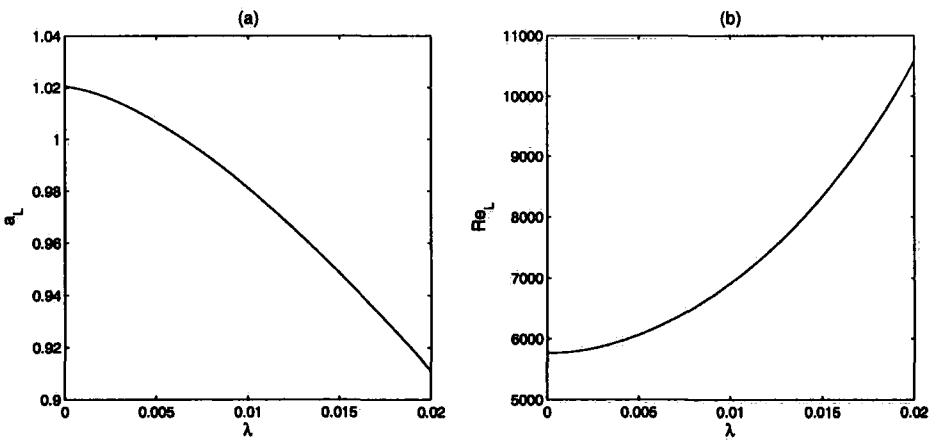

Figure 3.3: The dependence of critical point (a_L, Re_L) on slip length λ. Re_L is an increasing function of λ.

slip boundary conditions.

Having found boundary slip to be linearly stabilizing, we turn our attention to the results of our nonlinear analysis. The critical Reynolds number Re_E^{XY}, below which the flow is conditionally stable to $z-$independent perturbations, is observed to at first decrease with λ from the no-slip result of $Re_E^{XY} = 87.6$ (first calculated by Orr [47]) to a minimum of $Re_E^{XY} = 85.9$ at $\lambda = 0.045$, see Figure 3.6 (a). Then, the critical Reynolds number is an increasing function of λ, such that for $\lambda \sim O(10^0)$, Re_E^{XY} is observed to increase approximately linearly with λ.

Similar behaviour is observed in the case of $x-$independent perturbations. The critical Reynolds number Re_E^{YZ} decreases from the no-slip result of $Re_E^{YZ} = 49.6$ (as calculated by Joseph & Carmi [33] and Busse [7]) to a minimum value of $Re_E^{YZ} = 48.0$ at $\lambda = 0.08$. After this, Re_E^{YZ} is an increasing function of λ, such that, again, for $\lambda \sim O(10^0)$ Re_E^{YZ} increases with λ approximately linearly.

In our linear analysis we were able to show, by finding a Squire transform, that $z-$independent perturbations were the least stable, and so we could consider perturbations dependent upon (x, y, t) only. We then showed that there was no such transform for the equations governing the nonlinear analysis.

Although Orr [47] believed it sufficient to consider only $z-$independent disturbances in the nonlinear analysis, the results of [7,33] show that in the no-slip case, $x-$independent perturbations were the most critical. Our results show this is true for $\lambda \neq 0$. Moreover, if Re_L is an increasing function of λ with $Re_L|_{\lambda=0} = 5772$, and $Re_E = Re_E^{YZ}$ increases with λ from $Re_E|_{\lambda=0} = 49.6$, we cannot have convergence of $Re_L(\lambda)$ and $Re_E(\lambda)$ at $Re \sim 1000$, the critical figure from the experiments of [16].

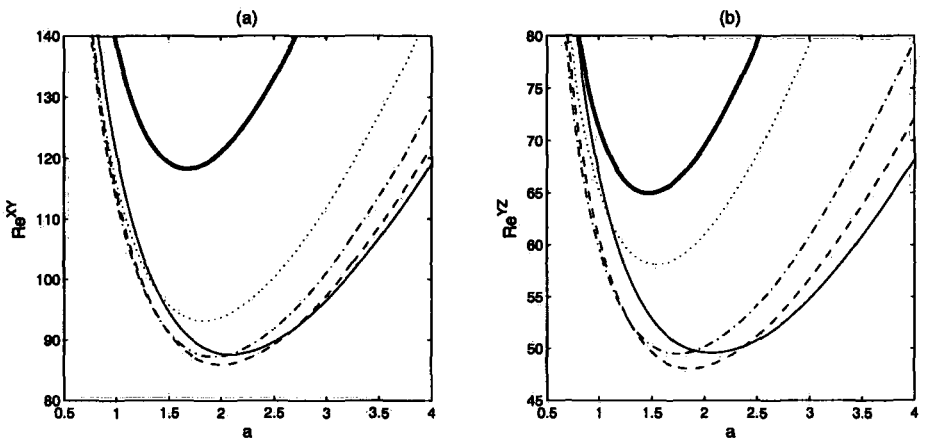

Figure 3.4: Effect of boundary slip on the neutral curves resulting from our nonlinear analysis. Graph (a) shows the neutral curves corresponding to a $z-$independent perturbation, where: $\lambda = 0$, '–'; $\lambda = 0.05$, '- -'; $\lambda = 0.1$, '-·'; $\lambda = 0.2$. '··'; $\lambda = 0.5$, dark '–'. Graph (b) shows the effect of λ for $x-$independent perturbations, with: $\lambda = 0$, '–'; $\lambda = 0.1$, '- -'; $\lambda = 0.2$, '-·'; $\lambda = 0.5$, '··'; $\lambda = 0.7$, dark '–'.

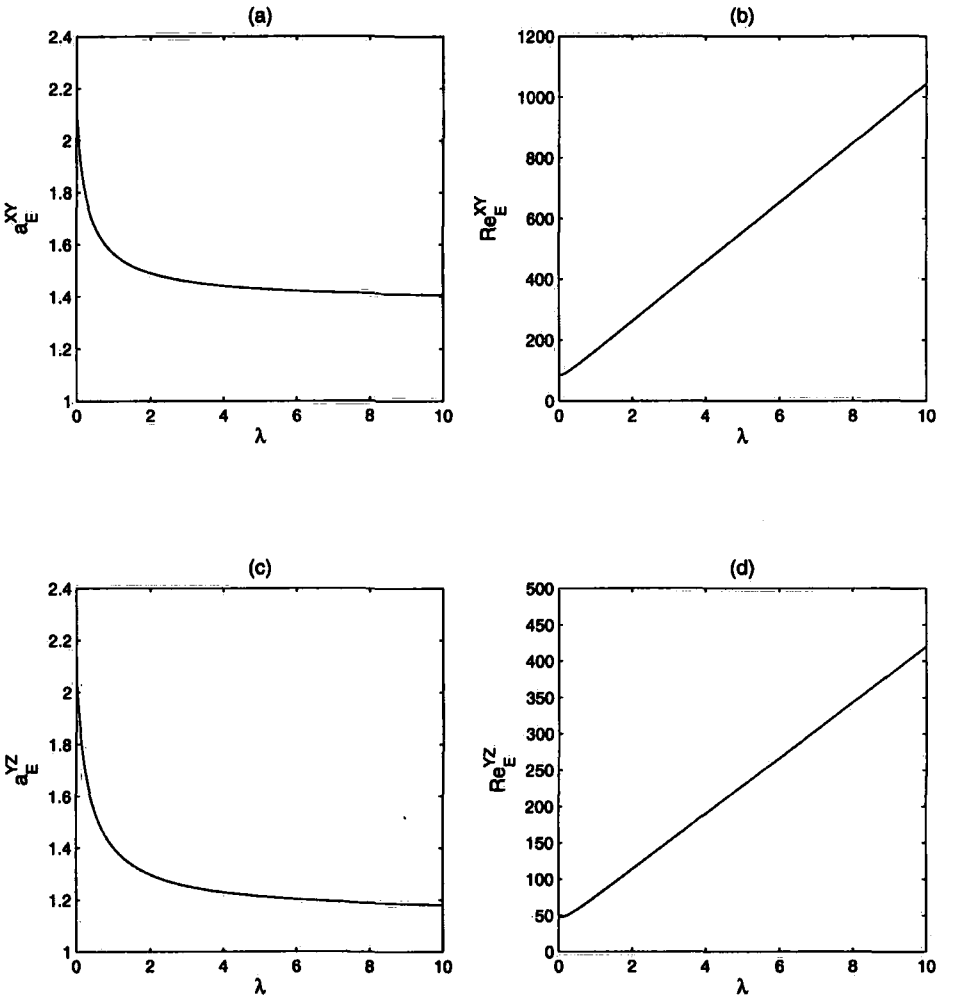

Figure 3.5: The dependence of critical point (a_E, Re_E) on slip length λ for: (a) and (b), $z-$independent disturbances; (c) and (d), $x-$independent disturbances.

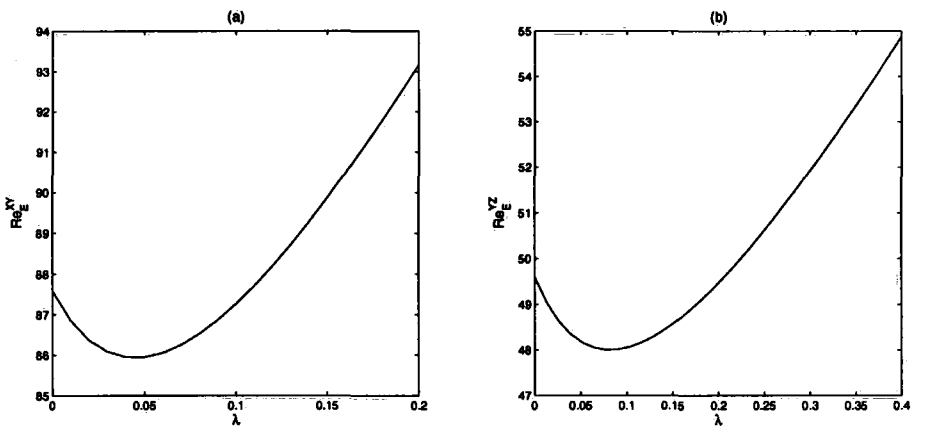

Figure 3.6: The dependence of critical Reynolds numbers Re_E^{XY} and Re_R^{YZ} on slip length λ, for small values of λ.

Chapter 4

Poiseuille flow with variable viscosity

We now consider the case of Poiseuille flow along a channel under non-isothermal conditions. A constant temperature difference is applied across the channel depth, and the viscosity of the fluid is considered to be a function of temperature, the form of its temperature dependence being at our disposal.

Controlling the temperature dependence of the viscosity allows us to observe the influence of slip boundary conditions on the instability of a variety of fluids. For instance, the viscosity of most liquids is a decreasing function of temperature, while at 'ordinary pressures' gases have viscosities that increase with temperature, [69]. However, there are some exceptions: for liquid sulphur and liquid helium there are a range of temperatures over which the viscosity increases as temperature is raised; highly compressed gases become less viscous as the temperature increases.

While boundary slip has been observed relatively recently in liquids [1,4,15,34, 46], it is more commonly associated with the behaviour of rarefied gases, see for example [41]. Therefore, controlling the form of the viscosity function makes for an interesting experiment, as it allows one to see whether, in the mathematical model, the slip length λ has a greater impact for liquid-like fluids or gas-like fluids.

Owing to the problems already mentioned (see previous chapter) in performing a fully nonlinear stability analysis of fluid systems where the velocity steady-state is non-zero, we perform a linear stability analysis only. While we retain control

over the viscosity function, we assume throughout that the fluid is incompressible, and that buoyancy effects are negligible. In doing this, the main point of reference for the work in this chapter is the linear stability analysis of Wall & Wilson [63], who assumed no-slip boundary conditions. Their results suggest that the base flow stabilizes when the viscosity is an increasing function of temperature. When the viscosity decreases with temperature, both increases and decreases in the critical Reynolds number ensuring instability were observed.

4.1 Fluid model

We let $\mathbf{x} = (x, y, z)$ denote the Cartesian coordinates of a point in $\mathbb{R}^3$, and consider a fluid in the channel defined by $\Omega = (-\infty, \infty) \times [-h, h] \times (-\infty, \infty)$. Then, for $\mathbf{x} \in \Omega$ and time $t \in [0, \infty)$, the fluid obeys the Navier-Stokes equations

$$\rho(u_{i,t} + u_j u_{i,j}) = -p_{,i} + \mu \Delta u_i + \mu_{,T} T_{,j}(u_{i,j} + u_{j,i}), \tag{4.1}$$

$$u_{j,j} = 0, \tag{4.2}$$

$$T_{,t} + u_j T_{,j} = \kappa \Delta T, \tag{4.3}$$

where $T(\mathbf{x}; t)$, $\mathbf{u}(\mathbf{x}; t)$, and $p(\mathbf{x}; t)$, are the temperature, velocity and pressure fields, and $\mu(T)$ is the viscosity. The constant terms are the density ρ, and thermometric conductivity κ. Note that in the absence of a body force term we are ignoring buoyancy, and that we consider the fluid to be incompressible. The components of the fluid velocity $\mathbf{u} = (u, v, w)$ satisfy the slip boundary conditions of (4.1) and (4.2), while the temperature satisfies

$$T|_{y=-h} = T_{-h}, \quad T|_{y=h} = T_h, \tag{4.4}$$

for nonzero constants T_{-h} and T_h.

We look for a steady-state solution to (4.1)-(4.3) of Poiseuille type, arising from a constant pressure gradient $p_{,x} = -g < 0$. With assumed forms for the velocity

and temperature $\mathbf{u} = (u(y), 0, 0)$ and $T = T(y)$, we have

$$0 = g + \mu u'' + \mu_{,T} T' u', \tag{4.5}$$

$$0 = p_{,y} = p_{,z}, \tag{4.6}$$

$$0 = T'', \tag{4.7}$$

where the prime denotes differentiation with respect to y. We see that the pressure is a linear function of x only, while from equation (4.7) we see that T is a linear function of y, which is easily found given (4.4). From equation (4.5) we have

$$\begin{aligned} g + \mu u'' + \mu_{,T} T' u' &= 0, \\ \Longrightarrow \frac{d}{dy}(\mu u') &= -g, \\ \Longrightarrow u' &= \frac{A - gy}{\mu} \quad \text{for some constant } A, \\ \Longrightarrow u(y) &= \int \frac{A - gy}{\mu(T(y))} dy + B \quad \text{for some constant } B. \end{aligned}$$

Therefore, we have the steady state solution

$$\bar{u}(y) = \int \frac{A - gy}{\mu(T(y))} dy + B, \quad \bar{p}(x) = \bar{p}_0 - gx, \quad \bar{T}(y) = \frac{1}{2}(T_h + T_{-h}) + \frac{1}{2h}(T_h - T_{-h})y. \tag{4.8}$$

4.2 Nondimensionalization

Denoting the constant $\mu_{-h} = \mu(T(y))|_{y=-h}$, we nondimensionalize equations (4.1) to (4.3) and steady state (4.8) according to the scales

$$\mathbf{x} = h\mathbf{x}^*, \quad \mathbf{u} = \frac{gh^2}{2\mu_{-h}}\mathbf{u}^*, \quad p = \rho\left(\frac{gh^2}{2\mu_{-h}}\right)^2 p^*, \quad \mu = \mu_{-h}\mu^*, \quad T = \frac{1}{2}(T_h - T_{-h})T^* + T_{-h},$$

and introduce the nondimensional numbers

$$Re = \frac{g\rho h^3}{2\mu_{-h}^2}, \quad Pr = \frac{\mu_{-h}}{\rho\kappa}, \tag{4.9}$$

where Re is our Reynolds number, and Pr is our Prandtl number. Then, our nondimensional equations of motion are

$$u_{i,t} + u_j u_{i,j} = -p_{,i} + \frac{1}{Re}\mu\Delta u_i + \frac{1}{Re}\mu_{,T} T_{,j}(u_{i,j} + u_{j,i}), \tag{4.10}$$

$$u_{j,j} = 0, \tag{4.11}$$

$$T_{,t} + u_j T_{,j} = \frac{1}{RePr}\Delta T, \tag{4.12}$$

while our base solution becomes

$$\bar{u}(y) = \int \frac{A-2y}{\mu(T(y))}dy + B, \quad \bar{p}(x) = \bar{p}_0 - \frac{2}{Re}x, \quad \bar{T}(y) = 1+y. \tag{4.13}$$

Wall & Wilson [63] considered three different models for the viscosity function: exponential dependence upon temperature; linear dependence upon temperature; combined linear and exponential temperature dependence. The exponential model $\mu(T) \propto \exp(const./T)$ is commonly used to model liquids and compressed gases [69]. However, Wall & Nagata [62] performed a linear stability analysis in the case of vanishing Péclet number, and found that the precise form of $\mu(T)$ was qualitatively irrelevant. What is important is whether μ is an increasing function of T, or a decreasing function.

Therefore, we choose a linear temperature dependence. Noting that our nondimensionalization results in $\mu(\bar{T}(y))|_{y=-1} = 1$, our model is then

$$\mu(T) = 1 + kT = 1 + k + ky, \tag{4.14}$$

and thus we can control our fluid type through our choice of constant k. In order that $\mu > 0$ we must choose $k > -1/2$. For sufficiently small $|k|$, model (4.14) may be thought of as a leading order approximation to an exponential viscosity model. Therefore, our model is a reasonable compromise, while its linear form aids simplicity of coding later on. With this choice of viscosity μ, our steady-state velocity profile becomes

$$\begin{aligned} \bar{u}(y) &= \int \frac{A-2y}{1+k+ky}dy + B, \\ &= \frac{(Ak+2+2k)\ln\{1+k+ky\} + Bk^2 - 2ky}{k^2}, \end{aligned}$$

and, upon reconciling the boundary conditions (3.9) and (3.10) and assuming $\lambda_{-1} = \lambda_1$ (i.e. symmetric slip), we arrive at the base solution

$$\begin{aligned} \bar{u}(y) = \frac{2}{k[\ln\{1+2k\} + 2\lambda k]}&[2(1+\lambda+\lambda k)\ln\{1+k+ky\} - (\ln\{1+2k\} + 2\lambda k)y \\ &-(1+\lambda)\ln\{1+2k\} + 2\lambda^2 k^2]. \end{aligned} \tag{4.15}$$

4.3 Perturbation equations

We perturb our equations of motion by $\bar{u}_i \mapsto u_i + v_i$, $\bar{p} \mapsto \bar{p} + q$ and $\bar{T} \mapsto \bar{T} + \theta$, where the components of $\mathbf{v} = (v_1, v_2, v_3) = (u, v, w)$ satisfy the slip boundary conditions of (3.9) and (3.10), and the temperature perturbation θ satisfies $\theta|_{y=\pm 1} = 0$. In particular, our viscosity function is also perturbed

$$\begin{aligned}\mu(\bar{T}+\theta) &= \mu(\bar{T}) + \theta\mu_{,T}(\bar{T}) + \frac{1}{2}\theta^2\mu_{,TT}(\bar{T}) + \ldots \\ &= \mu(\bar{T}) + \theta\mu_{,T}(\bar{T}) + \theta^2\eta(\bar{T},\theta),\end{aligned}$$

for some function $\eta(\bar{T},\theta)$. Making these substitutions, we obtain

$$\begin{aligned}v_{i,t} + v_j u_{i,j} + u_j v_{i,j} + v_j v_{i,j} &= -q_{,i} + \frac{1}{Re}(\theta\mu_{,T} + \theta^2\eta)\Delta u_i + \frac{1}{Re}(\mu + \theta\mu_{,T} + \theta^2\eta)\Delta v_i \\ &\quad + \frac{1}{Re}(\theta\mu_{,TT} + \theta^2\eta_{,T})(T_{,j} + \theta_{,j})(u_{i,j} + u_{j,i} + v_{i,j} + v_{j,i}) \\ &\quad + \frac{1}{Re}\mu_{,T}(T_{,j} + \theta_{,j})(v_{i,j} + v_{j,i}) + \frac{1}{Re}\mu_{,T}\theta_{,j}(u_{i,j} + u_{j,i}), \quad (4.16)\\ v_{j,j} &= 0, \quad (4.17)\\ \theta_{,t} + u_j\theta_{,j} + v_j T_{,j} + v_j\theta_{,j} &= \frac{1}{RePr}\Delta\theta. \quad (4.18)\end{aligned}$$

Eliminating terms nonlinear in $\mathbf{v}$ and θ, we find

$$\begin{aligned}v_{i,t} + v_j u_{i,j} + u_j v_{i,j} &= -q_{,i} + \frac{1}{Re}[\mu_{,T}\Delta u_i + \mu_{,TT}T_{,j}(u_{i,j} + u_{j,i})]\theta + \frac{1}{Re}\mu_{,T}(u_{i,j} + u_{j,i})\theta_{,j}, \\ &\quad + \frac{1}{Re}\mu\Delta v_i + \frac{1}{Re}\mu_{,T}T_{,j}(v_{i,j} + v_{j,i}), \quad (4.19)\\ v_{j,j} &= 0, \quad (4.20)\\ \theta_{,t} + u_j\theta_{,j} + v_j T_{,j} &= \frac{1}{RePr}\Delta\theta, \quad (4.21)\end{aligned}$$

before finally we substitute $\bar{T} = 1 + y$, $\bar{\mathbf{u}} = (\bar{u}, 0, 0)$

$$\begin{aligned}\left(\frac{\partial}{\partial t} + \bar{u}\frac{\partial}{\partial x}\right)u + \bar{u}'v &= -q_{,x} + \frac{1}{Re}\left(\mu_{,T}\bar{u}'' + \mu_{,TT}\bar{u}' + \mu_{,T}\bar{u}'\frac{\partial}{\partial y}\right)\theta \\ &\quad + \frac{1}{Re}\left(\mu\Delta + \mu_{,T}\frac{\partial}{\partial y}\right)u + \frac{1}{Re}\mu_{,T}v_{,x}, \quad (4.22)\\ \left(\frac{\partial}{\partial t} + \bar{u}\frac{\partial}{\partial x}\right)v &= -q_{,y} + \frac{1}{Re}\mu_{,T}\bar{u}'\theta_{,x} + \frac{1}{Re}\left(\mu\Delta + 2\mu_{,T}\frac{\partial}{\partial y}\right)v, \quad (4.23)\\ \left(\frac{\partial}{\partial t} + \bar{u}\frac{\partial}{\partial x}\right)w &= -q_{,z} + \frac{1}{Re}\mu_{,T}v_{,z} + \frac{1}{Re}\left(\mu\Delta + \mu_{,T}\frac{\partial}{\partial y}\right)w, \quad (4.24)\\ u_{,x} + v_{,y} + w_{,z} &= 0, \quad (4.25)\\ \left(\frac{\partial}{\partial t} + \bar{u}\frac{\partial}{\partial x}\right)\theta + v &= \frac{1}{RePr}\Delta\theta. \quad (4.26)\end{aligned}$$

4.4 Modal analysis

Since we are performing a linearized stability analysis, we wish to consider solutions to (4.22) to (4.26) of the form of single Fourier modes, i.e.

$$u = u(y)\exp\{i(\alpha x+\beta z-\alpha ct)\}, \quad v = v(y)\exp\{i(\alpha x+\beta z-\alpha ct)\}, \quad w = w(y)\exp\{i(\alpha x+\beta z-\alpha ct)\},$$

$$\theta = \theta(y)\exp\{i(\alpha x+\beta z-\alpha ct)\}, \quad q = q(y)\exp\{i(\alpha x+\beta z-\alpha ct)\}.$$

Wall & Wilson [63] neglect to detail the applicability of Squire's Theorem. Therefore, we now describe a Squire transform that shows that we may consider $z-$independent disturbances in the u and v components only. Substituting the above modal forms into equations (4.22)-(4.26) and removing exponential parts results in the system

$$\begin{aligned}
i\alpha(\bar{u}-c)u+\bar{u}'v &= -i\alpha q+\frac{1}{Re}\left(\mu_{,T}\bar{u}''+\mu_{,TT}\bar{u}'+\mu_{,T}\bar{u}'\frac{\partial}{\partial y}\right)\theta \\
&\quad +\frac{1}{Re}\left(\mu\frac{\partial^2}{\partial y^2}+\mu_{,T}\frac{\partial}{\partial y}-\mu(\alpha^2+\beta^2)\right)u+\frac{i\alpha}{Re}\mu_{,T}v, && (4.27)\\
i\alpha(\bar{u}-c)v &= -q'+\frac{i\alpha}{Re}\mu_{,T}\bar{u}'\theta+\frac{1}{Re}\left(\mu\frac{\partial^2}{\partial y^2}+2\mu_{,T}\frac{\partial}{\partial y}-\mu(\alpha^2+\beta^2)\right)v, && (4.28)\\
i\alpha(\bar{u}-c)w &= -i\beta q+\frac{i\beta}{Re}\mu_{,T}v+\frac{1}{Re}\left(\mu\frac{\partial^2}{\partial y^2}+\mu_{,T}\frac{\partial}{\partial y}-\mu(\alpha^2+\beta^2)\right)w, && (4.29)\\
i\alpha u+v'+i\beta w &= 0, && (4.30)\\
i\alpha(\bar{u}-c)\theta+v &= \frac{1}{RePr}\left(\frac{\partial^2}{\partial y^2}-(\alpha^2+\beta^2)\right)\theta. && (4.31)
\end{aligned}$$

However, if we define

$$a=\sqrt{\alpha^2+\beta^2}, \quad \hat{u}=\frac{\alpha u+\beta w}{a}, \quad \hat{v}=v, \quad \hat{Re}=\frac{\alpha}{a}Re, \quad \hat{q}=\frac{a}{\alpha}q, \quad \hat{\theta}=\frac{\alpha}{a}\theta,$$

and add $\alpha\times(4.27)$ to $\beta\times(4.29)$, we arrive at

$$\begin{aligned}
ia(\bar{u}-c)\hat{u}+\bar{u}'\hat{v} &= -ia\hat{q}+\frac{1}{\hat{Re}}\left(\mu_{,T}\bar{u}''+\mu_{,TT}\bar{u}'+\mu_{,T}\bar{u}'\frac{\partial}{\partial y}\right)\hat{\theta} \\
&\quad +\frac{1}{\hat{Re}}\left(\mu\frac{\partial^2}{\partial y^2}+\mu_{,T}\frac{\partial}{\partial y}-a^2\mu\right)\hat{u}+\frac{ia}{\hat{Re}}\mu_{,T}\hat{v}, && (4.32)\\
ia(\bar{u}-c)\hat{v} &= -\hat{q}_{,y}+\frac{ia}{\hat{Re}}\mu_{,T}\bar{u}'\hat{\theta}+\frac{1}{\hat{Re}}\left(\mu\frac{\partial^2}{\partial y^2}+2\mu_{,T}\frac{\partial}{\partial y}-a^2\mu\right)\hat{v}, && (4.33)\\
ia\hat{u}+\hat{v}' &= 0, && (4.34)\\
ia(\bar{u}-c)\hat{\theta}+\hat{v} &= \frac{1}{\hat{Re}Pr}\left(\frac{\partial^2}{\partial y^2}-a^2\right)\hat{\theta}, && (4.35)
\end{aligned}$$

which is exactly as we'd have had we set $\beta = w = 0$. Moreover, $\hat{Re} \leq Re$, therefore the least stable perturbation is associated with a $z-$independent disturbance in the $x-$ and $y-$ directions.

4.5 Thermal Orr-Sommerfeld equation

We begin by removing the pressure terms by subtracting $i\alpha\times$ equation (4.33) from $d/dy\times$ equation (4.32),

$$\begin{aligned} iaRe(\bar{u}-c)(u'-iav)+Re\bar{u}''v &= [(\mu_{,TTT}+a^2\mu_{,T})\bar{u}'+2\mu_{,TT}\bar{u}''+\mu_{,T}\bar{u}''']\theta \\ &\quad +2(\mu_{,TT}\bar{u}'+\mu_{,T}\bar{u}'')\theta'+2\mu_{,T}\bar{u}'\theta'' \\ &\quad -a^2\mu_{,T}u+(\mu_{,TT}-a^2\mu)u'+2\mu_{,T}u''+\mu u''' \\ &\quad +ia(\mu_{,TT}+a^2\mu)v-ia\mu_{,T}v'-ia\mu v'', \\ ia(\bar{u}-c)\theta+v &= \frac{1}{RePr}(\theta''-a^2\theta). \end{aligned}$$

We introduce a stream function ϕ such that

$$u(y)=\phi'(y), \quad \phi(y)=-ia\phi(y),$$

and thus the continuity equation $iau+v'=0$ is satisfied automatically. With this new variable ϕ we define $\psi(y)$ such that $\psi=\phi''-a^2\phi$. Then, our system becomes

$$\phi''-a^2\phi = \psi, \tag{4.36}$$

$$\begin{aligned} iaRe[(\bar{u}-c)\psi-\bar{u}''\phi] &= [(\mu_{,TTT}+a^2\mu_{,T})\bar{u}'+2\mu_{,TT}\bar{u}''+\mu_{,T}\bar{u}''']\theta \\ &\quad +2(\mu_{,TT}\bar{u}'+\mu_{,T}\bar{u}'')\theta'+2\mu_{,T}\bar{u}'\theta'' \\ &\quad +\mu\psi''+2\mu_{,T}\psi'+(\mu_{,TT}-a^2\mu)\psi \\ &\quad +2a^2\mu_{,TT}\phi, \end{aligned} \tag{4.37}$$

$$iaRePr[(\bar{u}-c)\theta-\phi] = \theta''-a^2\theta. \tag{4.38}$$

We must now transfer the boundary conditions on u and v onto ϕ.

$$\begin{aligned} v|_{y=\pm1} &= 0, \\ \Longrightarrow \phi|_{y=\pm1} &= 0, \end{aligned}$$

$$\begin{aligned} u|_{y=\pm1} &= \mp\lambda_{\pm1}u_{,y}|_{y=\pm1}, \\ \Longrightarrow \phi'|_{y=\pm1} &= \mp\lambda_{\pm1}\phi''|_{y=\pm1}. \end{aligned}$$

We solve this eigenproblem in eigenfunction ϕ, eigenvalue σ, using the Chebyshev tau method. We suppose that ϕ, ψ and θ can be expressed as an infinite series in

Chebyshev polynomials

$$\phi(y) = \sum_{n=0}^{\infty} \phi_n T_n(y), \quad \psi = \sum_{n=0}^{\infty} \psi_n T_n(y), \quad \theta = \sum_{n=0}^{\infty} \theta_n T_n(y). \tag{4.39}$$

We then substitute these series into system (4.36)-(4.38), and then truncate them at the $n = N$th term, so that we approximate ϕ, ψ and θ with the functions

$$\Phi(y) = \sum_{n=0}^{N} \Phi_n T_n(y), \quad \Psi(y) = \sum_{n=0}^{N} \Psi_n T_n(y), \quad \Theta(y) = \sum_{n=0}^{N} \Theta_n T_n(y).$$

Then, allowing for the error in our truncation, we aim to solve

$$\begin{aligned}
L_1(\Phi,\Psi) &= \left(\frac{d^2}{dy^2} - a^2\right)\Phi - \Psi = \tau_1 T_{N-1} + \tau_2 T_N, \\
L_2(\Phi,\Psi,\Theta) &= -(iaRe\bar{u}'' + 2a^2\mu_{,T})\Phi + \left(iaRe\bar{u} - \mu_{,TT} + a^2\mu - \mu\frac{d^2}{dy^2} - 2\mu_{,T}\frac{d}{dy}\right)\Psi \\
&\quad - \left[(\mu_{,TTT} + a^2\mu_{,T})\bar{u}' + 2\mu_{,TT}\bar{u}'' + \mu_{,T}\bar{u}''' \right. \\
&\quad \left. + 2(\mu_{,TT}\bar{u}' + \mu_{,T}\bar{u}'')\frac{d}{dy} + 2\mu_{,T}\bar{u}'\frac{d^2}{dy^2}\right]\Theta \\
&\quad - ciaRe\Psi = \tau_3 T_{N-1} + \tau_4 T_n, \\
L_3(\Phi,\Theta) &= \left(iaRePr\bar{u} + a^2 - \frac{d^2}{dy^2}\right)\Theta - iaRePr\Phi - ciaRePr\Theta \\
&= \tau_5 T_{N-1} + \tau_6 T_N.
\end{aligned}$$

We follow the now familiar procedure of taking the inner product (A.1.4) of $< L_i, T_j >$, where $i = 1, 2, 3$ and $j = 0, ..., N-2$, to remove the τ coefficients, and leave us with $3N-3$ linear equations for the $3N+3$ unknowns $\Phi_0, ..., \Phi_N$, $\Psi_0, ..., \Psi_N$, $\Theta_0, ..., \Theta_N$. The remaining six equations needed to close the system are found from our boundary conditions.

Letting D and D^2 be the first and second order Chebyshev differentiation matrices, and M and $\bar{U}$ be the Chebyshev representation matrices for the viscosity function μ and steady-state solution $\bar{u}$ (with derivatives similarly defined), we have the system

$$(A_r + iA_i)\,\mathbf{x} = c\,(B_r + iB_i)\,\mathbf{x}, \tag{4.40}$$

where A_r, A_i, B_r and B_i are $(3N+3) \times (3N+3)$ square matrices, and $\mathbf{x} = (\Phi_0, ..., \Psi_0, ..., \Theta_0, ...)^T$. Introducing the notation

$$X_\alpha = \begin{pmatrix} X_{\alpha\,11} & X_{\alpha\,12} & X_{\alpha\,13} \\ X_{\alpha\,21} & X_{\alpha\,22} & X_{\alpha\,23} \\ X_{\alpha\,31} & X_{\alpha\,32} & X_{\alpha\,33} \end{pmatrix},$$

where each $X_{\alpha\ ij}$ is a $(N+1)\times(N+1)$ square block, then

$$
\begin{aligned}
A_{r\ 11} &= D^2 - a^2 I,\\
A_{r\ 12} &= -I,\\
A_{r\ 13} &= 0,\\
A_{r\ 21} &= -2a^2 M'',\\
A_{r\ 22} &= a^2 M - M'' - MD^2 - 2M'D,\\
A_{r\ 23} &= -M'''\bar{U}' - a^2 M'\bar{U}' - 2M''\bar{U}'' - M'\bar{U}''' - 2M''\bar{U}'D - 2M'\bar{U}''D - 2M'\bar{U}'D^2,\\
A_{r\ 31} &= A_{r\ 32} = 0,\\
A_{r\ 33} &= a^2 I - D^2.
\end{aligned}
$$

$$
\begin{aligned}
A_{i\ 11} &= A_{i\ 12} = A_{i\ 13} = 0,\\
A_{i\ 21} &= -aRe\bar{U}'',\\
A_{i\ 22} &= aRe\bar{U}',\\
A_{i\ 23} &= 0,\\
A_{i\ 31} &= A_{i\ 32} = 0,\\
A_{i\ 33} &= aRePr\bar{U}'.
\end{aligned}
$$

$$
B_{r\ ij} = 0.
$$

$$
\begin{aligned}
B_{i\ 11} &= B_{i\ 12} = B_{i\ 13} = 0,\\
B_{i\ 21} &= 0,\\
B_{i\ 22} &= aReI,\\
B_{i\ 23} &= 0,\\
B_{i\ 31} &= B_{i\ 32} = 0,\\
B_{i\ 33} &= aRePrI.
\end{aligned}
$$

The boundary conditions are overwritten as rows in the usual way, using the identities $T_n(\pm 1) = (\pm 1)^n$ and $T_n'(\pm 1) = n^2(\pm 1)^{n+1}$.

$$
\sum_{n=0}^{N}\Phi_n = 0, \quad \sum_{n=0}^{N}\left(n^2\Phi_n + \lambda_1\Psi_n\right) = 0, \quad \sum_{n=0}^{N}\Theta_n = 0,
$$

$$
\sum_{n=0}^{N}(-1)^n\Phi_n = 0, \quad \sum_{n=0}^{N}\left(n^2(-1)^{n+1}\Phi_n - \lambda_{-1}(-1)^n\Psi_n\right) = 0, \quad \sum_{n=0}^{N}(-1)^n\Theta_n = 0.
$$

Therefore, for a given wave number a, Reynolds number Re, slip length λ and viscosity parameter k, we solve (4.40) using NAG routine F02GJF to find the spectrum $\{c_1, c_2, c_3, ...\}$ ordered such that $\Im m\{c_i\} \geq \Im m\{c_{i+1}\}$. We proceed to iterate over the wave number and Reynolds number finding pairs (a, Re) such that $\Im m\{c_1\} = 0$ (i.e. the system is neutrally stable) until we find the minimum Reynolds number Re_L (at corresponding wave number a_L) such that we have instability for $Re > Re_L$. The iterative methods are as in Chapter two.

4.6 Results

As in Chapter 2, we note that the Prandtl number Pr, unlike the Reynolds number Re, is not a measure of the fluid flow and therefore we do not expect our results to be strongly dependent upon it. The nondimensionalization of Wall & Wilson [63] made use of the Peclét number $Pe = PrRe$, and their results were calculated with the value $Pe = 1.0$. Although stating that their results were found to be qualitatively similar when they used $Pe \neq 1.0$, fixing the Peclét number does not seem the best way to proceed. Rather, fluids tend to be classed by their Prandtl number, for instance some typical Prandtl numbers are

- around 0.015 for mercury,
- around 0.7 for air and many other gases,
- around 7.0 for water,
- between 100 and 40,000 for engine oil,
- around 7×10^{21} for the Earth's mantle.

Wall & Nagata [62] argued that in the case of vanishing Peclét number (and so $Pr = 0$ also), the exact form of the viscosity was irrelevant, only whether $\mu_{,T} > 0$ or $\mu_{,T} < 0$ impacted on the stability of the flow. Also, very small Prandtl numbers may be associated with fluids exhibiting boundary slip, for example rarefied gas. We therefore performed calculations with a very small Prandtl number $Pr = 0.1 \times 10^{-5}$, tracking the critical point (a_L, Re_L) as a function of our viscosity parameter k, for six

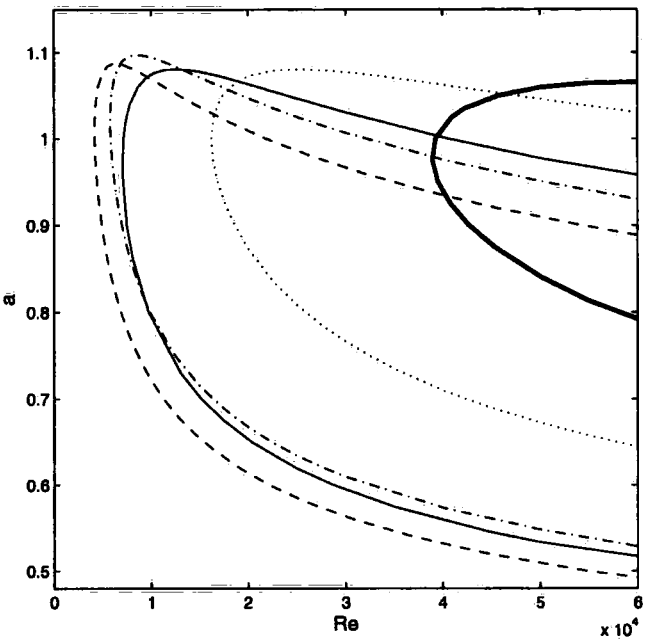

Figure 4.1: Neutral curves when $\lambda = 0$, and when: $k = -0.425$, '–'; $k = -0.2$, '- -'; $k = 0$, '–·'; $k = 0.5$, '··'; $k = 1.0$, '–' (dark).

different value of $\lambda \in [0, 0.05]$, see Figure 4.2. We remind the reader that for physical reasons we restrict $k > -\frac{1}{2}$, while in keeping $k < 1$ our viscosity $\mu(T) = 1 + kT$ might be considered a leading order approximation to an exponential dependence upon temperature.

The results show boundary slip to be stabilizing for all $k \in [-\frac{1}{2}, 1]$: holding k constant, increasing λ causes a corresponding increase in the critical Reynolds number Re_L. In this way we conclude that boundary slip is linearly stabilizing in the case of Poiseuille flow, even when the viscosity is allowed to vary with temperature. This increase in stability brought about by an increase in λ is observed to be greater for $k > 0$, i.e. when the viscosity function models a gas, than for $k < 0$, when $\mu(T)$ models a liquid, see Figure 4.2 (b). The effect of increasing λ on the neutral curves (for all k considered) was qualitatively similar to that shown in Figure 3.2.

For a fixed value of λ we see that increasing $k > 0$ always results in an increase in stability. For $k < 0$, increasing $|k|$ is seen to at first decrease Re_L to a minimum,

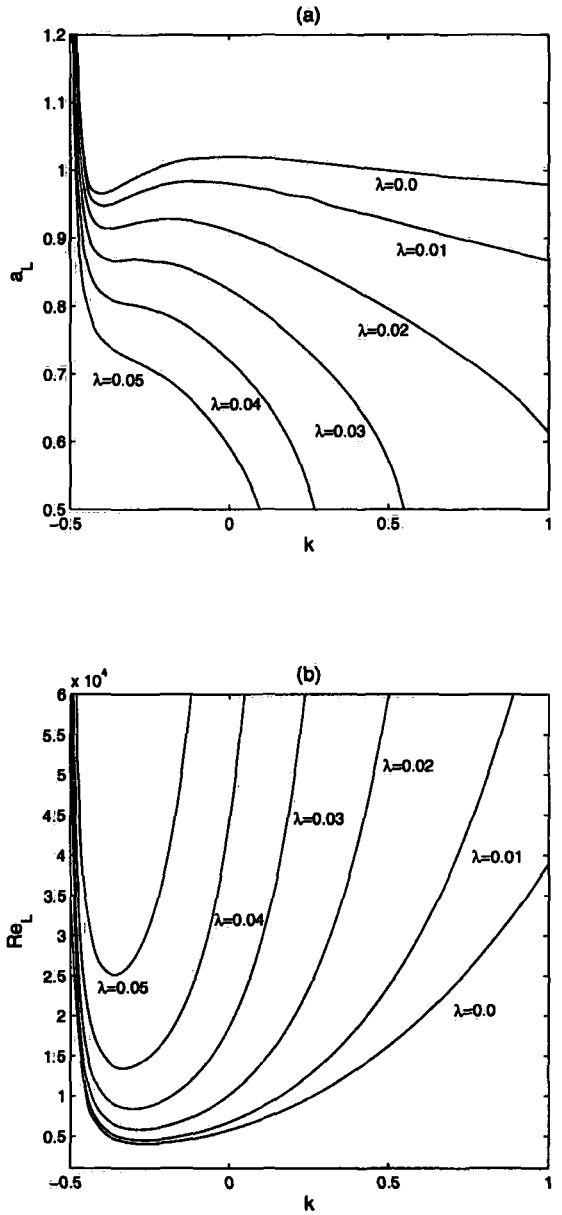

Figure 4.2: Variation of critical point (a_L, Re_L) with viscosity parameter k, for slip lengths in the range $\lambda \in [0, 0.05]$, and with $Pr = 0.1 \times 10^{-5}$.

before increasing Re_L explosively. Thus, there is global minimum critical Reynolds number of $Re_L \sim 4044$ below which the system is always linearly stable, at least for this viscosity model. When $k = 0$ we have $\mu \equiv 1$, and in this case the results for Re_L for each λ agree with the work of the previous chapter.

The explosive behaviour of Re_L (and a_L) in the limit $k \to -\frac{1}{2}$ is interesting. We note that in this limit

$$\lim_{k \to -\frac{1}{2}} \bar{u}(y) = \begin{cases} 4(1+\lambda+y) & \text{when } y \neq 1, \\ 0 & \text{when } y = 1, \end{cases} \tag{4.41}$$

and so the solution develops a discontinuity at $y = 1$, while in the region $y \in [-1, 1)$, $\bar{u}(y)$ is linear function of y, and so resembles the steady-state profile for Couette flow in the channel (see Chapter 1). Though the experiments of Reichardt [53] suggest instability of Couette flow around $Re \sim 750$, the flow has been shown to be linearly stable at all Reynolds numbers, see Romanov [55] and the book by Drazin and Reid for a discussion [18]. Therefore the rapid increase in stability of our system as $k \to -\frac{1}{2}$ is reasonable.

We repeated our calculations for different Prandtl numbers up to $Pr \sim O(10^0)$, and were able to verify that altering Prandtl was not observed to have any effect on the stability of the system. Not only were the results qualitatively the same as in Figure 4.2, but the actual values were in such close agreement as for any difference to be attributed to round off error from the difference in scaling.

Chapter 5

Thread-annular flow

The papers of Frei, Lüscher & Wintermantel [23] and Lüscher, Wintermantel & Annen [40] have succeeded in drawing attention back to an important problem from the field of hydrodynamic stability. Concerned with how to introduce a porous medium into a patient in a non-invasive way, Frei *et al* describe the modern technique of thread-injection, in which a hypodermic needle is connected to a syringe of fluid, which also contains a spool of surgical thread. One end of the thread is introduced into the needle, which in turn is inserted into the patient, see Figure 5.1.

A pressure gradient is applied by the syringe, and the thread is drawn through the needle with the fluid into the patient, the speed of the thread being controlled by a motor connected to the spool. In this way, a matrix of surgical thread approximating a porous mass builds up inside the patient. The thread-annular problem is the investigation into the stability of this type of fluid system, and is the motivation for this chapter.

Research into the thread-annular problem can be seen to have started with the work of Mott & Joseph [43], who presented a linear stability analysis for a viscous fluid flowing along a constant pressure gradient through a pipe with a solid core along its axis. Letting the pipe have inner radius R, the core have radius δ and setting $\eta = \delta/R$, Mott & Joseph investigated the instability of the system to axisymmetric perturbations, tracking the critical Reynolds number guaranteeing instability as a function of η. Their results showed the critical Reynolds number varying monoton-

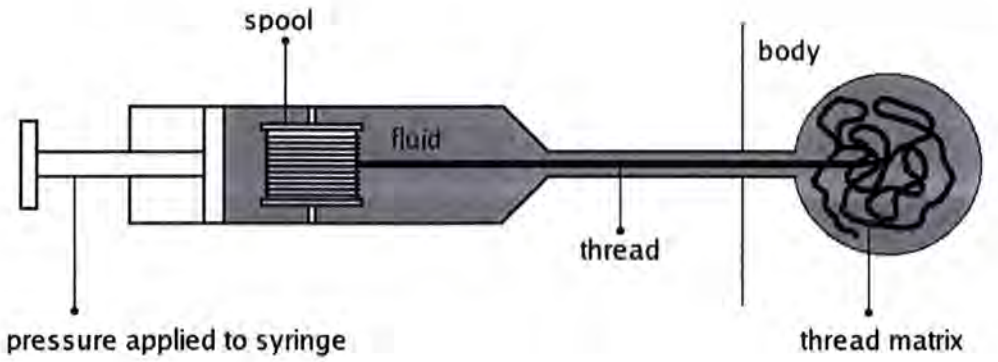

Figure 5.1: Diagram of thread-injection. A constant pressure gradient is applied to the fluid in the syringe, such that the thread is unspooled and drawn out into the body of the patient, to create a tangle of thread.

ically with η from a finite value at $\eta = 1$ (corresponding to Poiseuille flow in the plane), and approaching infinity as $\eta \to 0$ (corresponding to Hagen-Poiseuille pipe flow, see the book by Drazin & Reid for a discussion). This was verified later in the work of Strumolo [60].

More recent have been the contributions of Walton [64–66], whose model allows the inner cylinder to move axially with constant velocity $W \geq 0$ in the direction of the pressure gradient, and for algebraic neatness uses a different nondimensionalization to that of Mott & Joseph. Walton showed that multiple neutral curves can coexist when $W \neq 0$, making the problem of tracking the critical Reynolds number much more difficult.

We bring this model close to the problem considered by Frei *et al* [23] by including two further types of motion. The first, is we allow the solid core to rotate about the axis with constant angular frequency f. We show that this introduces another component into the steady-state solution, and that increasing the rate of rotation has a surprising, destabilizing effect on the stability of the system.

Finally, we introduce slip boundary conditions, which we allow since we consider our model to be valid on the interior of a hypodermic needle. Hypodermic needles

in common use can have inner diameters as small as 76.2×10^{-6} metres, and so we believe the thread-annular problem to have geometry on a scale such that boundary slip is an important part of the model.

5.1 The thread-annular model

Adopting the cylindrical polar coordinate system (r, θ, z), we consider a viscous, incompressible fluid on the annular domain $\Omega = \{(r, \theta, z) | r \in [\delta, R], \theta \in [0, 2\pi), z \in (-\infty, \infty)\}$ for lengths $0 \leq \delta \leq R$. At time $t \in [0, \infty)$ a fluid particle has velocity $\mathbf{u} = u(r, \theta, z; t)\hat{\mathbf{e}}_r + v(r, \theta, z; t)\hat{\mathbf{e}}_\theta + w(r, \theta, z; t)\hat{\mathbf{e}}_z$, which satisfies the Navier-Stokes equations on Ω,

$$u_{,t} + uu_{,r} + \frac{v}{r}u_{,\theta} + wu_{,z} - \frac{v^2}{r} = -\frac{1}{\rho}p_{,r} + \nu\left(u_{,rr} + \frac{1}{r}u_{,r} + \frac{1}{r^2}u_{,\theta\theta} + u_{,zz} - \frac{1}{r^2}u - \frac{2}{r^2}v_{,\theta}\right), \quad (5.1)$$

$$v_{,t} + uv_{,r} + \frac{v}{r}v_{,\theta} + wv_{,z} + \frac{uv}{r} = -\frac{1}{\rho r}p_{,\theta} + \nu\left(v_{,rr} + \frac{1}{r}v_{,r} + \frac{1}{r^2}v_{,\theta\theta} + v_{,zz} - \frac{1}{r^2}v + \frac{2}{r^2}u_{,\theta}\right), \quad (5.2)$$

$$w_{,t} + uw_{,r} + \frac{v}{r}w_{,\theta} + ww_{,z} = -\frac{1}{\rho}p_{,z} + \nu\left(w_{,rr} + \frac{1}{r}w_{,r} + \frac{1}{r^2}w_{,\theta\theta} + w_{,zz}\right), \quad (5.3)$$

$$u_{,r} + \frac{1}{r}u + \frac{1}{r}v_{,\theta} + w_{,z} = 0, \quad (5.4)$$

where $p(r, \theta, z; t)$ is the pressure field, and ρ and ν are the constant density and kinematic viscosity.

The thread-annular model is introduced through imposing appropriate conditions on the fluid at the surfaces $r = \delta$ and $r = R$. We suppose that the thread moves with constant velocity $W \geq 0$ along the z–axis, and rotates with constant angular frequency $f \geq 0$, such that points on the surface of the thread move with velocity $\delta f \hat{\mathbf{e}}_\theta + W\hat{\mathbf{e}}_z$. The surface $r = R$ is motionless.

We now need to prescribe our slip boundary conditions (1.3), (1.4) on the surfaces $\partial\Omega_\delta = \{(r, \theta, z) | r = \delta\}$ and $\partial\Omega_R = \{(r, \theta, z) | r = R\}$. In cylindrical polar coordinates the symmetric rate of strain tensor ϵ_{ij} is given by

$$\epsilon_{rr} = u_{,r}, \quad \epsilon_{\theta\theta} = \frac{1}{r}v_{,\theta} + \frac{1}{r}u, \quad \epsilon_{zz} = w_{,z},$$

$$\epsilon_{r\theta} = \frac{1}{2}\left(r\left(\frac{1}{r}v\right)_{,r} + \frac{1}{r}u_{,\theta}\right), \quad \epsilon_{\theta z} = \frac{1}{2}\left(\frac{1}{r}w_{,\theta} + v_{,z}\right), \quad \epsilon_{rz} = \frac{1}{2}\left(u_{,z} + w_{,r}\right).$$

Therefore, referring to the role of ϵ_{ij} in (1.3)-(1.4), our boundary conditions become

$$u|_{r=R} = 0, \quad v|_{r=R} = -\lambda_R\left(v_{,r} - \frac{1}{R}v\right)|_{r=R}, \quad w|_{r=R} = -\lambda_R w_{,r}|_{r=R}, \quad (5.5)$$

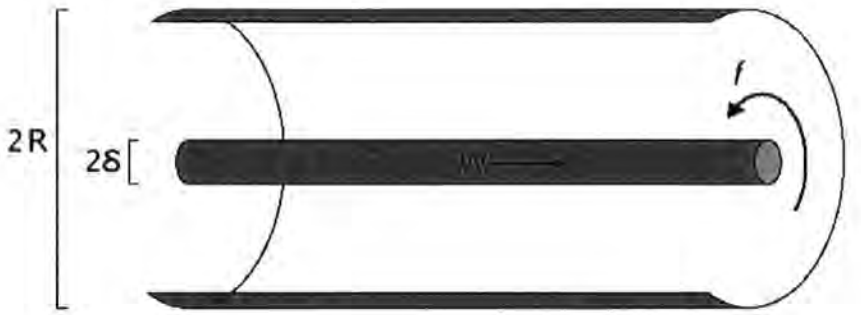

Figure 5.2: Diagram of thread of radius δ, centred within a hypodermic needle of radius R. The thread moves left to right with constant velocity $W \geq 0$, and rotates with angular frequency $f \geq 0$.

$$u|_{r=\delta} = 0, \quad v|_{r=\delta} = \lambda_\delta \left(v_{,r} - \frac{1}{\delta} v \right) |_{r=\delta} + \delta f, \quad w|_{r=\delta} = \lambda_\delta w_{,r}|_{r=\delta} + W. \tag{5.6}$$

We consider a time-independent solution of equations (5.1)-(5.4) where we assume the form

$$\bar{\mathbf{u}} = \bar{u}(r)\hat{\mathbf{e}}_r + \bar{v}(r)\hat{\mathbf{e}}_\theta + \bar{w}(r)\hat{\mathbf{e}}_z, \quad \bar{p} = \bar{p}(r, \theta, z), \quad \bar{p}_{,z} = -4g < 0,$$

arising from the shearing effect of the thread's motion, and the constant pressure gradient. In this way the flow may be regarded as being of combined Couette-Poiseuille type. Substituting these forms into equation (5.4) we obtain

$$\begin{aligned} \bar{u}' + \frac{1}{r}\bar{u} = 0 \Longrightarrow (r\bar{u})' &= 0, \\ \Longrightarrow \bar{u}(r) &= A/r, \end{aligned}$$

for some constant A, and where the prime denotes differentiation with respect to r. From the boundary conditions on u we see that $A = 0$, i.e. $\bar{u} \equiv 0$. We are left to

solve the system

$$-\frac{\bar{v}^2}{r} = -\frac{1}{\rho}\bar{p}_{,r}, \tag{5.7}$$

$$0 = -\frac{1}{\rho r}\bar{p}_{,\theta} + \nu\left(\bar{v}'' + \frac{1}{r}\bar{v}' - \frac{1}{r^2}\bar{v}\right), \tag{5.8}$$

$$0 = \frac{4g}{\rho} + \nu\left(\bar{w}'' + \frac{1}{r}\bar{w}'\right). \tag{5.9}$$

It is immediately clear that the $\bar{w}$ equation decouples, and so is easily solved,

$$\begin{aligned}
\bar{w}'' + \frac{1}{r}\bar{w}' = -\frac{4g}{\rho\nu} \Longrightarrow (r\bar{w}')' &= -\frac{4g}{\rho\nu}r, \\
\Longrightarrow \bar{w}' &= \frac{A}{r} - \frac{2g}{\rho\nu}r, \\
\Longrightarrow \bar{w}(r) &= B + A\ln r - \frac{g}{\rho\nu}r^2,
\end{aligned}$$

for constants A and B.

By differentiating equation (5.7) with respect to θ, we see that $\bar{p}_{,\theta} = h(z)$ only, for some function h. However, we have assumed the pressure's $z-$ dependence via the statement $\bar{p}_{,z} = -4g$, therefore $\bar{p}_{,\theta} = h$, constant. Finally, we see that we must impose $\bar{p}_{,\theta} = 0$, since $h \neq 0$ would result in the pressure varying as a saw-tooth wave, discontinuous at $\theta = 2\pi$. Therefore,

$$\begin{aligned}
\bar{v}'' + \frac{1}{r}\bar{v}' - \frac{1}{r^2}\bar{v} &= 0, \\
\Longrightarrow r\bar{s}'' + 3\bar{s}' &= 0, \quad \text{where we have let } \bar{v} = r\bar{s}, \\
\Longrightarrow \frac{\bar{s}''}{\bar{s}'} &= -\frac{3}{r}, \\
\Longrightarrow \ln\bar{s}' &= A - 3\ln r, \\
\Longrightarrow \bar{s}' &= \frac{A}{r^3} \quad \text{redefining } A, \\
\Longrightarrow \bar{s}(r) &= B - \frac{A}{r^2} \quad \text{again redefining } A, \\
\Longrightarrow \bar{v}(r) &= Br - \frac{A}{r}.
\end{aligned}$$

Reconciling the boundary conditions at $r = \delta$ and $r = R$, we obtain the dimensional

steady-state solution for the velocity

$$\bar{u}(r) = 0, \tag{5.10}$$

$$\bar{v}(r) = \frac{\delta^3 R^2 f}{R^3(\delta+2\lambda_\delta)-\delta^3(R-2\lambda_R)}\left[\left(\frac{2\lambda_R}{R}-1\right)\frac{r}{R}+\frac{R}{r}\right], \tag{5.11}$$

$$\begin{aligned}\bar{w}(r) = {} & \frac{\delta R}{R\lambda_\delta+\delta\lambda_R-\delta R\ln(\delta/R)}\left(\frac{g}{\rho\nu}\right)\left[R^2-\delta^2+2(R\lambda_R+\delta\lambda_\delta)-\frac{\rho\nu}{g}W\right]\ln r \\ & +\frac{\delta R}{R\lambda_\delta+\delta\lambda_R-\delta R\ln(\delta/R)}\left(\frac{g}{\rho\nu}\right)\left[\left(\frac{\lambda_\delta}{\delta}-\ln\delta\right)(R^2+2R\lambda_R)+\left(\frac{\lambda_R}{R}+\ln R\right)(\delta^2-2\delta\lambda_\delta)\right] \\ & +\frac{\delta R}{R\lambda_\delta+\delta\lambda_R-\delta R\ln(\delta/R)}\left(\frac{\lambda_R}{R}+\ln R\right)W-\frac{g}{\rho\nu}r^2.\end{aligned} \tag{5.12}$$

5.2 Instability equations

For algebraic neatness, we nondimensionalize using the scalings of Walton [64–66] rather than employing the scalings usual to the treatment of parallel flow problems. Denoting non-dimensional quantities by the '*' notation, the scalings we use are

$$r = Rr^*, \quad z = Rz^*, \quad \delta = R\delta^*, \quad \lambda_\delta = R\lambda_\delta^*, \quad \lambda_R = R\lambda_1^*, \quad t = \frac{\rho\nu}{gR}t^*,$$

$$\mathbf{u} = \frac{gR^2}{\rho\nu}\mathbf{u}^*, \quad f = \frac{gR}{\rho\nu}f^*, \quad W = \frac{gR^2}{\rho\nu}W^*, \quad p = \frac{g^2R^3}{\rho\nu^2}p^*, \quad Re = \frac{gR^3}{\rho\nu^2},$$

where Re is our Reynolds number.

Following non-dimensionalization and upon dropping the '*' notation, our equations of motion (5.1)-(5.3) become the familiar non-dimensional Navier-Stokes equations

$$u_{,t}+uu_{,r}+\frac{v}{r}u_{,\theta}+wu_{,z}-\frac{v^2}{r} = -p_{,r}+\frac{1}{Re}\left(u_{,rr}+\frac{1}{r}u_{,r}+\frac{1}{r^2}u_{,\theta\theta}+u_{,zz}-\frac{1}{r^2}u-\frac{2}{r^2}v_{,\theta}\right), \tag{5.13}$$

$$v_{,t}+uv_{,r}+\frac{v}{r}v_{,\theta}+wv_{,z}+\frac{uv}{r} = -\frac{1}{r}p_{,\theta}+\frac{1}{Re}\left(v_{,rr}+\frac{1}{r}v_{,r}+\frac{1}{r^2}v_{,\theta\theta}+v_{,zz}-\frac{1}{r^2}v+\frac{2}{r^2}u_{,\theta}\right), \tag{5.14}$$

$$w_{,t}+uw_{,r}+\frac{v}{r}w_{,\theta}+ww_{,z} = -p_{,z}+\frac{1}{Re}\left(w_{,rr}+\frac{1}{r}w_{,r}+\frac{1}{r^2}w_{,\theta\theta}+w_{,zz}\right), \tag{5.15}$$

$$u_{,r}+\frac{1}{r}u+\frac{1}{r}v_{,\theta}+w_{,z} = 0, \tag{5.16}$$

valid on the domain $\lambda = \{(r,\theta,z)|r \in [\delta,1], \theta \in [0,2\pi), z \in (-\infty,\infty)\}$. The steady-state solution satisfies

$$\bar{u}(r) = 0, \tag{5.17}$$

$$\bar{v}(r) = \frac{\delta^3 f}{\delta-\delta^3+2(\lambda_\delta+\delta^3\lambda_1)}\left[(2\lambda_1-1)r+\frac{1}{r}\right], \tag{5.18}$$

$$\bar{w}(r) = \frac{\delta}{\lambda_\delta+\delta\lambda_1-\delta\ln\delta}\left[1-\delta^2+2(\lambda_1+\delta\lambda_\delta)-W\right](\ln r-\lambda_1)+1+2\lambda_1-r^2. \tag{5.19}$$

Our aim is to investigate the instability of the steady-state $\bar{\mathbf{u}}, \bar{p}$ to three-dimensional disturbances $\mathbf{v}(r,\theta,z;t)$, $q(r,\theta,z;t)$. We begin by perturbing the steady-state $\bar{\mathbf{u}} \mapsto \bar{\mathbf{u}} + \mathbf{v}$, $\bar{p} \mapsto \bar{p} + q$, and substituting this perturbed form into equations (5.13)-(5.16). Upon removing terms nonlinear in $\mathbf{u}$, we obtain the linearized perturbation equations

$$u_{,t} + \frac{\bar{v}}{r}u_{,\theta} + \bar{w}u_{,z} - \frac{2\bar{v}}{r}v = -q_{,r} + \frac{1}{Re}\left(u_{,rr} + \frac{1}{r}u_{,r} + \frac{1}{r^2}u_{,\theta\theta} + u_{,zz} - \frac{1}{r^2}u - \frac{2}{r^2}v_{,\theta}\right), \quad (5.20)$$

$$v_{,t} + \left(\bar{v}' + \frac{\bar{v}}{r}\right)u + \frac{\bar{v}}{r}v_{,\theta} + \bar{w}v_{,z} = -\frac{1}{r}q_{,\theta} + \frac{1}{Re}\left(v_{,rr} + \frac{1}{r}v_{,r} + \frac{1}{r^2}v_{,\theta\theta} + v_{,zz} - \frac{1}{r^2}v + \frac{2}{r^2}u_{,\theta}\right), \quad (5.21)$$

$$w_{,t} + \bar{w}'u + \frac{\bar{v}}{r}w_{,\theta} + \bar{w}w_{,z} = -q_{,z} + \frac{1}{Re}\left(w_{,rr} + \frac{1}{r}w_{,r} + \frac{1}{r^2}w_{,\theta\theta} + w_{,zz}\right), \quad (5.22)$$

$$u_{,r} + \frac{1}{r}u + \frac{1}{r}v_{,\theta} + w_{,z} = 0, \quad (5.23)$$

where the components of $\mathbf{v}$ satisfy the boundary conditions

$$u|_{r=1} = 0, \quad v|_{r=1} + \lambda_1(v_{,r} - v)|_{r=1} = 0, \quad w|_{r=1} + \lambda_1 w_{,r}|_{r=1} = 0, \quad (5.24)$$

$$u|_{r=\delta} = 0, \quad v|_{r=\delta} - \lambda_\delta(v_{,r} - \frac{v}{\delta})|_{r=\delta} = 0, \quad w|_{r=1} - \lambda_\delta w_{,r}|_{r=1} = 0. \quad (5.25)$$

Rather than performing the instability analysis in the primitive variables (u,v,w,q), we employ an Orr-Sommerfeld technique. Although this sacrifices simplicity of coding and incurs the presence of spurious eigenvalues, the Orr-Sommerfeld approach has been seen to converge faster (see the work of Kerswell & Davey [37] on the similar problem of flow through an elliptical pipe) and spurious eigenvalues may easily be identified and filtered out of our algorithm.

We suppose that $u(r,\theta,z;t)$ may be expressed as an expansion of Fourier modes, specifically

$$u(r,\theta,z;t) = \sum_{m=0}^{\infty}\sum_{n=0}^{\infty} u_{nm}(r)\exp\{ia_m(z - c_m t)\}\exp\{in\theta\}, \quad (5.26)$$

with a similar expression for v and q, for positive wave numbers a_m and complex growth factors c_m. However, since unbounded growth of a single mode is sufficient for instability, we need only consider travelling wave solutions of the form

$$\mathbf{v} = \mathbf{v}(r)e^{ia(z-ct)}e^{in\theta}, \quad q = q(r)e^{ia(z-ct)}e^{in\theta}. \quad (5.27)$$

Substituting these into equations (5.20) to (5.23) and removing exponential parts

reveals

$$ia(\bar{w}-c)u+in\frac{\bar{v}}{r}u-2\frac{\bar{v}}{r}v = -q'+\frac{1}{Re}\left(u''+\frac{1}{r}u'-\left(\frac{n^2+1}{r^2}+a^2\right)u-2\frac{in}{r^2}v\right), \quad (5.28)$$

$$ia(\bar{w}-c)v+in\frac{\bar{v}}{r}v+\left(\bar{v}'+\frac{\bar{v}}{r}\right)u = -\frac{in}{r}q+\frac{1}{Re}\left(v''+\frac{1}{r}v'-\left(\frac{n^2+1}{r^2}+a^2\right)v+2\frac{in}{r^2}u\right), \quad (5.29)$$

$$ia(\bar{w}-c)w+\bar{w}'u+in\frac{\bar{v}}{r}w = -iaq+\frac{1}{Re}\left(w''+\frac{1}{r}w'-\left(\frac{n^2}{r^2}+a^2\right)w\right), \quad (5.30)$$

$$u'+\frac{1}{r}u+\frac{in}{r}v+iaw = 0. \quad (5.31)$$

5.3 Generalized Orr-Sommerfeld system

We remove the pressure terms by absorbing the $u_{,t}$ equation into the equations for $v_{,t}$ and $w_{,t}$, giving

$$ia(\bar{w}-c)\left(iav-\frac{in}{r}w\right)+\frac{in\bar{v}}{r}\left(iav-\frac{in}{r}w\right)+\left[ia\left(\bar{v}'+\frac{\bar{v}}{r}\right)-\frac{in\bar{w}'}{r}\right]u$$
$$=\frac{1}{Re}\left[\frac{d^2}{dr^2}+\frac{1}{r}\frac{d}{dr}-\left(\frac{1+n^2}{r^2}+a^2\right)\right]\left(iav-\frac{in}{r}w\right)+\frac{2in}{r^2Re}\left(iau-w'\right), \quad (5.32)$$

$$ia(\bar{w}-c)\left(\frac{in}{r}u-v'-\frac{1}{r}v\right)+\frac{in\bar{v}}{r}\left(\frac{in}{r}u-v'-\frac{1}{r}v\right)+ia\left(\bar{v}'+\frac{\bar{v}}{r}\right)w-ia\bar{w}'v$$
$$=\frac{1}{Re}\left[\frac{d^2}{dr^2}+\frac{1}{r}\frac{d}{dr}-\left(\frac{n^2}{r^2}+a^2\right)\right]\left(\frac{in}{r}u-v'-\frac{1}{r}v\right), \quad (5.33)$$

$$u'+\frac{1}{r}u+\frac{in}{r}v+iaw=0. \quad (5.34)$$

We then eliminate w using the continuity equation, and upon multiplying out the singularities we arrive at

$$\left[n(nr\bar{v}+ar^2\bar{w})\left(r\frac{d}{dr}+1\right)+a^2(r^4\bar{v}'+r^3\bar{v})-anr^3\bar{w}'\right]u$$
$$+\frac{1}{Re}\left[n^4-n^2+(2a^2n^2+a^2)r^2+a^4r^4-(a^2r^3-n^2r)\frac{d}{dr}-(a^2r^4+n^2r^2)\frac{d^2}{dr^2}\right]v$$
$$+\frac{in}{Re}\left[1-n^2-3a^2r^2-(a^2r^3+n^2r+r)\frac{d}{dr}+2r^2\frac{d^2}{dr^2}+r^3\frac{d^3}{dr^3}\right]u$$
$$+i(nr\bar{v}+ar^2\bar{w})(a^2r^2+n^2)v$$
$$=c\left[anr^2\left(r\frac{d}{dr}+1\right)u+iar^2(a^2r^2+n^2)v\right] \quad (5.35)$$

$$\left[n(nr\bar{v}+ar^2\bar{w})+(r^2\bar{v}'+r\bar{v})\left(r\frac{d}{dr}+1\right)\right]u$$
$$+\frac{1}{Re}\left[n^2-1+a^2r^2+(n^2r+a^2r^3+r)\frac{d}{dr}-2r^2\frac{d^2}{dr^2}-r^3\frac{d^3}{dr^3}\right]v$$
$$+\frac{in}{Re}\left[1-n^2-a^2r^2-r\frac{d}{dr}+r^2\frac{d^2}{dr^2}\right]u+i\left[n(r^2\bar{v}'+r\bar{v})+ar^3\bar{w}'+(nr\bar{v}+ar^2\bar{w})\left(r\frac{d}{dr}+1\right)\right]v$$
$$=c\left[anr^2u+iar^2\left(r\frac{d}{dr}+1\right)v\right] \quad (5.36)$$

subject to the boundary conditions

$$u = 0, \quad (\lambda_1 + 1)u' + \lambda_1 u'' = 0, \quad (\lambda_1 - 1)v - \lambda_1 v' = 0 \quad \text{at } r = 1, \tag{5.37}$$

$$u = 0, \quad (\lambda_\delta - \delta)u' + \lambda_\delta \delta u'' = 0, \quad (\lambda_\delta + \delta)v - \lambda_\delta \delta v' = 0 \quad \text{at } r = \delta. \tag{5.38}$$

To implement the Chebyshev tau method we must first transform our variable from $r \in [\delta, 1]$ to $x \in [-1, 1]$ via

$$x = \frac{2r - (1+\delta)}{1-\delta},$$

and so we now consider the functions u, v, $\bar{v}$ and $\bar{w}$ to be functions of x, and for convenience we define the functions f_1 and f_2 by

$$f_1(x) = nr(x)\bar{v}(x) + ar^2(x)\bar{w}(x), \quad f_2 = \frac{2}{1-\delta} r^2(x)\bar{v}(x)' + r(x)\bar{v}(x) \tag{5.39}$$

where $r(x) = [(1-\delta)x + 1 + \delta]/2$.

As usual, we suppose that u and v have the Chebyshev expansions $u(x) = \sum_{n=0}^{\infty} u_n T_n(x)$ and $v(x) = \sum_{n=0}^{\infty} v_n T_n(x)$, which we then truncate at the $n = N$th term so that we approximate u and v by $U(x) = \sum_{n=0}^{N} U_n T_n(x)$ and $V(x) = \sum_{n=0}^{N} V_n T_n(x)$. We then substitute U and V for u and v in equations (5.35) and (5.36) so that we are left to solve

$$\begin{aligned} L_1(U,V) = &\left[nf_1\left(r\left(\frac{2}{1-\delta}\right)\frac{d}{dx} + 1\right) + a^2r^2f_2 - \left(\frac{2}{1-\delta}\right)anr^3\bar{w}'\right]U \\ &+\frac{1}{Re}\left[n^4 - n^2 + (2a^2n^2 + a^2)r^2 + a^4r^4 - (a^2r^3 - n^2r)\left(\frac{2}{1-\delta}\right)\frac{d}{dx} - (a^2r^4 + n^2r^2)\left(\frac{2}{1-\delta}\right)^2\frac{d^2}{dx^2}\right]V \\ &+\frac{in}{Re}\left[1 - n^2 - 3a^2r^2 - (a^2r^3 + n^2r + r)\left(\frac{2}{1-\delta}\right)\frac{d}{dx} + 2r^2\left(\frac{2}{1-\delta}\right)^2\frac{d^2}{dx^2} + r^3\left(\frac{2}{1-\delta}\right)^3\frac{d^3}{dx^3}\right]U \\ &+if_1(a^2r^2 + n^2)V - c\left[anr^2\left(r\left(\frac{2}{1-\delta}\right)\frac{d}{dx} + 1\right)U + iar^2(a^2r^2 + n^2)V\right] \\ &= \tau_1 T_{N-2} + \tau_2 T_{N-1} + \tau_3 T_N, \end{aligned} \tag{5.40}$$

$$\begin{aligned} L_2(U,V) = &\left[nf_1 + f_2\left(r\left(\frac{2}{1-\delta}\right)\frac{d}{dx} + 1\right)\right]U \\ &+\frac{1}{Re}\left[n^2 - 1 + a^2r^2 + (n^2r + a^2r^3 + r)\left(\frac{2}{1-\delta}\right)\frac{d}{dx} - 2r^2\left(\frac{2}{1-\delta}\right)^2\frac{d^2}{dx^2} - r^3\left(\frac{2}{1-\delta}\right)^3\frac{d^3}{dx^3}\right]V \\ &+\frac{in}{Re}\left[1 - n^2 - a^2r^2 - r\left(\frac{2}{1-\delta}\right)\frac{d}{dx} + r^2\left(\frac{2}{1-\delta}\right)^2\frac{d^2}{dx^2}\right]U + i\left[nf_2 + \left(\frac{2}{1-\delta}\right)ar^3\bar{w}' + f_1\left(r\left(\frac{2}{1-\delta}\right)\frac{d}{dx} + 1\right)\right]V \\ &-c\left[anr^2U + iar^2\left(r\left(\frac{2}{1-\delta}\right)\frac{d}{dx} + 1\right)V\right] \\ &= \tau_4 T_{N-2} + \tau_5 T_{N-1} + \tau_6 T_N, \end{aligned} \tag{5.41}$$

and r is understood to be a function of $x \in [-1, 1]$.

We take the Chebyshev innerproducts $< L_i, T_j >$ for $i = 1, 2$ and $j = 0, 1, 2, ..., N-3$ to obtain $2N - 4$ equations in the $2N + 2$ unknowns U_k and V_k. The system is

closed with the six boundary conditions

$$U = 0, \quad (1-\delta)(\lambda_1+1)U'+2\lambda_1 U'' = 0, \quad (1-\delta)(\lambda_1-1)V-2\lambda_1 V' = 0 \quad \text{at } x = 1, \tag{5.42}$$

$$U = 0, \quad (1-\delta)(\lambda_\delta-\delta)U'+2\lambda_\delta\delta U'' = 0, \quad (1-\delta)(\lambda_\delta+\delta)V-2\lambda_\delta\delta V' = 0 \quad \text{at } x = -1. \tag{5.43}$$

Noting that $T_n(\pm1) = (\pm1)^n$, $T_n'(\pm1) = n^2(\pm1)^{n+1}$ and $T_n''(\pm1) = \frac{1}{3}(n^4-n^2)(\pm1)^n$, these boundary conditions become the equations

$$\sum_{n=0}^{N} U_n = 0, \tag{5.44}$$

$$(1-\delta)(\lambda_1+1)\sum_{n=0}^{N} n^2 U_n + 2\lambda_1\frac{1}{3}\sum_{n=0}^{N}(n^4-n^2)U_n = 0, \tag{5.45}$$

$$(1-\delta)(\lambda_1-1)\sum_{n=0}^{N} V_n - 2\lambda_1\sum_{n=0}^{N} n^2 V_n = 0, \tag{5.46}$$

$$\sum_{n=0}^{N}(-1)^n U_n = 0, \tag{5.47}$$

$$(1-\delta)(\lambda_\delta-\delta)\sum_{n=0}^{N} n^2(-1)^{n+1}U_n + 2\lambda_\delta\delta\frac{1}{3}\sum_{n=0}^{N}(n^4-n^2)(-1)^n U_n = 0, \tag{5.48}$$

$$(1-\delta)(\lambda_\delta+\delta)\sum_{n=0}^{N}(-1)^n V_n - 2\lambda_\delta\delta\sum_{n=0}^{N} n^2(-1)^{n+1}V_n = 0. \tag{5.49}$$

Once more we arrive at a generalized eigenvalue problem $(A_r + iA_i)\mathbf{x} = c(B_r + iB_i)\mathbf{x}$, where $\mathbf{x} = (U_0, .., U_N, V_0, ..., V_N)^T$, which we solve using NAG routine F02GJF. For fixed values of n, δ, f, λ, and W we vary wave number a and Reynolds number Re to find pairs (a, Re) such that the imaginary part of the leading eigenvalue is zero (and thus we have neutral stability), before iterating over the wave number to find the minimum Reynolds number Re_L below which the system is linearly stable. The iteration methods are as in Chapter two.

5.4 Results

5.4.1 Variation of Re_L with aspect ratio

With such a large parameter space (δ, f, λ, W), and for each of these the possibility of performing calculations for many values of n (where, we remind the reader, n

determines the periodicity of the θ–dependence of the perturbations via $e^{in\theta}$), we choose to investigate the effects of each of f, λ and W in isolation of each other, in each case for at least the two values $\delta = 0.4$ and $\delta = 0.7$. The reasons for these specific values of δ will be made clear in our results.

We begin, though, by setting $f = \lambda = W = 0$, and calculate the critical Reynolds number Re_L as a function of the aspect ratio δ, the results of which are in Figure 5.3. The $n = 0$ curve agrees with the axisymmetric results of Walton [65] whose nondimensionalization we share, and we remind the reader that this is not the nondimensionalization employed by Mott & Joseph. [43], who found a monotonic relation between aspect ratio and the critic Reynolds number under their definition. However, we also performed calculations to thoroughly investigate Re_L as a function of δ for the asymmetric cases of $n > 0$.

For all aspect ratios in the range $0.1 < \delta < 0.9$ we found the critical Reynolds number to be the minimum point of a unique neutral curve, qualitatively similar to that for plane Poiseuille flow, see the illustrations in Drazin & Reid [18] and Walton [65]. We find that axisymmetric perturbations appear to dominate only as δ approaches 1, i.e. as we tend towards Poiseuille flow in the plane, while the $n = 4$ and $n = 5$ perturbations never dominate, see Table 5.1. The wave number a_L at which the critical Reynolds number Re_L occurs is seen to decrease as n increments, and to increase as $\delta \to 1$, see Figure 5.3. There also appears to be convergence of the a_L for each n in this limit.

The behaviour of Re_L at $\delta = 0$ and $\delta = 1$ is unclear, owing to lack of convergence of the numerical method at high Reynolds numbers. For the same reason, instability could not be found for $n \geq 6$.

5.4.2 The stabilizing effect of thread velocity W

We now investigate the effect of W, setting $f = \lambda = 0$. The most relevant work on this problem is that of Walton [66] who performed calculations for the two cases $\delta = 0.4$ and $\delta = 0.55$, for disturbances with periodicities $n = 1, 2$. In obtaining our results on the effect of varying δ (above) we can corroborate Walton's assertion that in the case $W = 0$ (while $f = 0$) the neutral curve is always unique.

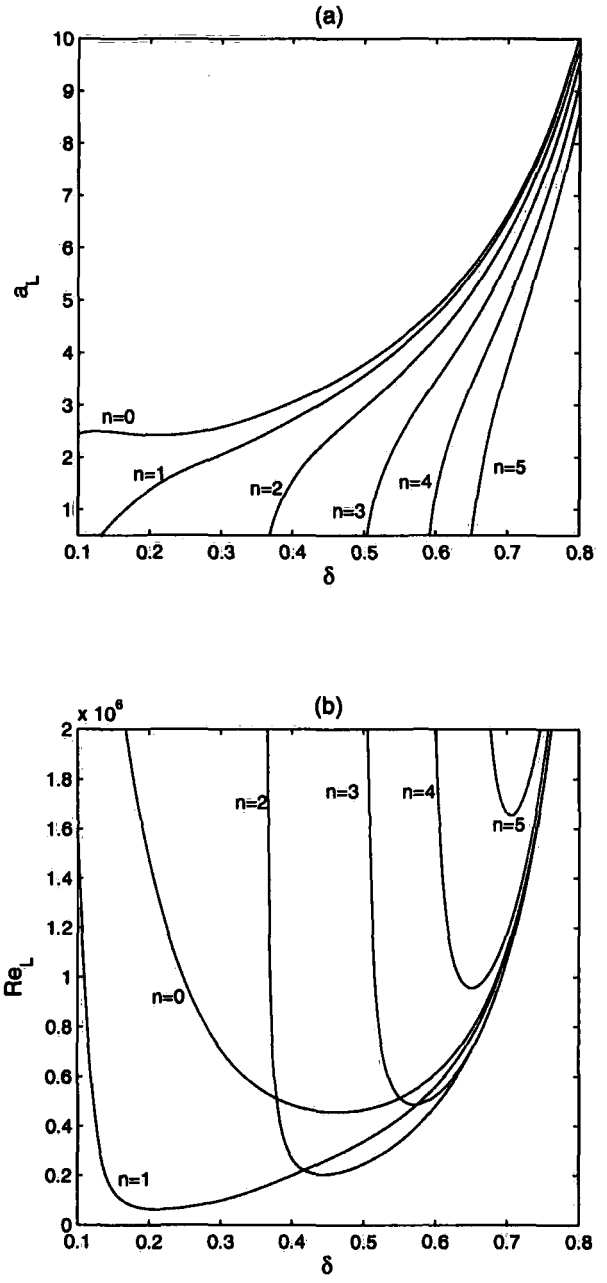

Figure 5.3: Effect on location of critical point (a_L, Re_L) of varying aspect ratio δ, for $n = 0, 1, 2, 3, 4, 5$.

Aspect ratio	Periodicity of critical mode
$0.100 < \delta < 0.419$	$n = 1$
$0.419 < \delta < 0.665$	$n = 2$
$0.665 < \delta < 0.701$	$n = 3$
$0.701 < \delta < 0.758$	$n = 2$
$0.758 < \delta < 0.762$	$n = 1$
$0.762 < \delta < 0.800$	$n = 0$

Table 5.1: The changing periodicity of the least stable mode, for aspect ratios in the range $0.1 < \delta < 0.8$.

For the axisymmetric case ($n = 0$) and $\delta = 0.55$, Walton found that for $W > 0$ a stable intrusion appears in the neutral curve, from the direction of increasing Reynolds number, which grew as W was increased until the neutral curve was split into two separate curves. The 'upper' curve (in the domain of higher wave numbers) was observed to close up at finite W, whilst the lower curve retreated to infinity, such that ultimately the system became linearly stable to axisymmetric perturbations. He did not find this behaviour when $\delta = 0.4$. Instead he reports of a unique neutral curve which closes with increasing W.

We now refer the reader to Figure 5.4 where we present our calculations for an aspect ratio of $\delta = 0.4$. In Figure 5.4 (b) we see that a stable intrusion does in fact appear, splitting the curve from the direction of higher Reynolds numbers. By Figure 5.4 (d), the intrusion has split the neutral curve in two. The new curve closes up at finite W, while the remaining curve closes at a higher thread velocity (see Figure 5.4 (f)). It is likely that this behaviour was missed owing to the relatively small scale of the new neutral curve, and the small thread velocities ($W \sim O(10^{-3})$) at which the stable intrusion appears.

We observed similar behaviour in the axisymmetric case, when $\delta = 0.7$, see Figure 5.7. However, for this aspect ratio the division of the neutral curve is seen to be much more equal, and it is the upper curve that closes first, the lower curve persisting for high values of Re.

Thread velocity	Periodicity of critical mode
$0.0 < W < 0.9 \times 10^{-5}$	$n = 3$
$0.9 \times 10^{-5} < W < 0.147 \times 10^{-2}$	$n = 2$
$0.147 \times 10^{-2} < W < 0.328 \times 10^{-2}$	$n = 1$
$0.328 \times 10^{-2} < W < 0.889 \times 10^{-2}$	$n = 2$
$0.889 \times 10^{-2} < W < 0.03$	$n = 1$

Table 5.2: The changing periodicity of the least stable mode when $\delta = 0.7$ and $f = \lambda = 0$, in the range $0 < W < 0.03$.

Walton [66] also performed computations for the cases $\delta = 0.4$, $n = 1, 2$. He reported that for both types of θ–dependent perturbation, the neutral curve was seen to be unique. However, for $n = 1$ the results of our computations again show the process of stable intrusion followed by curve splitting for, see Figure 5.5.

Our results for $n = 2$ are shown in Figure 5.6. For this value of n we were unable to find splitting of the neutral curve. However, we note that the scale of the neutral curve is very different from the $n < 2$ cases, existing over an especially narrow interval of wave numbers. This makes the presence of a stable intrusion easy to miss in our algorithm. Also, the neutral curve is observed to retreat rapidly in the direction of high Reynolds numbers. Therefore, curve splitting may occur at high Re, outside the range of the numerical method.

When curve splitting was observed, the critical Reynolds number was found to belong to the larger, easier to detect of the two resulting curves. Therefore, our numerical results would indicate that new, smaller curves resulting from stable intrusion exist in the region of higher Reynolds numbers, and so do not affect the system's transition to instability. Based on this, we present what we believe to be the critical Reynolds number at $\delta = 0.4$ and $\delta = 0.7$ in Figure 5.11.

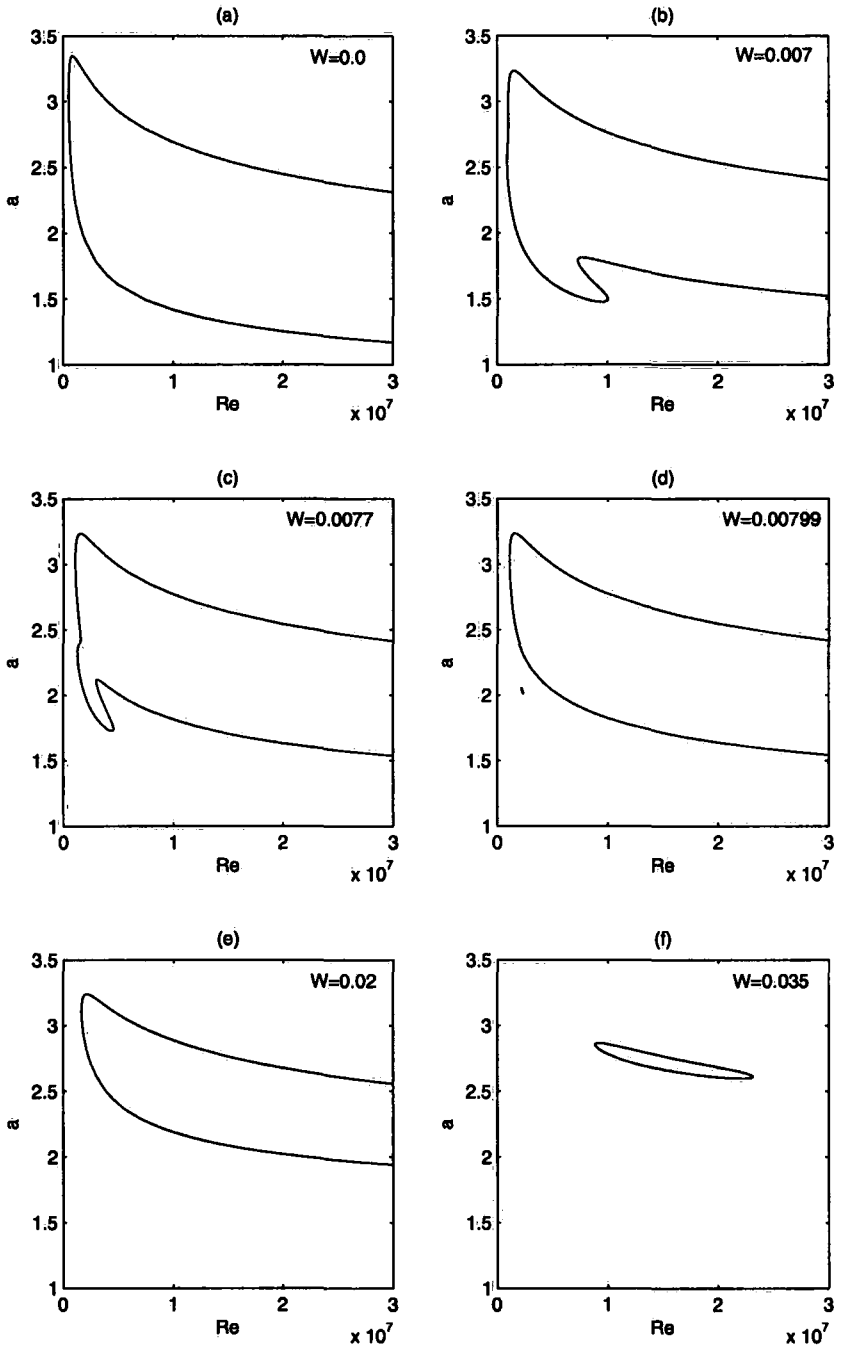

Figure 5.4: Neutral curves for $n = 0$ (i.e. axisymmetric) perturbations with aspect ratio $\delta = 0.4$, and: (a) $W = 0.0$; (b) $W = 0.007$; (c) $W = 0.0077$; (d) $W = 0.00799$; (e) $W = 0.02$; (f) $W = 0.035$.

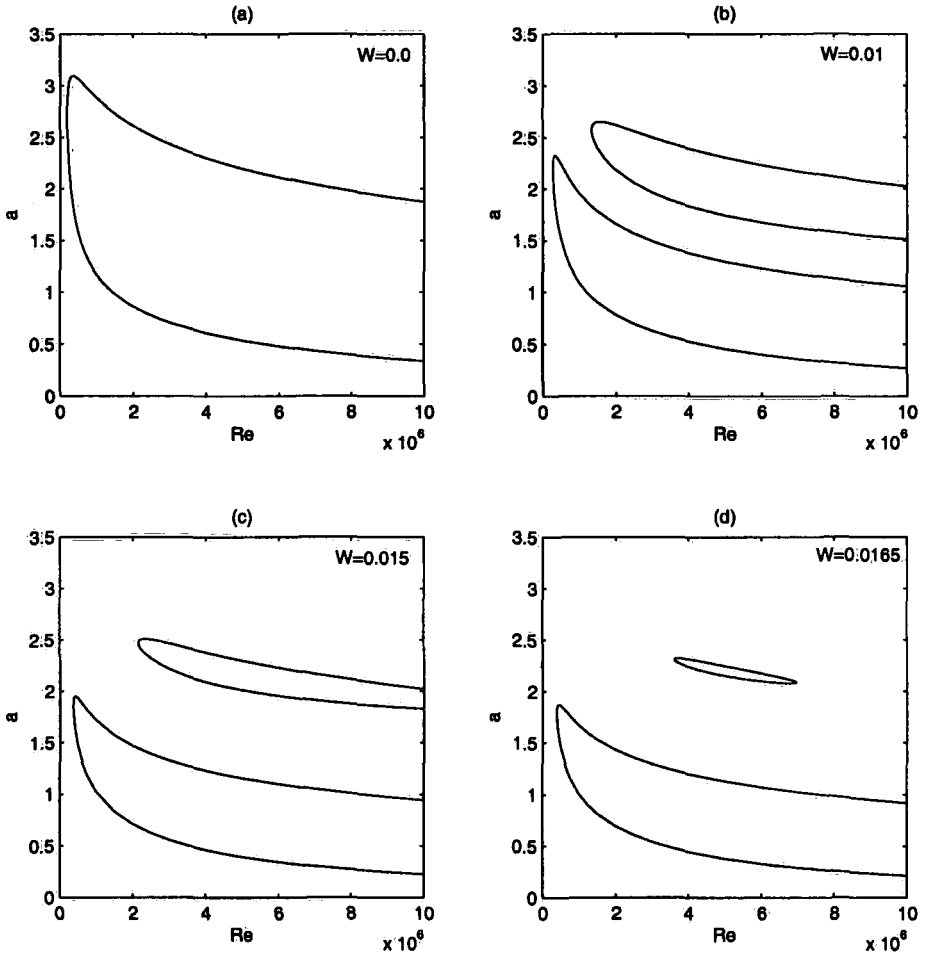

Figure 5.5: Neutral curves for $n = 1$ perturbations with aspect ratio $\delta = 0.4$, and: (a) $W = 0.0$; (b) $W = 0.01$; (c) $W = 0.015$; (d) $W = 0.0165$.

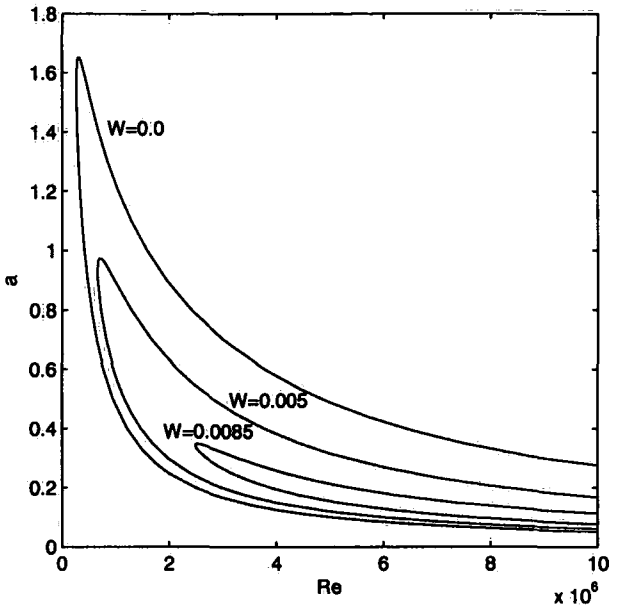

Figure 5.6: Neutral curves for $n = 2$ perturbations with aspect ratio $\delta = 0.4$, and (outer to inner): $W = 0.0$; $W = 0.005$; $W = 0.0085$.

5.4.3 The stabilizing influence of boundary slip

The linear analyses of Spille *et al* [57], Lauga & Cossu [38] and the linear and non-linear analyses of Webber & Straughan [68] (see Chapter 3) have shown boundary slip to have a stabilizing effect on Poiseuille flow in the plane. That is, Re_L becomes higher with increasing slip length λ. Our results for the thread-annular case support the assertion that boundary slip is stabilizing in the case of parallel flows.

Setting $W = f = 0$ we find that the neutral curve is unique, and resembles the classic neutral curve for Poiseuille flow in the plane, as was the case for channel flow. As we increase λ, the critical Reynolds number increases, and the wave number at which Re_L occurs decreases. However, in Figure 5.12 (b) we obeserve the neutral curve to close up for $\lambda \leq 0.011$. Though we did not observe this for other values of n and δ, it implies that at finite λ the system becomes linearly stable to at least some types of perturbation.

Figure 5.14 shows the variation of Re_L with λ, for various values of n and δ.

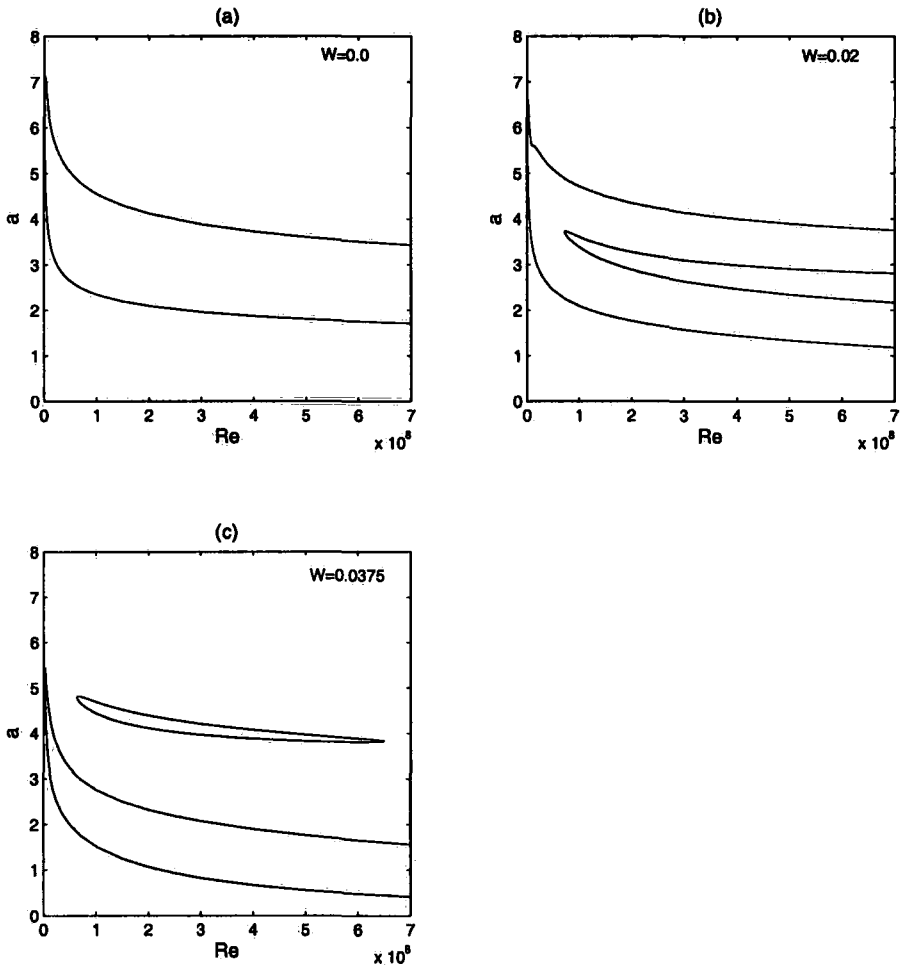

Figure 5.7: Neutral curves for $n = 0$ perturbations with aspect ratio $\delta = 0.7$, and: (a) $W = 0$; (b) $W = 0.002$; (c) $W = 0.0075$.

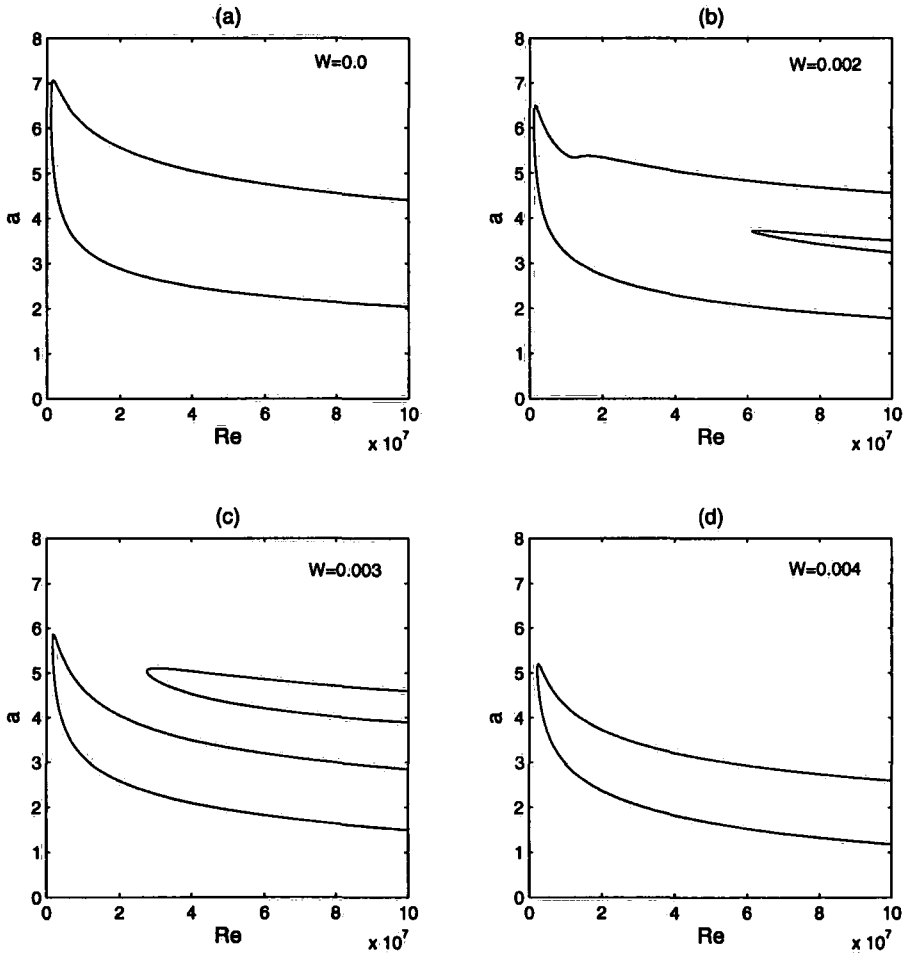

Figure 5.8: Neutral curves for $n = 1$ perturbations with aspect ratio $\delta = 0.7$, and: (a) $W = 0$; (b) $W = 0.002$; (c) $W = 0.003$; (d) $W = 0.004$.

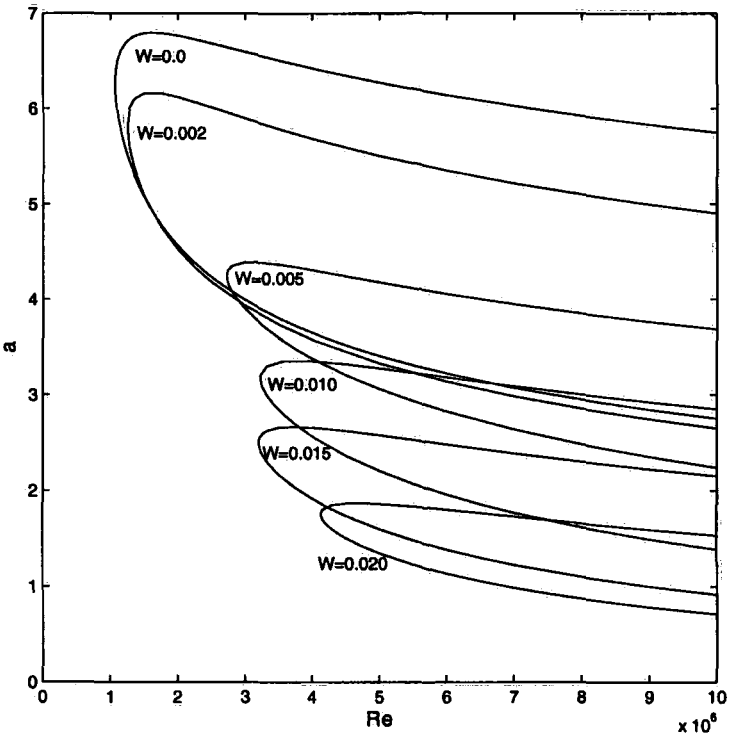

Figure 5.9: Neutral curves for $n = 2$ perturbations with aspect ratio $\delta = 0.7$, and $W = 0$, $W = 0.002$, $W = 0.005$, $W = 0.010$, $W = 0.015$, and $W = 0.020$ (descending).

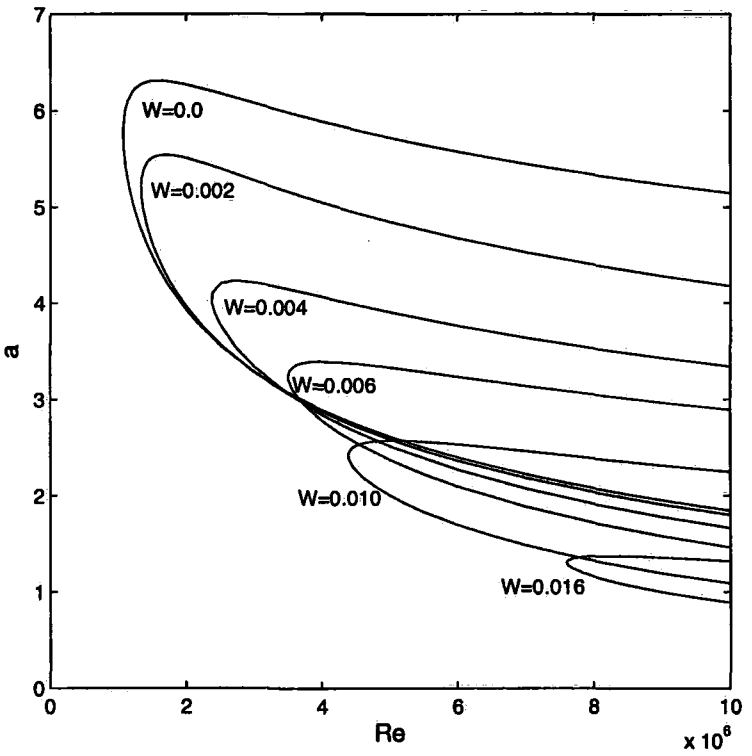

Figure 5.10: Neutral curves for $n = 3$ perturbations with aspect ratio $\delta = 0.7$, and $W = 0$, $W = 0.002$, $W = 0.004$, $W = 0.006$, $W = 0.010$, and $W = 0.016$ (descending).

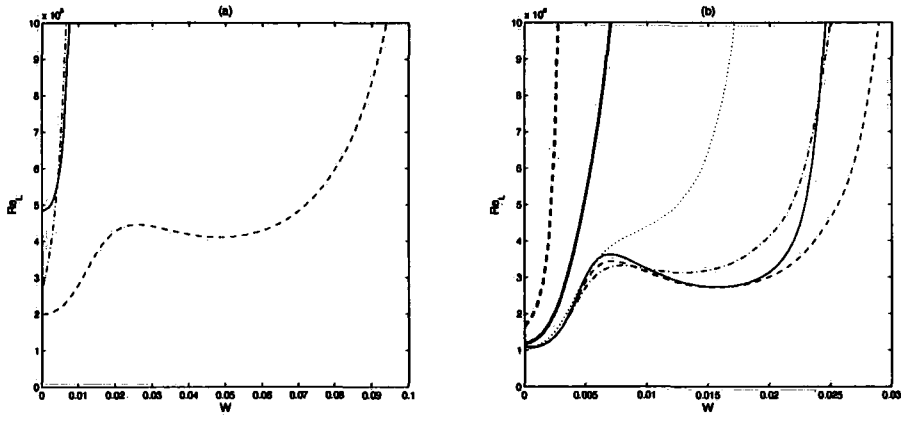

Figure 5.11: Critical Reynolds number Re_L as a function of thread velocity W, for: (a) $\delta = 0.4$; (b) $\delta = 0.7$. Perturbations are of periodicity: $n = 0$, —; $n = 1$, - - - ; $n = 2$, — · —; $n = 3$, · · ·; $n = 4$, dark —; $n = 5$, dark - - - .

The slip length is seen to influence the ordering of the second and third least stable perturbations: in the $\delta = 0.4$ case, the second least stable disturbance is seen to switch from being the $n = 2$ mode to the axisymmetric mode at $\lambda \sim 0.0035$. A similar reordering is seen when $\delta = 0.6$ around $\lambda \sim 0.0038$.

5.4.4 The destabilizing effect of rotation

Finally, we set $W = \lambda = 0$ and investigate the effect of allowing the thread to rotate. We remind the reader of the role of f in the boundary conditions (5.6): f is the angular frequency with which our thread of radius δ spins around the $z-$axis, such that points on the thread surface have velocity $\delta f \hat{\mathbf{e}}_\theta$ (when $W = 0$), and we showed that $f > 0$ introduced a new component into the steady-state flow.

For both $\delta = 0.4$ and $\delta = 0.7$, our results for axisymmetric perturbations showed the neutral curve to be unique. Increasing f had the effect of slowly decreasing the value of Re_L, so that rotation was seen to be destabilizing, see Figure 5.15. However, this was not true in the case of asymmetric perturbations.

For an aspect ratio $\delta = 0.7$ and asymmetric perturbations $n = 1, 2, 3$, increasing f caused a stable intrusion to appear, splitting the neutral curve into two separate

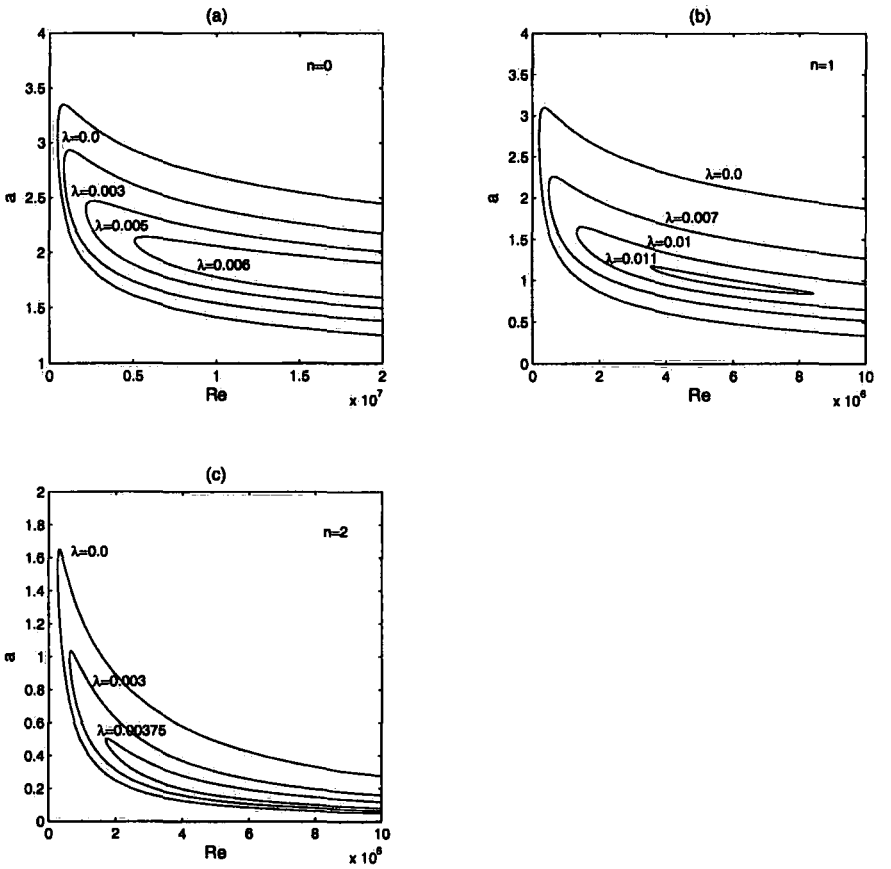

Figure 5.12: Effect of increasing slip length λ on neutral curves when $\delta = 0.4$, and: (a) $n = 0$; (b) $n = 1$; (c) $n = 2$.

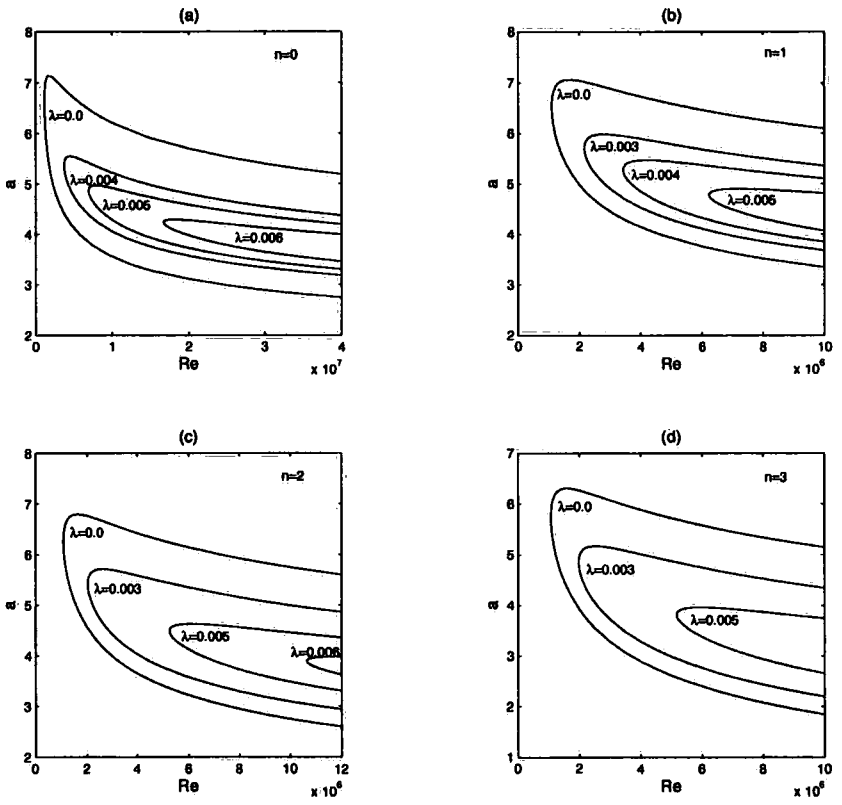

Figure 5.13: Effect of increasing slip length λ on neutral curves when $\delta = 0.7$, and: (a) $n = 0$; (b) $n = 1$; (c) $n = 2$; (d) $n = 3$.

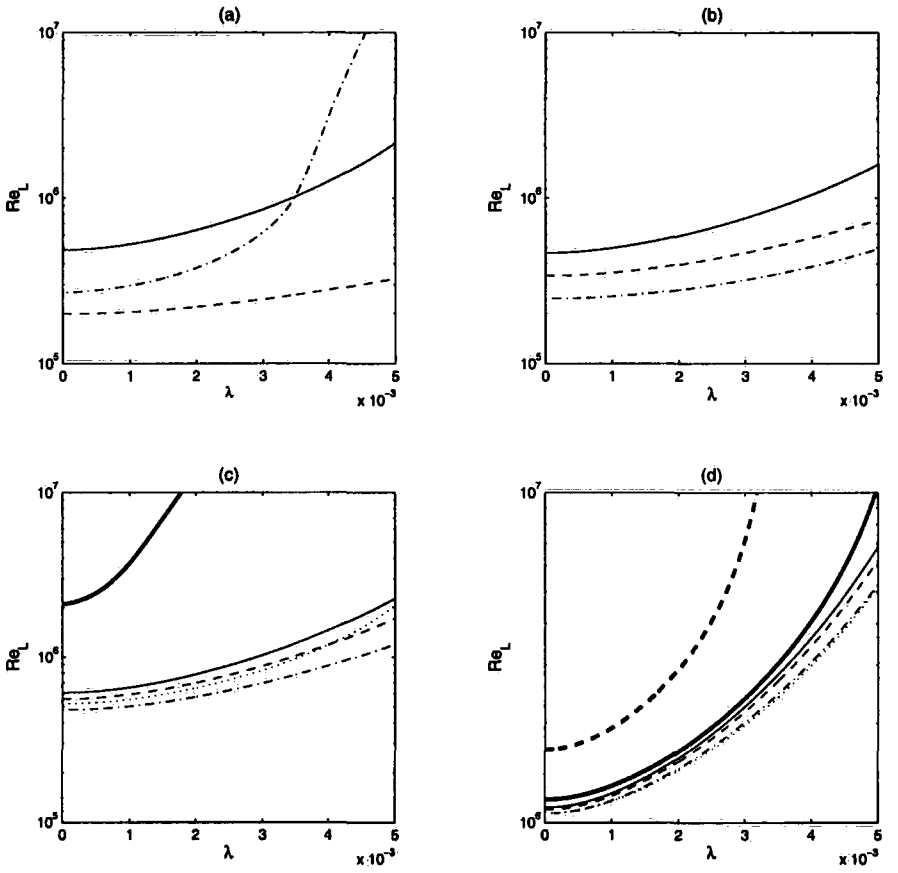

Figure 5.14: Critical Reynolds number Re_L as a function of slip length λ, for: (a) $\delta = 0.4$; (b) $\delta = 0.5$; (c) $\delta = 0.6$; (d) $\delta = 0.7$. Perturbations are of periodicity: $n = 0$, –; $n = 1$, - -; $n = 2$, -·; $n = 3$, ···; $n = 4$, dark –; $n = 5$, dark - -.

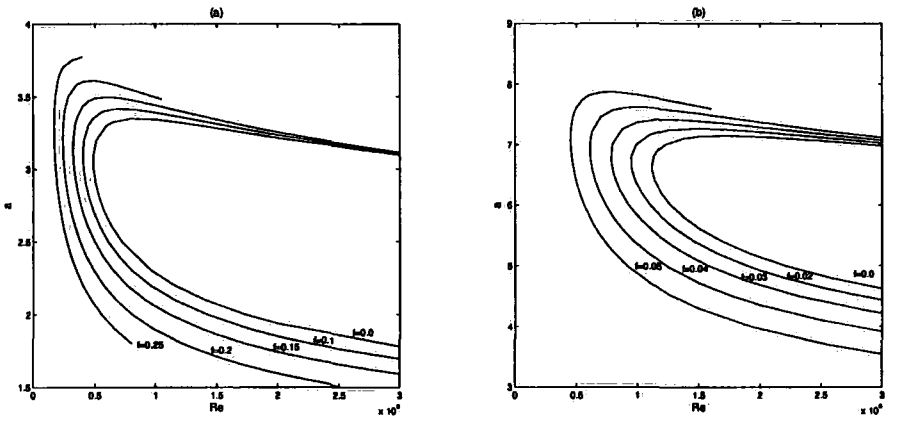

Figure 5.15: Neutral curves for axisymmetric ($n = 0$) perturbations when: (a) $\delta = 0.4$, and $0.0 < f < 0.25$; (b) $\delta = 0.7$, and $0.0 < f < 0.05$.

neutral curves. The minimum Reynolds number of the two curves was tracked and shown to increase with f, stabilizing the flow.

However, when $f > 0$ a new, separate neutral curve appears in the region of very small wave numbers. We can see in Figure 5.18 that as f increases this neutral curve creeps from right to left, until eventually it contains the critical Reynolds number. From this point on, Re_L is a decreasing function of f. This behaviour was also seen $\delta = 0.4$ for $n = 1$ perturbations.

For other combinations of aspect ratio and $n > 0$, we observed this new, destabilizing neutral curve appear, but we did not see curve splitting by stable intrusion. There are a variety of possible explanations as to why we did not observe curve splitting (if a stable intrusion does indeed occur): often the neutral curve becomes very 'thin', and so curve splitting can be easily missed by our iteration over a and Re; the numerical method becomes unstable at high Reynolds numbers, especially as f is increased, and curve splitting occurs in this numerically unstable region; the new neutral curve expands and obscures the other neutral curve before curve splitting takes place.

The eventual dominance of this new neutral curve is interesting, in that it implies

a sudden change in the system's instability. At a critical value of f, long wave (i.e. small wave number) perturbations suddenly become the most unstable form of disturbance. This also means that Re_L does not vary as a smooth function of f, as is illustrated in Figure 5.21. We see that, as f increases and so the new neutral curve takes over, the most unstable mode is of high periodicity n. Therefore, we conclude that for a rotating thread/core, perturbations of low frequency along the $z-$axis, and high frequency in the azimuthal direction, become the least stable.

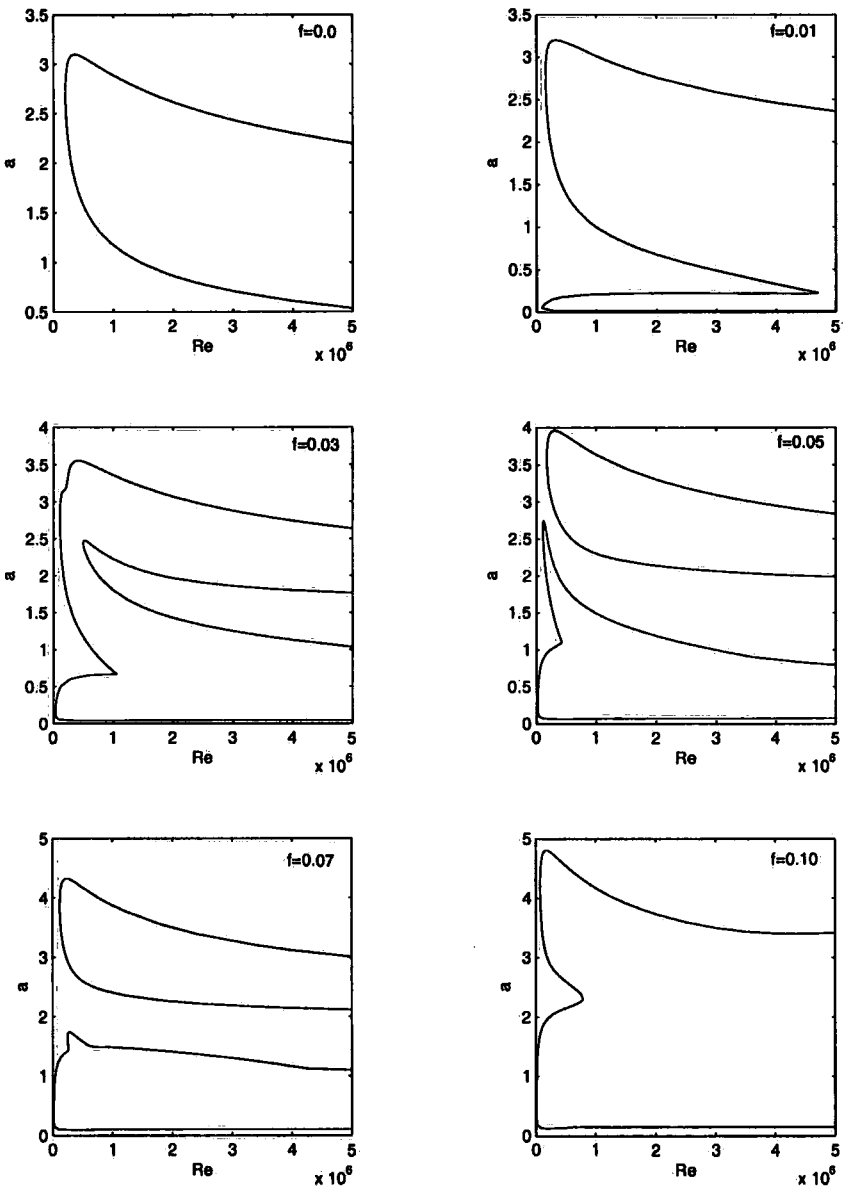

Figure 5.16: Effect of increasing frequency f when $\delta = 0.4$, and $n = 1$. We see a new neutral curve, overlapping the original, appear at low wave numbers for small f. As f increases a stable intrusion begins to split the original neutral curve, while the new neutral curve grows.

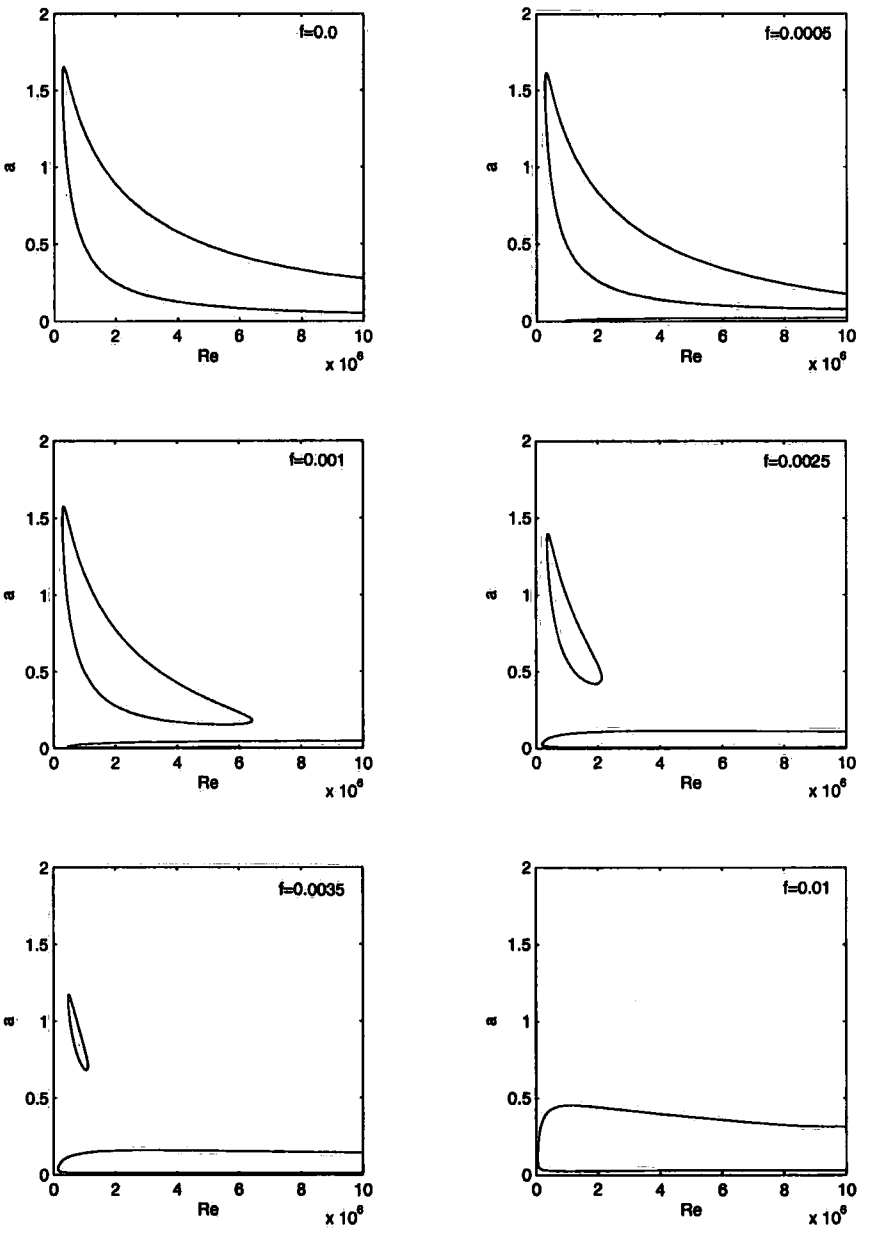

Figure 5.17: Effect of increasing frequency f when $\delta = 0.4$ and $n = 2$. In this case we did not observe stable intrusion.

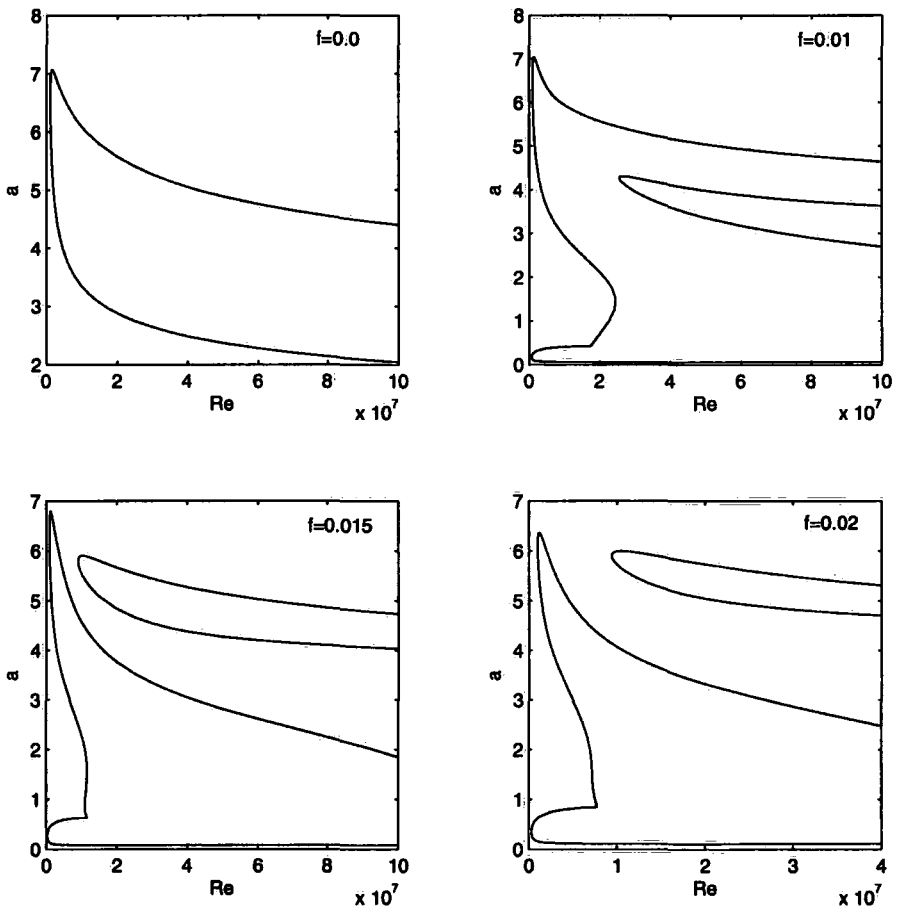

Figure 5.18: Effect of increasing frequency f when $\delta = 0.7$ and $n = 1$.

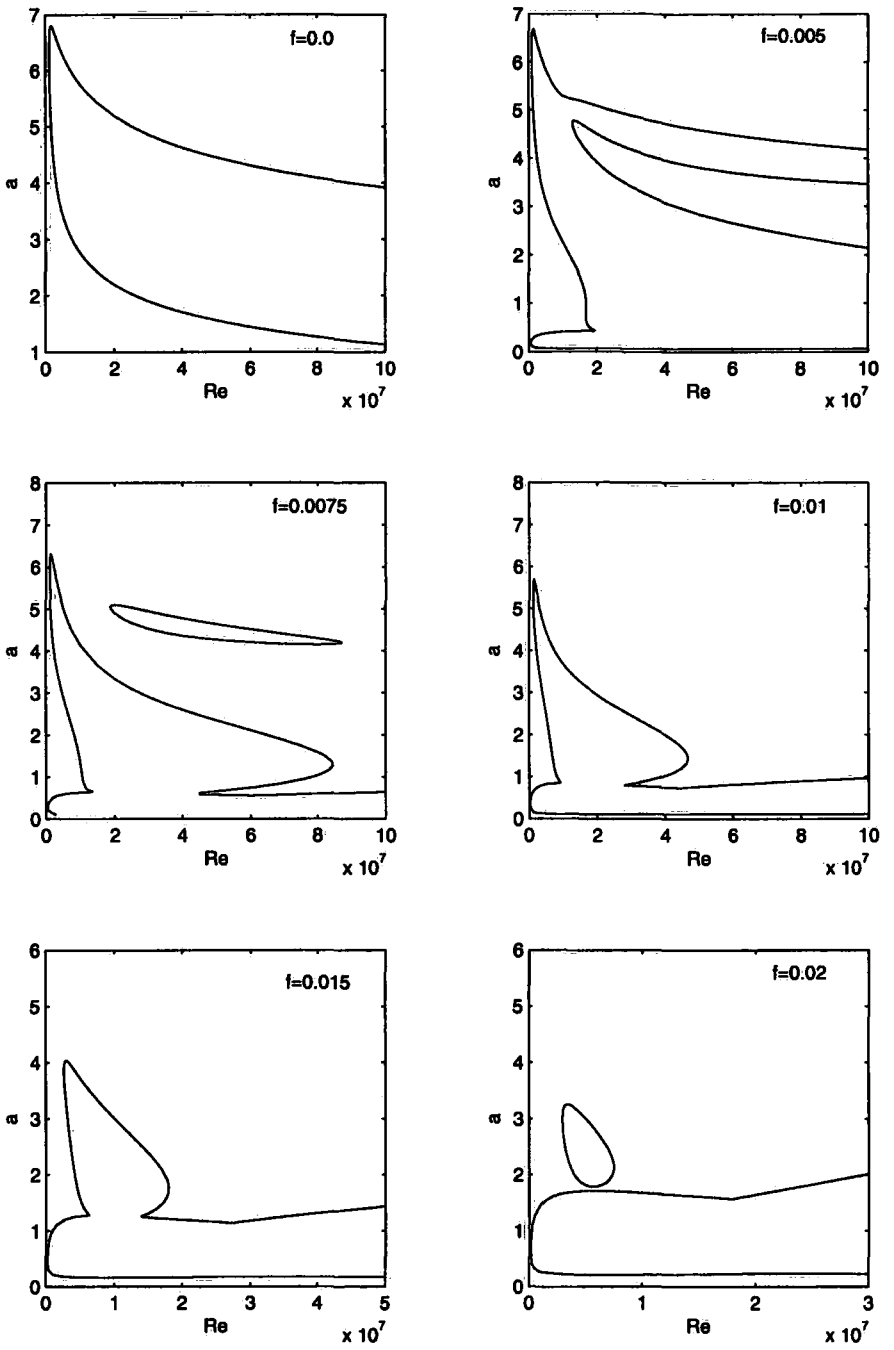

Figure 5.19: Effect of increasing frequency f when $\delta = 0.7$ and $n = 2$.

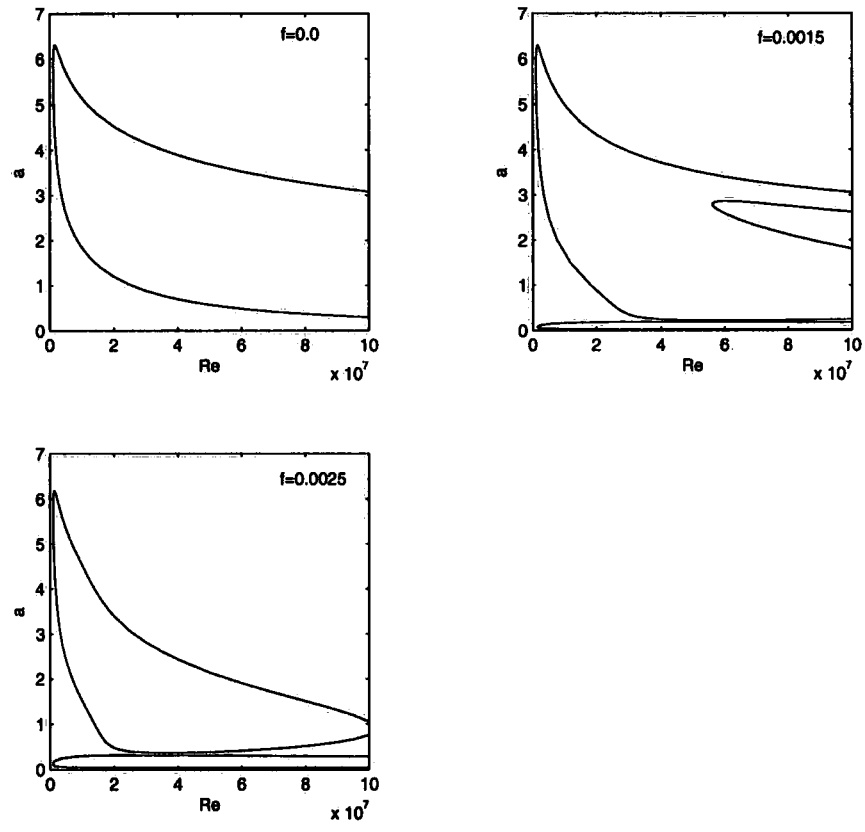

Figure 5.20: Effect of increasing frequency f when $\delta = 0.7$ and $n = 3$.

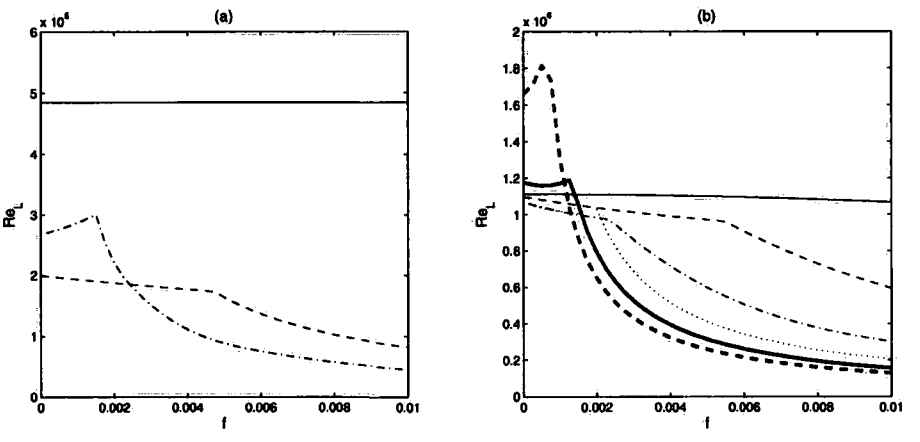

Figure 5.21: Critical Reynolds number as a function of angular frequency f, for: (a) $\delta = 0.4$; (b) $\delta = 0.7$. Perturbations are of periodicity: $n = 0$, –; $n = 1$, - -; $n = 2$, -·; $n = 3$, ··; $n = 4$, dark –; $n = 5$, dark –.

Chapter 6

Instability of fluids obeying higher order differential equations

There has recently been interest in equations of motion for viscous fluids that contain higher order derivatives than the Navier-Stokes equations. Although one of the main reasons for these alternative fluid models is that of regularity, another reason is the understanding of turbulence in fluids, see for example Chen *et al* [10], and Foias *et al* [20, 21].

Motivated by evidence suggesting that the structure of turbulent flows is affected by fluid vorticity and spin of vorticity, Green & Naghdi [25] developed a theory of continuum mechanics based on an entropy equality rather than an inequality. For an incompressible fluid on some domain $\Omega \subset \mathbb{R}^3$ with zero body force, and denoting $\mathbf{u} = \mathbf{u}(\mathbf{x}; t)$ the fluid velocity at the point $\mathbf{x} = (x, y, z) \in \Omega$ and time $t \in [0, \infty)$, the Green-Naghdi equations are

$$\rho\left(1 - \frac{\mu_1}{\mu}\Delta\right) u_{i,t} + \rho u_j \left(1 - \frac{\mu_1}{\mu}\Delta\right) u_{i,j} = -p_{,i} + \mu\left(1 - 2\frac{\mu_1}{\mu}\Delta\right)\Delta u_i, \quad (6.1)$$

$$u_{j,j} = 0, \quad (6.2)$$

for constants ρ, μ and μ_1, and for $p = p(\mathbf{x}; t)$. We see that this is a fourth-order system, and resembles the Navier-Stokes equations in the limit $\mu_1/\mu \to 0$.

Bleustein & Green [3] developed the equations governing a dipolar fluid, which,

assuming incompressibility and zero body force, are

$$\rho\left(1-d^2\Delta\right)\left(u_{i,t}+u_j u_{i,j}\right)+\rho d^2\sigma_{ji,j} = -p_{,i}+\mu\left(1-l^2\Delta\right)\Delta u_i, \quad (6.3)$$

$$u_{j,j} = 0, \quad (6.4)$$

where l and d are known as the dipolar constants, and σ_{ij} is the dipolar inertia. The similarity between many high derivative models for fluid flow such as equations (6.1) and (6.3) invites comparison. In particular, Quintanilla & Straughan [51] have shown that the dipolar equations are essentially the same as the Camassa-Holm or Navier-Stokes-alpha equations, after a certain mapping of parameters.

In this chapter we investigate the onset of instability of Poiseuille flow in both the setting of the Green-Naghdi equations and dipolar equations.

6.1 Pressure driven flow

Once more we consider the domain $\Omega=(-\infty,\infty)\times(-h,h)\times(-\infty,\infty)$, containing an incompressible viscous fluid obeying either of equations (6.1) or (6.3). At $y=\pm h$ the velocity $\mathbf{u}=(u,v,w)$ satisfies

$$u|_{y=\pm h}=u_{,yy}|_{y=\pm h}=0, \quad v|_{y=\pm h}=v_{,y}|_{y=\pm h}=0, \quad w|_{y=\pm h}=w_{,yy}|_{y=\pm h}=0, \quad (6.5)$$

after the boundary conditions of Green & Naghdi [25] and Bleustein & Green [3]. For either fluid model, we can consider the time-independent solution arising from a constant 'pressure gradient' in the $x-$direction. We assume that this constant pressure gradient maintains a certain steady state velocity profile $\bar{\mathbf{u}}(y)$, where our solutions are of the form

$$p_{,x}=-g<0, \quad \bar{\mathbf{u}}=(\bar{u}(y),0,0), \quad \text{such that } \bar{u}(y)|_{y=\pm h}=\bar{u}''(y)|_{y=\pm h}=0. \quad (6.6)$$

6.2 Green-Naghdi flow

We first concern ourselves with the Green-Naghdi model. Substituting the above forms into (6.1) we obtain the system

$$\begin{aligned} 0 &= g + \mu\bar{u}'' - 2\mu_1\bar{u}'''', \\ 0 &= p_{,y}, \\ 0 &= p_{,z}, \end{aligned}$$

and upon considering the boundary conditions at $y = \pm h$ we find the base solution to be

$$\bar{u}(y) = \frac{g}{\mu}\left[\frac{1}{2}\left(h^2 - y^2\right) + 2\frac{\mu}{\mu_1}\left(\frac{\cosh\left(\sqrt{\frac{\mu}{2\mu_1}}y\right)}{\cosh\left(\sqrt{\frac{\mu}{2\mu_1}}h\right)} - 1\right)\right], \quad \bar{p}(x) = p_0 - gx. \tag{6.7}$$

Equation (6.1) and (6.2) can be nondimensionalized via the scalings usual to the Navier-Stokes equations when investigating Poiseuille flow, specifically

$$\mathbf{x} = h\mathbf{x}^*, \quad \mathbf{u} = \bar{u}_0\mathbf{u}^*, \quad t = \frac{h}{\bar{u}_0}t^*, \quad p = \rho\bar{u}_0^2 p^*, \quad Re = \frac{\rho h\bar{u}_0}{\mu}, \tag{6.8}$$

where Re is our Reynolds number, and $\bar{u}_0 = \bar{u}(0) = gh^2/2\mu$, and we use '*' to denote a nondimensional quantity. We also define the nondimensional constant $\gamma^2 = h^2\mu/2\mu_1$. Then, upon dropping the '*' notation equations (6.1) and (6.2) become

$$\left(1 - \frac{1}{2\gamma^2}\Delta\right)u_{i,t} + u_j\left(1 - \frac{1}{2\gamma^2}\Delta\right)u_{i,j} = -p_{,i} + \frac{1}{Re}\left(1 - \frac{1}{\gamma^2}\Delta\right)\Delta u_i, \tag{6.9}$$

$$u_{j,j} = 0, \tag{6.10}$$

for $\mathbf{x} \in \{(-\infty, \infty) \times (-1, 1) \times (-\infty, \infty)\}$ and time $t \in [0, \infty)$, while our steady state velocity becomes

$$\bar{u}(y) = \frac{\left[\frac{1}{2}\gamma^2\left(1 - y^2\right) - 1\right]\cosh(\gamma) + \cosh(\gamma y)}{\left[\frac{1}{2}\gamma^2 - 1\right]\cosh(\gamma) + 1}. \tag{6.11}$$

We aim to investigate the instability of solution (6.11) to disturbances periodic in the $x-$ and $z-$ directions. Therefore, we begin by perturbing the steady state solution

$$\bar{\mathbf{u}}(y) \mapsto \bar{\mathbf{u}}(y) + \mathbf{v}(\mathbf{x}, t), \quad \bar{p}(x) \mapsto \bar{p}(x) + q(\mathbf{x}, t),$$

and substitute these perturbations into equations (6.9), (6.10). After removal of nonlinear terms, we arrive at the linearized perturbation equations

$$\left(1-\frac{1}{2\gamma^2}\Delta\right)v_{i,t}+v_j\left(1-\frac{1}{2\gamma^2}\Delta\right)\bar{u}_{i,j}+\bar{u}_j\left(1-\frac{1}{2\gamma^2}\Delta\right)v_{i,j} = -q_{,i}+\frac{1}{Re}\left(1-\frac{1}{\gamma^2}\Delta\right)\Delta v_i, \quad (6.12)$$

$$v_{j,j} = 0. \quad (6.13)$$

We follow the now familiar method of letting the components of $\mathbf{v}=(u,v,w)$ have the form of travelling waves, i.e.

$$u = u(y)\exp\{i(\alpha x+\beta z-\alpha ct)\}, \quad (6.14)$$

for positive real numbers α and β, and growth rate $c\in\mathbb{C}$, with similar forms for v, w, and the perturbation q. After substituting these expressions and removing exponential parts, we arrive at the system

$$-i\alpha c\left(1-\frac{1}{2\gamma^2}\left[\frac{d^2}{dy^2}-(\alpha^2+\beta^2)\right]\right)u+v\left(1-\frac{1}{2\gamma^2}\frac{d^2}{dy^2}\right)\bar{u}'+i\alpha\bar{u}\left(1-\frac{1}{2\gamma^2}\left[\frac{d^2}{dy^2}-(\alpha^2+\beta^2)\right]\right)u=-i\alpha q$$
$$+\frac{1}{Re}\left(1-\frac{1}{\gamma^2}\left[\frac{d^2}{dy^2}-(\alpha^2+\beta^2)\right]\right)\left(\frac{d^2}{dy^2}-(\alpha^2+\beta^2)\right)u, \quad (6.15)$$

$$-i\alpha c\left(1-\frac{1}{2\gamma^2}\left[\frac{d^2}{dy^2}-(\alpha^2+\beta^2)\right]\right)v+i\alpha\bar{u}\left(1-\frac{1}{2\gamma^2}\left[\frac{d^2}{dy^2}-(\alpha^2+\beta^2)\right]\right)v=-q'$$
$$+\frac{1}{Re}\left(1-\frac{1}{\gamma^2}\left[\frac{d^2}{dy^2}-(\alpha^2+\beta^2)\right]\right)\left(\frac{d^2}{dy^2}-(\alpha^2+\beta^2)\right)v, \quad (6.16)$$

$$-i\alpha c\left(1-\frac{1}{2\gamma^2}\left[\frac{d^2}{dy^2}-(\alpha^2+\beta^2)\right]\right)w+i\alpha\bar{u}\left(1-\frac{1}{2\gamma^2}\left[\frac{d^2}{dy^2}-(\alpha^2+\beta^2)\right]\right)w=-i\beta q$$
$$+\frac{1}{Re}\left(1-\frac{1}{\gamma^2}\left[\frac{d^2}{dy^2}-(\alpha^2+\beta^2)\right]\right)\left(\frac{d^2}{dy^2}-(\alpha^2+\beta^2)\right)w, \quad (6.17)$$

$$i\alpha u+v'+i\beta w=0. \quad (6.18)$$

We now observe that upon adding $\alpha\times$(equation 6.15)$+\beta\times$(equation 6.17), and defining

$$a=\sqrt{\alpha^2+\beta^2}, \quad \hat{u}=\frac{\alpha u+\beta w}{a} \quad \hat{v}=v, \quad \hat{q}=\frac{a}{\alpha}q, \quad \hat{Re}=\frac{\alpha}{a}Re, \quad (6.19)$$

we arrive at the system

$$-i\alpha c\left(1-\frac{1}{2\gamma^2}\left[\frac{d^2}{dy^2}-a^2\right]\right)\hat{u}+\hat{v}\left(1-\frac{1}{2\gamma^2}\frac{d^2}{dy^2}\right)\bar{u}'+i\alpha\bar{u}\left(1-\frac{1}{2\gamma^2}\left[\frac{d^2}{dy^2}-a^2\right]\right)\hat{u}=-i\alpha\hat{q}$$
$$+\frac{1}{Re}\left(1-\frac{1}{\gamma^2}\left[\frac{d^2}{dy^2}-a^2\right]\right)\left(\frac{d^2}{dy^2}-a^2\right)\hat{u}, \quad (6.20)$$

$$-i\alpha c\left(1-\frac{1}{2\gamma^2}\left[\frac{d^2}{dy^2}-a^2\right]\right)\hat{v}+i\alpha\bar{u}\left(1-\frac{1}{2\gamma^2}\left[\frac{d^2}{dy^2}-a^2\right]\right)\hat{v}=-\hat{q}' \quad (6.21)$$
$$+\frac{1}{Re}\left(1-\frac{1}{\gamma^2}\left[\frac{d^2}{dy^2}-a^2\right]\right)\left(\frac{d^2}{dy^2}-a^2\right)\hat{v}, \quad (6.22)$$

$$ia\hat{u}+v'=0. \quad (6.23)$$

We note that this is exactly as we would have, had we set $u=u(y)\exp\{i(ax-ct)\}$, $v=v(y)\exp\{i(ax-ct)\}$, $w=w(y)\exp\{i(ax-ct)\}$, and $q=q(y)\exp\{i(ax-ct)\}$,

i.e. had we considered a $z-$independent perturbation, since then we would have found $w = 0$.

Since $\hat{Re} \leq Re$, we see that for every unstable fully three dimensional perturbation, there is a $z=$independent perturbation that is unstable at the same or lower Reynolds number. Therefore we can limit ourselves to studying this reduced system.

We remove the pressure terms by performing $d/dy\times$(equation 6.20)$-ia\times$(equation 6.22), and introduce a stream function $\phi(y)$ such that $u = \phi'(y)$ and $v = -ia\phi(y)$ (so that equation 6.23 is satisfied). Thus we arrive at our generalization of the Orr-Sommerfeld equation

$$iaRe\left[(\bar{u}-c)\left(1-\frac{1}{2\gamma^2}\left[\frac{d^2}{dy^2}-a^2\right]\right)-\left(\bar{u}''-\frac{1}{2\gamma^2}\bar{u}''''\right)-\frac{1}{2\gamma^2}\left(\bar{u}'\left[\frac{d^2}{dy^2}-a^2\right]-\bar{u}'''\right)\frac{d}{dy}\right]\phi = \frac{1}{Re}\left(1-\frac{1}{\gamma^2}\left[\frac{d^2}{dy^2}-a^2\right]\right)\left(\frac{d^2}{dy^2}-a^2\right)^2\phi, \tag{6.24}$$

where the boundary conditions of (6.5) become

$$\phi|_{y=\pm1} = \phi'_{y=\pm1} = \phi'''_{y=\pm1} = 0. \tag{6.25}$$

6.3 Dipolar flow

6.3.1 Bleustein & Green inertia term

We now look to equations (6.3) and (6.4). Bleustein & Green [3] proposed an inertia term for equation (6.3) of the form $\sigma_{ij} = u_{j,k}u_{k,i}$. With this form for σ, we see that the terms multiplying d^2 in equation (6.3) are

$$\begin{aligned}
\sigma_{ji,j} - \Delta(u_{i,t} + u_j u_{i,j}) &= (u_{i,k}u_{k,j})_{,j} - \Delta u_{i,t} - u_j\Delta u_{i,j} = u_{i,j}\Delta u_j - 2u_{j,k}u_{i,jk}, \\
&= u_{i,jk}u_{k,j} + u_{i,j}\Delta u_j - \Delta u_{i,t} - u_j\Delta u_{i,j} - u_{i,j}\Delta u_j - 2u_{j,k}u_{i,jk}, \\
&= u_{i,jk}(u_{k,j} - u_{j,k}) - \Delta u_{i,t} - u_j\Delta u_{i,j} - u_{j,k}u_{i,jk}, \\
&= -\Delta u_{i,t} - u_j\Delta u_{i,j} - u_{j,k}u_{i,jk},
\end{aligned}$$

since $u_{i,jk}$ is symmetric in j and k, while $(u_{j,k} - u_{k,j})$ is antisymmetric, and so their product is zero. Therefore we arrive at the equations of motion for a dipolar fluid with Bleustein & Green's inertia tensor,

$$\rho(1-d^2\Delta)u_{i,t} + \rho u_j(1-d^2\Delta)u_{i,j} - \rho d^2 u_{j,k}u_{i,jk} = -p_{,i} + \mu(1-l^2\Delta)\Delta u_i, \tag{6.26}$$

$$u_{j,j} = 0. \tag{6.27}$$

Looking for a steady-state solution of the form (6.6) leads us to the system

$$\begin{aligned} 0 &= g + \mu\bar{u}'' - l^2\mu\bar{u}'''', \\ 0 &= p_{,x}, \\ 0 &= p_{,y}, \end{aligned}$$

from which we obtain

$$\bar{u}(y) = \frac{g}{\mu}\left[\frac{1}{2}(h^2 - y^2) + l^2\left(\frac{\cosh(y/l)}{\cosh(h/l)} - 1\right)\right], \quad \bar{p}(x) = p_0 - gx. \tag{6.28}$$

With this $\bar{u}(y)$ we nondimensionalize equations (6.26) and (6.27) using the scalings of (6.8), and introduce the nondimensional constants $l_1 = d/h$ and $l_2 = l/h$, giving us the nondimensional equations

$$(1 - l_1^2\Delta)u_{i,t} + u_j(1 - l_1^2\Delta)u_{i,j} - l_1^2 u_{j,k}u_{i,jk} = -p_{,i} + \frac{1}{Re}(1 - l_2^2\Delta)\Delta u_i, \tag{6.29}$$

$$u_{j,j} = 0, \tag{6.30}$$

and nondimensional base flow

$$\bar{u}(y) = \frac{\left[\frac{1}{2}(1 - y^2) - l_2^2\right]\cosh(1/l_2) + l_2^2\cosh(y/l_2)}{\left[\frac{1}{2} - l_2^2\right]\cosh(1/l_2) + l_2^2}. \tag{6.31}$$

We proceed as before, by perturbing our steady state solution, substituting this into the equations of motion, and then linearizing. The linearized perturbations equations (for a velocity perturbation $\mathbf{v}$ and pressure pertubation q) are

$$\begin{aligned} (1 - l_1^2\Delta)u_{i,t} + v_j(1 - l_1^2\Delta)\bar{u}_{i,j} + \bar{u}_j(1 - l_1^2\Delta)v_{i,j} & \\ -l_1^2 v_{j,k}\bar{u}_{i,jk} - l_1^2\bar{u}_{j,k}v_{i,jk} &= -q_{,i} + \frac{1}{Re}(1 - l_2^2\Delta)\Delta v_i, \end{aligned} \tag{6.32}$$

$$v_{j,j} = 0. \tag{6.33}$$

Again, we suppose that the velocity perturbation $\mathbf{v} = (u, v, w)$ and pressure perturbation q are periodic in the $x-$ and $z-$ directions, such that they have the form

$$\mathbf{v} = \mathbf{v}(y)e^{i(\alpha x + \beta z - \alpha c t)}, \quad q = q(y)e^{i(\alpha x + \beta z - \alpha c t)}, \tag{6.34}$$

and we substitute these forms into our linearized perturbation equations. Upon removal of exponential parts, we see that $(u(y), v(y), w(y))$ and $q(y)$ satisfy

$$-i\alpha c\left(1-l_1^2\left[\frac{d^2}{dy^2}-(\alpha^2+\beta^2)\right]\right)u+v\left(1-l_1^2\frac{d^2}{dy^2}\right)\bar{u}'+i\alpha\bar{u}\left(1-l_1^2\left[\frac{d^2}{dy^2}-(\alpha^2+\beta^2)\right]\right)u$$
$$-l_1^2v'\bar{u}''-i\alpha l_1^2\bar{u}'u'=-i\alpha q$$
$$+\frac{1}{Re}\left(1-l_2^2\left[\frac{d^2}{dy^2}-(\alpha^2+\beta^2)\right]\right)\left(\frac{d^2}{dy^2}-(\alpha^2+\beta^2)\right)u, \quad (6.35)$$

$$-i\alpha c\left(1-l_1^2\left[\frac{d^2}{dy^2}-(\alpha^2+\beta^2)\right]\right)v+i\alpha\bar{u}\left(1-l_1^2\left[\frac{d^2}{dy^2}-(\alpha^2+\beta^2)\right]\right)v$$
$$-i\alpha l_1^2\bar{u}'v'=-q'$$
$$+\frac{1}{Re}\left(1-l_2^2\left[\frac{d^2}{dy^2}-(\alpha^2+\beta^2)\right]\right)\left(\frac{d^2}{dy^2}-(\alpha^2+\beta^2)\right)v, \quad (6.36)$$

$$-i\alpha c\left(1-l_1^2\left[\frac{d^2}{dy^2}-(\alpha^2+\beta^2)\right]\right)w+i\alpha\bar{u}\left(1-l_1^2\left[\frac{d^2}{dy^2}-(\alpha^2+\beta^2)\right]\right)w$$
$$-i\alpha l_1^2\bar{u}'w'=-i\beta q$$
$$+\frac{1}{Re}\left(1-l_2^2\left[\frac{d^2}{dy^2}-(\alpha^2+\beta^2)\right]\right)\left(\frac{d^2}{dy^2}-(\alpha^2+\beta^2)\right)w, \quad (6.37)$$

$$i\alpha u+v'+i\beta w=0 \quad (6.38)$$

We note that by again applying transform (6.19) and adding multiples of the above equations as in the example of the Green-Naghdi model (i.e. performing $\alpha\times$(equation 6.35)$+\beta\times$(equation 6.37)) we obtain the system

$$iac\left(1-l_1^2\left[\frac{d^2}{dy^2}-a^2\right]\right)\hat{u}+\hat{v}\left(1-l_1^2\frac{d^2}{dy^2}\right)\bar{u}'+ia\bar{u}\left(1-l_1^2\left[\frac{d^2}{dy^2}-a^2\right]\right)\hat{u}$$
$$-l_1^2\hat{v}'\bar{u}''-ial_1^2\bar{u}'\hat{u}'=-ia\hat{q}$$
$$+\frac{1}{\hat{Re}}\left(1-l_2^2\left[\frac{d^2}{dy^2}-a^2\right]\right)\left(\frac{d^2}{dy^2}-a^2\right)\hat{u}, \quad (6.39)$$

$$-iac\left(1-l_1^2\left[\frac{d^2}{dy^2}-a^2\right]\right)\hat{v}+ia\bar{u}\left(1-l_1^2\left[\frac{d^2}{dy^2}-a^2\right]\right)\hat{v}$$
$$-ial_1^2\bar{u}'\hat{v}'=-\hat{q}'$$
$$+\frac{1}{\hat{Re}}\left(1-l_2^2\left[\frac{d^2}{dy^2}-a^2\right]\right)\left(\frac{d^2}{dy^2}-a^2\right)\hat{v}, \quad (6.40)$$

$$ia\hat{u}+\hat{v}'=0. \quad (6.41)$$

Therefore, we have found a Squire transform, and need only consider perturbations dependent upon x and y, as before.

We remove the pressure terms by differentiating equation (6.39) with respect to y, multiplying equation (6.40) by ia, and subtracting, and by defining a stream function $\phi(y)$ as before, we arrive at the generalized Orr-Sommerfeld equation for this problem,

$$iaRe\left[(\bar{u}-c)\left(1-l_1^2\left[\frac{d^2}{dy^2}-a^2\right]\right)\left(\frac{d^2}{dy^2}-a^2\right)-(\bar{u}''-l_1^2\bar{u}'''')-2l_1^2\left(\bar{u}'\left[\frac{d^2}{dy^2}-a^2\right]-\bar{u}'''\right)\frac{d}{dy}\right]\phi=$$
$$\left(1-l_2^2\left[\frac{d^2}{dy^2}-a^2\right]\right)\left(\frac{d^2}{dy^2}-a^2\right)^2\phi. \quad (6.42)$$

Again, we have $\phi|_{y=\pm 1} = \phi'|_{y=\pm 1} = \phi'''|_{y=\pm 1} = 0$.

6.3.2 Green & Naghdi inertia term

If we use the inertia term of Green & Naghdi [24] given as $\sigma_{ij} = u_{j,k}u_{k,i} + u_{j,k}u_{i,k} - u_{k,i}u_{k,j}$, then terms multiplying d^2 in equation (6.3) become

$$\begin{aligned}
\sigma_{ji,j} - \Delta(u_{i,t} + u_j u_{i,j}) &= (u_{i,k}u_{k,j} + u_{i,k}u_{j,k} - u_{k,j}u_{k,i})_{,j} - \Delta u_{i,t} - u_j \Delta u_{i,j} - u_{i,j}\Delta u_j \\
&\quad -2u_{j,k}u_{i,jk}, \\
&= u_{i,jk}(u_{k,j} - u_{j,k}) - \Delta u_{i,t} - u_{j,i}\Delta u_j - u_j \Delta u_{i,j} - \frac{1}{2}(u_{k,j}u_{k,j})_{,i}, \\
&= -\Delta u_{i,t} - u_{j,i}\Delta u_j - u_j \Delta u_{i,j} - \frac{1}{2}(u_{k,j}u_{k,j})_{,i},
\end{aligned}$$

where we have disposed of the $u_{i,jk}(u_{k,j} - u_{j,k})$ term as before. However, we notice that a gradient term is present, which can be absorbed into a modified pressure term.

Upon doing so, our equations of motion are

$$\rho(1 - d^2\Delta)u_{i,t} + \rho u_j(1 - d^2\Delta)u_{i,j} - d^2 u_{j,i}\Delta u_j = -p_{,i} + \mu(1 - l^2\Delta)\Delta u_i, \tag{6.43}$$

$$u_{j,j} = 0. \tag{6.44}$$

Assuming $\mathbf{u} = (\bar{u}(y), 0, 0)$ and $p_{,x} = -g < 0$, then our steady-state satisfies

$$0 = g + \mu\bar{u}'' - \mu l^2 \bar{u}'''', \tag{6.45}$$

$$d^2\bar{u}'\bar{u}'' = p_{,y}, \tag{6.46}$$

$$0 = p_{,z}, \tag{6.47}$$

where clearly $\bar{u}(y)$ has the same solution as before (given in 6.28), although this time the pressure is solved for by

$$\bar{p}(x, y) = p_0 - gx + \frac{1}{2}d^2(\bar{u}')^2. \tag{6.48}$$

Following the nondimensionalization of (6.8) and again letting $l_1 = d/h$ and $l_2 = l/h$, we obtain the nondimensional equations of motion

$$(1 - l_1^2\Delta)u_{i,t} + u_j(1 - l_1^2\Delta)u_{i,j} - l_1^2 u_{j,i}\Delta u_j = -p_{,i} + \frac{1}{Re}(1 - l_2^2\Delta)\Delta u_i, \tag{6.49}$$

$$u_{j,j} = 0, \tag{6.50}$$

where p is understood to be the modified pressure, and $\bar{u}(y)$ nondimensionalizes to the form given in (6.31).

An important difference from the previous dipolar case arises when we look at the linearized perturbation equations, which are

$$(1 - l_1^2\Delta)u_{i,t} + u_j(1 - l_1^2\Delta)\bar{u}_{i,j} + \bar{u}_j(1 - l_1^2\Delta)u_{i,j} \tag{6.51}$$

$$-l_1^2\bar{u}_{j,i}\Delta u_j - l_1^2 u_{j,i}\Delta\bar{u}_j = -q_{,i} + \frac{1}{Re}(1 - l_2^2\Delta)\Delta u_i, \tag{6.52}$$

$$u_{j,j} = 0. \tag{6.53}$$

Substituting travelling wave solutions as before into these equations we obtain

$$\begin{aligned} -i\alpha c\left(1 - l_1^2\left[\frac{d^2}{dy^2} - (\alpha^2+\beta^2)\right]\right)u + v\left(1 - l_1^2\frac{d^2}{dy^2}\right)\bar{u}' + i\alpha\bar{u}\left(1 - l_1^2\left[\frac{d^2}{dy^2} - (\alpha^2+\beta^2)\right]\right)u \\ -i\alpha l_1^2\bar{u}''u = -i\alpha q \\ +\frac{1}{Re}\left(1 - l_2^2\left[\frac{d^2}{dy^2} - (\alpha^2+\beta^2)\right]\right)\left(\frac{d^2}{dy^2} - (\alpha^2+\beta^2)\right)u, \end{aligned} \tag{6.54}$$

$$\begin{aligned} -i\alpha c\left(1 - l_1^2\left[\frac{d^2}{dy^2} - (\alpha^2+\beta^2)\right]\right)v + i\alpha\bar{u}\left(1 - l_1^2\left[\frac{d^2}{dy^2} - (\alpha^2+\beta^2)\right]\right)v - l_1^2\bar{u}''u' \\ -l_1^2\bar{u}'\left(\frac{d^2}{dy^2} - (\alpha^2+\beta^2)\right)u = -q' \\ +\frac{1}{Re}\left(1 - l_2^2\left[\frac{d^2}{dy^2} - (\alpha^2+\beta^2)\right]\right)\left(\frac{d^2}{dy^2} - (\alpha^2+\beta^2)\right)v \end{aligned} \tag{6.55}$$

$$\begin{aligned} -i\alpha c\left(1 - l_1^2\left[\frac{d^2}{dy^2} - (\alpha^2+\beta^2)\right]\right)w + i\alpha\bar{u}\left(1 - l_1^2\left[\frac{d^2}{dy^2} - (\alpha^2+\beta^2)\right]\right)w \\ -i\beta l_1^2\bar{u}''u = -i\beta q \\ +\frac{1}{Re}\left(1 - l_2^2\left[\frac{d^2}{dy^2} - (\alpha^2+\beta^2)\right]\right)\left(\frac{d^2}{dy^2} - (\alpha^2+\beta^2)\right)w, \end{aligned} \tag{6.56}$$

$$i\alpha u + v' + i\beta w = 0. \tag{6.57}$$

There is no Squire transform for these equations owing to the terms in u, in equation (6.55). Therefore for reasons of consistency we set $\alpha = a$, $\beta = 0$ and $w = 0$, and so consider the equations

$$\begin{aligned} -iac\left(1 - l_1^2\left[\frac{d^2}{dy^2} - a^2\right]\right)u + v\left(1 - l_1^2\frac{d^2}{dy^2}\right)\bar{u}' + -a\left(1 - l_1^2\left[\frac{d^2}{dy^2} - a^2\right]\right)u \\ -ial_1^2\bar{u}''u = -iaq \\ +\frac{1}{Re}\left(1 - l_2^2\left[\frac{d^2}{dy^2} - a^2\right]\right)\left(\frac{d^2}{dy^2} - a^2\right)u, \end{aligned} \tag{6.58}$$

$$\begin{aligned} -iac\left(1 - l_1^2\left[\frac{d^2}{dy^2} - a^2\right]\right)v + ia\bar{u}\left(1 - l_1^2\left[\frac{d^2}{dy^2} - a^2\right]\right)v - l_1^2\bar{u}''u' \\ -l_1^2\bar{u}'\left[\frac{d^2}{dy^2} - a^2\right]u = -q' \\ +\frac{1}{Re}\left(1 - l_2^2\left[\frac{d^2}{dy^2} - a^2\right]\right)v, \end{aligned} \tag{6.59}$$

$$iau + v' = 0, \tag{6.60}$$

and, upon introducing the stream function ϕ as before, we obtain the generalized

Orr-Sommerfeld equation for this problem,

$$iaRe\left[(\bar{u}-c)\left(1-l_1^2\left[\frac{d^2}{dy^2}-a^2\right]\right)\left(\frac{d^2}{dy^2}-a^2\right)-(\bar{u}''-l_1^2\bar{u}'''')\right]\phi=\left(1-l_2^2\left[\frac{d^2}{dy^2}-a^2\right]\right)\left(\frac{d^2}{dy^2}-a^2\right)^2\phi. \tag{6.61}$$

6.3.3 Generalized Orr-Sommerfeld problem

We can summarise our findings so far by proposing a generalized Orr-Sommerfeld equation, given by

$$iaRe\left[(\bar{u}-c)\left(1-\lambda_1^2\left[\frac{d^2}{dy^2}-a^2\right]\right)\left(\frac{d^2}{dy^2}-a^2\right)=(\bar{u}''-\lambda_1^2\bar{u}'''')-\lambda_2^2\left(\bar{u}'\left[\frac{d^2}{dy^2}-a^2\right]-\bar{u}'''\right)\frac{d}{dy}\right]\phi=$$
$$\left(1-\lambda_3^2\left[\frac{d^2}{dy^2}-a^2\right]\right)\left(\frac{d^2}{dy^2}-a^2\right)^2\phi, \tag{6.62}$$

to be solved subject to the boundary conditions $\phi(\pm1)=\phi'(\pm1)=\phi'''(\pm1)=0$, and where $\bar{u}(y)$ is given by

$$\bar{u}(y)=\frac{\left[\frac{1}{2}(1-y^2)-\lambda_3^2\right]\cosh(1/\lambda_3)+\lambda_3^2\cosh(y/\lambda_3)}{\left[\frac{1}{2}-\lambda_3^2\right]\cosh(1/\lambda_3)+\lambda_3^2}. \tag{6.63}$$

The Green-Naghdi model and both dipolar models are to be found within the parameter space $(\lambda_1^2,\lambda_2^2,\lambda_3^2)$, as follows.

$$\begin{aligned}\text{Green-Naghdi model:}\quad &(\lambda_1^2,\lambda_2^2,\lambda_3^2)=\left(\tfrac{1}{2\gamma^2},\tfrac{1}{2\gamma^2},\tfrac{1}{\gamma^2}\right).\\ \text{Dipolar model, Bleustein \& Green inertia:}\quad &(\lambda_1^2,\lambda_2^2,\lambda_3^2)=(l_1^2,2l_1^2,l_2^2).\\ \text{Dipolar model, Green \& Naghdi inertia:}\quad &(\lambda_1^2,\lambda_2^2,\lambda_3^2)=(l_1^2,0,l_2^2).\end{aligned}$$

6.4 Numerical solution

Anticipating the Chebyshev tau method, we introduce the functions $\psi(y)$ and $\theta(y)$ such that

$$\psi(y)=\phi''(y)-a^2\phi(y),\quad \theta(y)=\psi''(y)-a^2\psi(y).$$

Then equation (6.62) becomes

$$iaRe\left[(\bar{u}-c)(\psi-\lambda_1^2\theta)-(\bar{u}''-\lambda_1^2\bar{u}'''')\phi-\lambda_2^2\bar{u}'\psi'+\lambda_2^2\bar{u}'''\phi'\right]=\theta-\lambda_3^2\left(\frac{d^2}{dy^2}-a^2\right)\theta, \tag{6.64}$$

with the boundary conditions

$$\phi(\pm1)=\phi'(\pm1)=\psi'(\pm1)=0. \tag{6.65}$$

We suppose that $\phi(y)$ is expressible as a Chebyshev polynomial series $\phi(y) = \sum_{n=0}^{\infty} \phi_n T_n(y)$, with ψ and θ having similar expansions. Then, we aim to approximate ϕ, ψ and θ with the functions Φ, Ψ and Θ, with the finite expansions

$$\Phi(y) = \sum_{n=0}^{N} \Phi_n T_n(y), \quad \Psi(y) = \sum_{n=0}^{N} \Psi_n T_n(y), \quad \Theta(y) = \sum_{n=0}^{N} \Theta_n T_n(y),$$

for some integer N. We then substitute these finite dimensional functions into equation (6.64), and so aim to solve

$$\begin{aligned}
L_1(\Phi,\Psi) &= \Phi'' - a^2\Phi - \Psi = \tau_1 T_{N-1} + \tau_2 T_N, \\
L_2(\Psi,\Theta) &= \Psi'' - a^2\Psi - \Theta = \tau_3 T_{N-1} + \tau_4 T_N, \\
L_3(\Phi,\Psi,\Theta) &= iaRe\left[(\bar{u}-c)\left(\psi - \lambda_1^2\theta\right) - \left(\bar{u}'' - \lambda_1^2\bar{u}''''\right)\phi - \lambda_2^2\bar{u}'\psi' + \lambda_2^2\bar{u}'''\phi'\right] \\
&\quad -\theta + \lambda_3^2\left(\frac{d^2}{dy^2} - a^2\right)\theta = \tau_5 T_{N-1} + \tau_6 T_N.
\end{aligned}$$

We then take the weighted Chebyshev inner product of $< L_i, T_j >$ for $i = 1,2,3$ and $j = 0,1,..,N-2$ to remove the τ coefficients, and so obtain $3N-3$ linear equations in $3N+3$ unknowns Φ_i, Ψ_i, Θ_i. The system is closed using our six homogeneous boundary conditions, and thus we arrive at the generalized eigenvalue problem $(A_r + A_i)\mathbf{x} = c(B_r + B_i)\mathbf{x}$ for eigenvalue c and eigenvector $\mathbf{x} = (\Phi_0,...,\Phi_N,\Psi_0,...,\Psi_N,\Theta_0,...,\Theta_N)^T$, with $(3N+3)\times(3N+3)$ square matrices

$$A_r = \begin{pmatrix}
D^2 - a^2 I & -I & 0 \\
BC1 & 0...0 & 0...0 \\
BC2 & 0...0 & 0...0 \\
0 & D^2 - a^2 I & -I \\
BC3 & 0...0 & 0...0 \\
BC4 & 0...0 & 0...0 \\
0 & 0 & -I + \lambda_3^2(D^2 - a^2 I) \\
0...0 & BC5 & 0...0 \\
0...0 & BC6 & 0...0
\end{pmatrix},$$

$$A_i = \begin{pmatrix} 0 & 0 & 0 \\ 0...0 & 0...0 & 0...0 \\ 0...0 & 0...0 & 0...0 \\ 0 & 0 & 0 \\ 0...0 & 0...0 & 0...0 \\ 0...0 & 0...0 & 0...0 \\ -aRe\left(\bar{U}'' - \lambda_1^2\bar{U}''''\right) + aRe\lambda_2^2\bar{U}''D & aRe\bar{U} - aRe\lambda_2^2\bar{U}' & -aRe\lambda_1^2\bar{U} \\ 0...0 & 0...0 & 0...0 \\ 0...0 & 0...0 & 0...0 \end{pmatrix},$$

$$B_r = (0),$$

$$B_i = \begin{pmatrix} 0 & 0 & 0 \\ 0...0 & 0...0 & 0...0 \\ 0...0 & 0...0 & 0...0 \\ 0 & 0 & 0 \\ 0...0 & 0...0 & 0...0 \\ 0...0 & 0...0 & 0...0 \\ 0 & aReI & -aRe\lambda_1^2 I \\ 0...0 & 0...0 & 0...0 \\ 0...0 & 0...0 & 0...0 \end{pmatrix}.$$

Here, D and D^2 are the first and second order Chebyshev differentiation matrices, I is the identity matrix, and $\bar{U}$ is the Chebyshev representation matrix for multiplication by $\bar{u}$ (with $\bar{U}'$ and so on defined similarly).

The rows $BC1$ to $BC6$ are our boundary conditions, which, upon noting that $T_n(\pm 1) = (\pm 1)^n$ and $T_n'(\pm 1) = n^2(\pm 1)^{n+1}$ are overwritten as

$$\sum_{n=0}^{N} \Phi_n = 0, \quad \sum_{n=0}^{N} n^2\Phi_n = 0, \quad \sum_{n=0}^{N} n^2\Psi_n = 0, \tag{6.66}$$

$$\sum_{n=0}^{N} (-1)^n\Phi_n = 0, \quad \sum_{n=0}^{N} n^2(-1)^{n+1}\Phi_n = 0, \quad \sum_{n=0}^{N} n^2(-1)^{n+1}\Psi_n = 0. \tag{6.67}$$

For a given set of parameters $(\lambda_1, \lambda_2, \lambda_3)$ we solve this generalized eigenvalue problem using NAG routine F02GJF, finding points (a, Re) such that we have neutral linear stability (i.e. the leading eigenvalue in the spectrum has zero imaginary part)

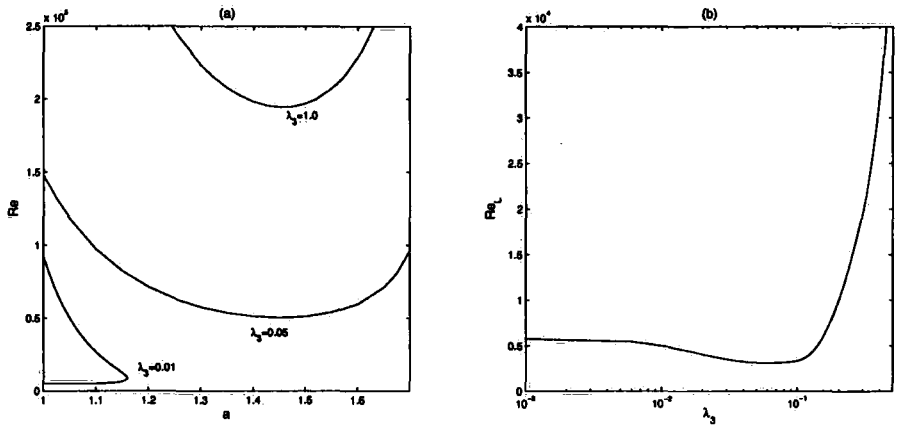

Figure 6.1: The effect of increasing λ_3 (when $\lambda_1 = \lambda_2 = 0$) on: (a) the neutral curves, when $\lambda_3 = 0.01$, 0.05 and 1.0; (b) the critical Reynolds number Re_L as a function of λ_3.

over which we iterate until we have the minimum Reynolds number above which instability is assured, Re_L. The iterative methods are as in Chapter two.

6.5 Results

Before presenting our results for the cases of a Green-Naghdi fluid or a dipolar fluid, we consider the effect of the highest order derivative in our generalized eigenvalue equation (6.64), by setting $\lambda_1 = \lambda_2 = 0$. Figure 6.1 (a) shows the unique neutral curves for this case, and it is clearly seen that, for the three choices of λ_3 shown, the minimum Reynolds number increases with increasing λ_3.

However, there is a small initial interval over which the effect of increasing λ_3 is to destabilize the flow. Figure 6.1 (b) shows the variation of the critical Reynolds number Re_L as a function of λ_3. The critical Reynolds number decreases from $Re_L \sim 5772$ at $\lambda_3 = 0$ (the classical, Navier-Stokes case) to $Re_L \sim 3080$ at $\lambda_3 \sim 0.06$. For λ_3 greater than approximately 0.06, the flow rapidly stabilizes.

When we turn to the case of a Green-Naghdi fluid, we lose the initial destabilizing effect of λ_3. In the Green-Naghdi parameter γ $(= 1/\lambda_3)$, our base solution $\bar{u}(y)$

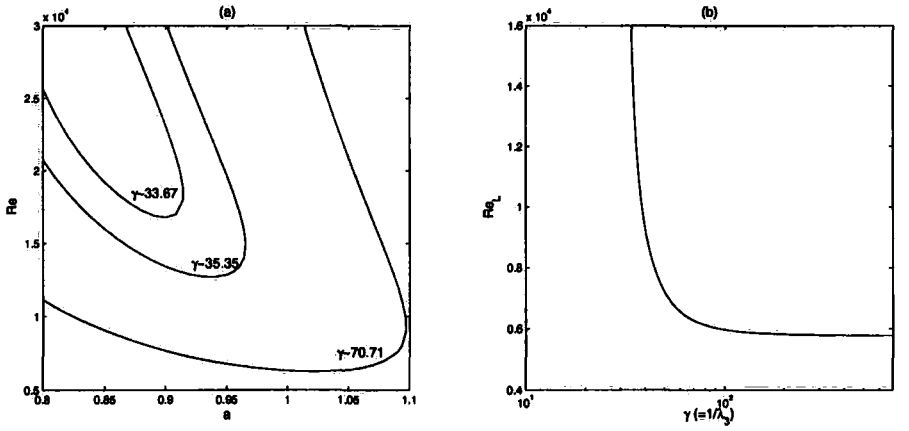

Figure 6.2: Green-Naghdi fluid model. (a) shows neutral curves for $\lambda_3 = 2.1\sqrt{2} \times 10^{-2}$ ($\gamma \sim 33.67$), $\lambda_3 = 2\sqrt{2} \times 10^{-2}$ ($\gamma \sim 35.35$), and $\lambda_3 = \sqrt{2} \times 10^{-2}$ ($\gamma \sim 70.71$). Graph (b) shows the critical Reynolds number Re_L against $\gamma(= 1/\lambda_3)$.

satisfies the Navier-Stokes equations in the limit $\gamma \to \infty$ (i.e. $\lim_{\gamma\to\infty} \bar{u}(y) = 1-y^2$). Therefore, in Figure 6.2 (b) we see that the critical Reynolds number Re_L tends asymptotically to 5772 as γ becomes large.

Figure 6.2 (a) shows the neutral curves for different choices of γ, and in 6.2 (b) we see that as γ decreases, the base solution rapidly stabilizes. Therefore, despite the apparent monotone dependence of Re_L upon γ, we conclude that the behaviour is very similar the case $\lambda_1 = \lambda_2 = 0$. It appears that the sixth order derivative terms of equation (6.64) dominate the linear stability of Green-Naghdi pressure driven flow.

For a dipolar fluid with either of the inertia terms considered, the critical Reynolds number at first falls with increasing dipolar constant l_2, before reaching some critical value close to $l_2 = 0.05$ from where Re_L becomes an increasing function of l_2. Therefore, nonzero values of l_2 are see to be destabilizing if l_2 is small, and stabilizing if l_2 is sufficiently large. This is seen clearly in Figures 6.3 and 6.4.

For both inertia terms, providing that l_2 is small, the effect of increasing the other dipolar constant l_1 is to stabilize the flow, that is, increase the critical Reynolds number. In the case of the Bleustein & Green inertia term, Figure 6.4 shows that

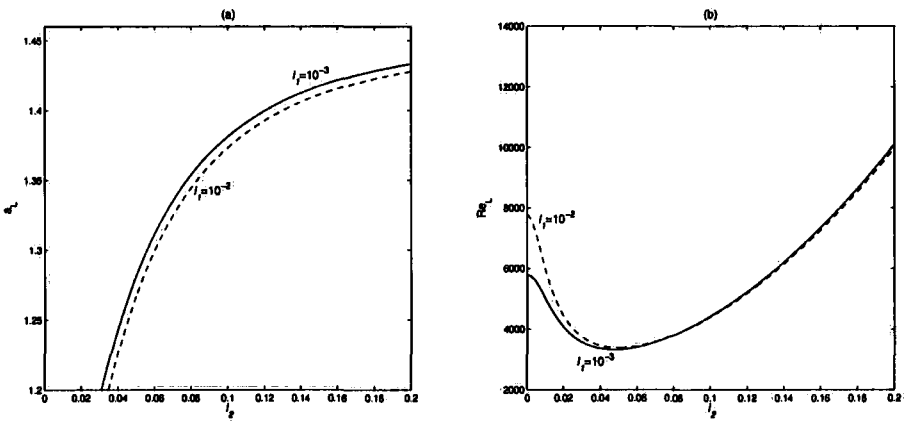

Figure 6.3: Dipolar fluid with Green-Naghdi inertia term. Graph (b) shows the variation of the critical Reynolds number for instability Re_L as a function of the dipolar constant l_2, for $l_1 = 0.001$ ('–') and $l_1 = 0.01$ ('- -'). In graph (a) we see the corresponding variation in the wave number a_L at which Re_L occurs.

this is also true at higher values of l_2, where as with the Green & Naghdi inertia (Figure 6.3) a small increase in l_1 was observed to lower the value of Re_L.

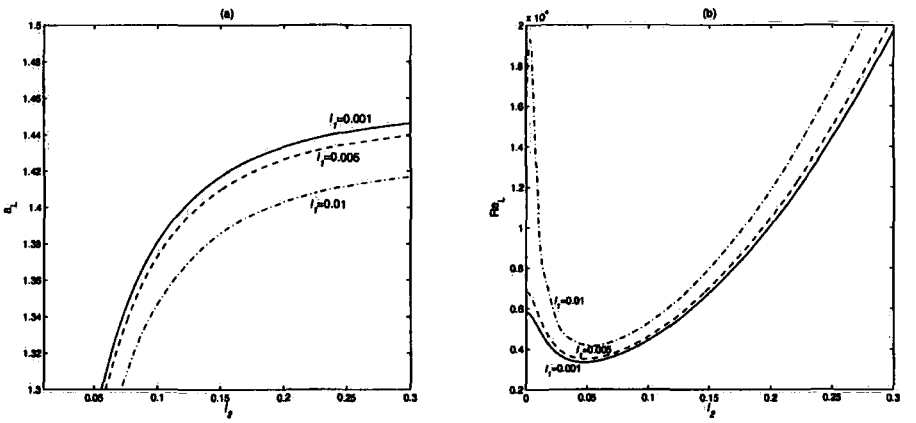

Figure 6.4: Dipolar fluid with Bleustein & Green inertia. In graph (b) we show the variation of Re_L with l_2 when the dipolar constant $l_1 = 0.001$ ('–'), when $l_1 = 0.005$ ('- -') and when $l_1 = 0.01$ ('·–'). Graph (a) shows the corresponding variation in a_L.

Chapter 7

Conclusions

In chapters two through to five, we investigated the role of slip length in the instability of various fluid systems, and there was a difference between the effect of slip length λ in convective instability, and in the transition to turbulence of parallel flows.

In Chapter two we showed that the presence of boundary slip did not alter the steady state, nor the property of exchange of stabilities, in Bénard convection. Our computations, however, showed the critical Rayleigh number Ra_{crit} at which thermal convection occurs varied as a strictly decreasing function of λ, i.e. as the slip length is increased, thermal instability occurs at lower Rayleigh numbers. This suggests that for very thin fluid layers, convection is possible at smaller temperature gradients than predicted by no-slip theory. However, our results were generated using the Chebyshev tau method, whereas the usual method for such problems is that of compound matrices, since exchange of stabilities ensures that this is computationally and algorithmically simple.

We showed that non-homogeneous boundary conditions require a special formulation of the compound matrix method, and the norm of the solutions generated in this way became very large, leading to loss of significance problems in our numerical integration.

Given that, in the context of thermal stability, increasing λ was seen to have a destabilizing effect, it was natural to turn to the problem of Poisuille flow in the

plane, since the subcritical transition to turbulence of such flows has been problematic since Orszag [48] first accurately computed the value $Re_L = 5772$. A thorough investigation was all the more necessary owing to disagreement in the literature as to the effect of λ on linear stability.

We found the linear stability result Re_L to be an increasing function of slip length λ, and thus boundary slip was seen to have a stabilizing effect. One possibility for the disagreement in the literature over the effect of λ on this system's linear stability was identified to be the incorrect boundary conditions employed by [13, 14] for the velocity perturbations.

We followed this with a nonlinear analysis. Being unable to find a Squire transform for the equations governing the system's nonlinear stability, we considered in turn different types of two dimensionally dependent perturbations, and found that Re_E became an increasing function of λ, after a small initial interval for which it was a decreasing function of λ.

A possible modification to the work in Chapter three would be to model Poiseuille flow in a channel of finite width, rather than the infinite channel we considered. This would make for interesting comparison with experiments.

A further modification is to develop the actual equations of motion further, which we did in Chapter four by allowing the viscosity to vary as a function of temperature. After setting the viscosity to be a linear function of temperature at our disposal, we still observed boundary slip to increase the value of Re_L, regardless of exact form of the viscosity (i.e. regardless of the value of $k = \mu_{,T}$).

We were able to investigate both the case when fluid became increasingly viscous with increasing temperature, and when the fluid viscosity decreased with temperature. In this way we were interested in both when the fluid resembled a gas and when it resembled a liquid, but a possible modification that may be made in future work is to consider compressible fluids, since boundary slip is historically associated with rarefied gases.

Increasing the value of λ was observed to bring about the greatest increases in critical Reynolds number Re_L when the viscosity was gas-like (in the region

$k = \mu_{,T} > 0$). However, some liquids such as liquid helium inhabit this viscosity regime, and therefore our results on the effects of boundary slip may be of use in understanding fluid flows involving liquid helium.

In Chapter five we described the modern surgical method of thread injection, before posing the problem of instability of thread-annular flow. The most recent model, due to Walton [64–66], was developed to include boundary slip at the needle wall and at the thread surface, and to allow for rotation of the thread about its axis. We showed that this rotation introduced a second component into the steady-state, which we believe has not been studied before.

Our results showed the importance of non-axisymmetric pertubations in the linear stability of core-annular problems. We also found the problem to be algorithmically stiff, in that, for instance, one must iterate over small increments in wave number, Reynolds number and thread velocity in order to observe the appearance of a stable intrusion.

There is much scope for future work on this problem. For instance: allowing the thread to lie off the axis of the needle; treating the thread as an elastic body; treating the thread as a porous medium. The inclusion of end effects may also be important.

Finally, in Chapter six we introduced two alternative equations of motion, the Green-Naghdi equations and the dipolar equations, that, although not equivalent to each other, are at least comparable. Both models have fourth order derivatives, and the Navier-Stokes equations can be obtained from them in the limit as various parameters (whether Green-Naghdi coefficients or dipolar constants) tend to zero.

We showed that the behaviour of the high order derivatives dominated the stability of Poiseuille flow-type solutions to these equations, such that as we move through the parameter space away from the Navier-Stokes equations the fluid rapidly stabilizes.

Bibliography

[1] J. Baudry, E. Charlaix, A. Tonck, & D. Mazuyer (2001), *Experimental evidence for a large slip effect at a nonwetting fluid-solid interface*, Langmuir, **17**, pp 5232–5236.

[2] H. Bénard (1900), *Les tourbillons cellulaires des unde nappe liquide*, Revue Générale des Sciences Pures et Appliquées, **11**, pp 1261–1271.

[3] J. L. Bleustein & A. E. Green (1967), *Dipolar fluids*, Int. J. Eng. Sci., **5**, pp 323–340.

[4] E. Bonaccurso, H. S. Butt & V. S. J. Craig (2003), *Surface roughness and hydrodynamic boundary slip of a Newtonian fluid in a completely wetting system*, Phys. Rev. Lett., **90**, 144501.

[5] E, Bonaccurso, M. Kappl & H. S. Butt (2002) *Hydrodynamic force measurements: boundary slip of water on hydrophilic surfaces and electrokinetics effects*, Phys. Rev. Lett., **88**, 076103.

[6] J. Boussinesq (1903), *Théorie Analytique de la Chaleur*, vol. 2. Gauthier-Villars: Paris; 172.

[7] F. H. Busse (1969), *Bounds on the transport of mass and momentum by turbulent flow between parallel plates*, Zeit. Angew. Math. Phys., **20**, pp 1–14.

[8] S. Chandrasekhar (1961), *Hydrodynamic and Hydromagnetic Stability*, Oxford University Press, Oxford.

[9] C. Cheikh & G. Koper (2003), *Stick-slip transition at the nanometre scale*, Phys. Rev. Lett., **91**, 156102.

[10] S. Chen, C. Foias, D. D. Holm, E. Olson, E. S. Titi & S. Wynne (1999), *The Camassa-Holm equations and turbulence,* Physica D, **133**, pp 49–65.

[11] J. T. Cheng & N. Giordano (2002), *Fluid flow through nanometre-scale channels,* Phys. Rev. E, **65** 031206.

[12] C. -H. Choi, K. Johan, A. Westin & K. S. Breur (2003), *Apparent slip flows in hydrophilic and hydrophobic microchannels*, Phys. Fluids, **15**, pp 2897–2902.

[13] A. K.-H. Chu (2004), *Instability of Navier slip flow of liquids*, C. R. Mecanique, **332**, pp 895-900.

[14] W. K. -H. Chu (2000), *Stability of incompressible helium II: a two-fluid system*, J. Phys.: Condens. Matter, **12**, pp 8065–8069.

[15] V. S. J. Craig, C. Neto & D. R. M. Williams (2001), *Shear-dependent boundary slip in an aqueous Newtonian liquid*, Phys. Rev. Lett., **87**, 054504.

[16] S. J. Davies & C. M. White (1928), *An experimental study of the flow of water in pipes of rectangular section*, Proc. Roy. Soc. A, **119**, pp 92–107.

[17] J. J. Dongarra, B. Straughan & D. W. Walker (1996), *Chebyshev tau-QZ algorithm methods for calculating spectra of hydrodynamic stability problems*, App. Num. Math., **22**, pp 399–434.

[18] P. G. Drazin & W. H. Reid (1981), *Hydrodynamic Stability*, Cambridge University Press, Cambridge.

[19] G. Evans (1993), *Practical Numerical Integration*, Wiley, Chichester.

[20] C. Foias, D. D. Holm & E. S. Titi (2001), *The Navier-Stokes-alpha model of fluid turbulence*, Physica D, **152**, pp 505–519.

[21] C. Foias, D. D. Holm & E. S. Titi (2002), *The three dimensional viscous Camassa-Holm equations, and their relation to the Navier-Stokes equations and turbulence theory*, J. Dyn. Diff. Eqns., **14** pp 1–35.

[22] L. Fox (1962), *Chebyshev methods for ordinary differential equations*, Comput. J., **4**, pp 318-331.

[23] Ch. Frei, P. Lüscher & E. Wintermantel (2000), *Thread-annular flow in vertical pipes*, J. Fluid. Mech., **410**, pp 185–210.

[24] A. E. Green & P. M. Naghdi (1970), *A note on dipolar flows*, Q. Appl. Math., **28**, pp 458–460.

[25] A. E. Green & P. M. Naghdi (1996), *An extended theory for incompressible viscous fluid flow*, J. non-Newtonian Fluid Mech., **66**, pp 233–255.

[26] G. Hall & J. M. Watt (1976), *Modern Numerical Methods for Ordinary Differential Equations*, Clarendon, Oxford.

[27] D. L. Harris & W. H. Reid (1958), *Some further results on the Bénard problem*, Phys. Fluids, **1**, pp 102–110.

[28] S. Ivansson (2004), *Compound-matrix Riccati method for solving boundary value problems*, Zeit. Angew. Math. Mech., **83**, pp 535–548.

[29] H. Jeffreys (1926), *The stability of a layer of fluid heated below*, Phil. Mag., **2**(7), pp 833–844.

[30] H. Jeffreys (1928), *Some cases of instability in fluid motion*, Proc. Roy. Soc. A, **118**, pp 195–208.

[31] D. D. Joseph (1965), *On the stability of the Boussinesq equations*, Arch. Rat. Mech. Anal., **20**(1), pp 59–71.

[32] D. D. Joseph (1966), *Nonlinear stability of the Boussinesq equations by the method of energy*, Arch. Rat. Mech. Anal., **22**(3), pp 163–184.

[33] D. D. Joseph & S. Carmi (1969), *Stability of the Orr-Sommerfeld stability equation*, Quart. App. Math., **26**, pp 575–599.

[34] P. Joseph & P. Tabeling (2005), *Direct measurement of the apparent slip length*, Phys. Rev. E., **71**, 035303.

[35] R. Kaiser & G. Mulone (2005), *A note on the nonlinear stability of plane parallel shear flows*, J. Math. Anal. Appl., **302**, pp 543–556.

[36] R. Kaiser & B. J. Schmitt (2001), *Bounds on the energy stability limit of plane parallel shear flows*, Z. Angew. Math. Phys., **52**, pp 573–596.

[37] R. R. Kerswell & A. Davey (1996), *On the linear instability of elliptic pipe flow*, J. Fluid Mech., **316**, pp 307–324.

[38] E. Lauga & C. Cossu (2005), *A note on the stability of slip channel flows*, Phys. Fluids, **17**(8), 088106.

[39] E. Lauga, M. P. Brenner & H. A. Stone, *Microfluidics: The No-Slip Boundary Condition*, to appear as chapter 15 in *Handbook of Experimental Fluid Dynamics*, Editors J. Foss, C. Tropea & A. Yarin, Springer, New-York (2007).

[40] P. Lüscher, E. Wintermantel & M. Annen (1995), *A new injectable open-porous implant system*, 21st Annual Meeting of the Society for Biomaterials, San Francisco, California, USA.

[41] J. C. Maxwell (1879), *On stresses in rarefied gases arising from inequalities of temperature*, Phil. Trans. Roy. Soc. Lond., **170**, pp 231–256.

[42] C. B. Moler & G. W. Stewart (1973), *An algorithm for generalized matrix eigenproblems*, SIAM J. Numer. Anal., **10**, pp 241-256.

[43] J. E. Mott & D. D. Joseph (1968), *Stability of parallel flow between concentric cylinders*, Phys. Fluids, **11**(10), pp 2065–2073.

[44] E. P. Muntz (1989), *Rarefied-gas dynamics*, Ann. Rev. Fluid. Mech., **21**, pp 387–417.

[45] C. L. M. H. Navier (1823), *Mémoire sur les lois du mouvement des fluides*, Mémoires de l'Académie Royale des Sciences d l'Institut de France, **6**, pp 389–440.

[46] C. Neto, V. S. J. Craig & D. R. M. Williams (2003), *Evidence of shear-dependent boundary slip in Newtonian liquids*, Eur. Phys. J. E, **12**, S71–S74.

[47] W. M'F. Orr (1907), *The stability or instability of the steady motions of a perfect liquid and of a viscous liquid*, Proc. Roy. Irish. Acad. A, **27**, pp 9–68 and pp 69–138,

[48] S. Orszag (1971), *Accurate solution of the Orr-Sommerfeld stability equation*, J. Fluid Mech., **50**(4), pp 689-703.

[49] R. Pit, H. Hervert & L. Léger (2000), *Direct experimental evidence of slip in hexadecane:solid interfaces*, Phys. Rev. Lett., **85**, pp 980–983.

[50] H. Poincaré (1885), *Sur l'equilibre d'une masse fluide animée d'un mouvement de rotation*, Acta. Math., **7**, pp 259–380.

[51] R. Quintanilla & B. Straughan (2005), *Bounds for some non-standard problems in porous fluid flow and viscous Green-Naghdi fluids*, Proc. Roy. Soc. A, **461**, pp 3159–3168.

[52] Lord Rayleigh (1916), *On convective currents in a horizontal layer of fluid, when the higher temperature is on the under side*, Philosophical Magazine, **32**(6), pp 529–546.

[53] H. Reichardt (1956), *Über die Geschwindigkeitsverteilung in einer geradlinigen turbulenten Couetteströmung*, Z, Angew. Math. Mech., **36**, S26–9.

[54] O. Reynolds (1883), *An experimental investigation of the circumstances which determine whether the motion of water shall be direct or sinuous, and of the law of resistance in parallel channels*, Phil. Trans. Roy. Soc., **174**, pp 935–982.

[55] V. A. Romanov (1973), *Stability of plane-parallel Couette flow*, Funkcional Anal. & Its Applics., **7**, pp 137-146.

[56] D. H. Sattinger (1969), *The mathematical problem of hydrodynamic stability*, J. Math. Fluid Mech., **19**, pp 797-817.

[57] A. Spille, A. Rauh & H. Bühring (2000), *Critical curves of plane Poiseuille flow with slip boundary conditions*, Nonlinear Phenomena in Complex Systems, **3**(2), pp 171-173.

[58] H. B. Squire (1933), *On the stability for three-dimensional disturbances of viscous fluid flow between parallel walls*, Proc. R. Soc. Lond. A, **142**, pp 621–628.

[59] B. Straughan (2004), *The Energy Method, Stability, and Nonlinear Convection*,2nd ed., Springer Verlag, New York.

[60] G. S. Strumolo (1982), *Perturbed bifurcation theory for Poiseuille annular flow*, J. Fluid Mech., **130**, pp 59–72.

[61] D. C. Tretheway & C. D. Meinhart (2002), *Apparent fluid slip at hydrophobic microchannel walls*, Phys. Fluids, **14**, L9–L12.

[62] D. P. Wall & M. Nagata (2000), *Nonlinear equilibrium solutions for the channel flow of fluid with temperature dependent-dependent viscosity*, J. Fluid Mech., **406**, pp 1–26.

[63] D. P. Wall & S. K. Wilson (1996), *The linear stability of channel flow of fluid with temperature-dependent viscosity*, J. Fluid Mech., **323**, pp 107–132.

[64] A. G. Walton (2003), *The nonlinear instability of thread-annular flow at high Reynolds number*, J. Fluid Mech., **477**, pp 227–257.

[65] A. G. Walton (2004), *Stability of circular Poiseuille-Couette flow to axisymmetric disturbances*, J. Fluid Mech., **500**, pp 169–210.

[66] A. G. Walton (2005), *The linear and nonlinear stability of thread-annular flow*, Phil. Trans. R. Soc. A, **363**, pp 1223–1233.

[67] M. Webber (2006), *The destabilizing effect of boundary slip on Bénard convection*, Math. Meth. Appl. Sci., **29**, pp 819–838.

[68] M. Webber & B. Straughan (2006), *Stability of pressure driven flow in a microchannel*, Rend. Circolo. Matem. Palermo, **78**(2), pp 343–357.

[69] P. G. Wright (1977), *The variation of viscosity with temperature*, Phys. Educ., **12**(5), pp 323–325.

[70] Y. Zhu & S. Granick (2001), *Rate-dependent slip of Newtonian liquid at smooth surfaces*, Phys. Rev. Lett., **87**, 096105.

[71] Y. Zhu & S. Granick (2002), *Limits of the hydrodynamic no-slip boundary condition*, Phys. Rev. Lett., **88**, 106102.

Appendix A

The Chebyshev tau method

In this chapter we introduce the set of Chebyshev polynomials, and explain some important relations used in the computational work described in this thesis. We then present a description of the Chebyshev tau method, which we clarify through a simple example of its use, as well as explaining a technical detail known as Curtis-Clenshaw quadrature.

A.1 The Chebyshev polynomials

For $n \in \{0, 1, 2, 3, ...\}$ we define the function $T_n : [-1, 1] \to [-1, 1]$ by the relation

$$T_n(\cos(\theta)) = \cos(n\theta). \tag{A.1.1}$$

Then we call T_n the nth Chebyshev polynomial, and if we set $x = \cos(\theta)$ it is seen immediately from setting $n = 0$ and $n = 1$ in (A.1.1) that

$$\begin{aligned} T_0(x) &= 1, \\ T_1(x) &= x. \end{aligned}$$

Using the standard result $2\cos(A)\cos(B) = \cos(A+B) + \cos(A-B)$, we see that from the definition (A.1.1)

$$\begin{aligned} 2T_n(x)T_m(x) &= 2T_n(\cos(\theta))T_m(\cos(\theta)), \\ &= 2\cos(n\theta)\cos(m\theta), \\ &= \cos((n+m)\theta) + \cos((n-m)\theta), \\ &= \cos((n+m)\theta) + \cos((m-n)\theta), \end{aligned}$$

and so we have the relation

$$2T_n(x)T_m(x) = T_{n+m}(x) + T_{|n-m|}(x), \tag{A.1.2}$$

which is central to much of the numerical work in this thesis. Upon letting $m = 1$ we obtain a recurrence relation for $T_{n+1}(x)$, specifically

$$T_{n+1}(x) = 2xT_n(x) - T_{n-1}(x), \quad n = 1, 2, 3, \ldots \tag{A.1.3}$$

and since we have already found T_0 and T_1, we can now construct the rest of the set of Chebyshev polynomials $\{T_n\}_{n=0}^{\infty}$,

$$\begin{aligned} T_2(x) &= 2x^2 - 1, \\ T_3(x) &= 4x^3 - 3x, \\ T_4(x) &= 8x^4 - 8x^2 + 1, \\ T_5(x) &= 16x^5 - 20x^3 + 5x, \\ &\text{etc.} \end{aligned}$$

Clearly, T_n is an nth order polynomial, and so is an odd or even function according to n.

The Chebyshev tau method exploits the orthogonality of Chebyshev polynomials. We start by considering a weighted integral of $T_n(x)T_m(x)$ over the interval $(-1, 1)$,

$$\begin{aligned} \int_{-1}^{1} \frac{T_n(x)T_m(x)}{\sqrt{1-x^2}}dx &= \int_0^{\pi} T_n(\cos(\theta))T_m(\cos(\theta))d\theta \quad \text{letting } x = \cos(\theta), \\ &= \int_0^{\pi} \cos(n\theta)\cos(m\theta)d\theta \quad \text{by definition (A.1.1)}, \\ &= \int_0^{\pi} d\theta \quad \text{when } n = m = 0, \\ &= \pi. \end{aligned}$$

When $n \neq m$, then

$$\begin{aligned}\int_0^\pi \cos(n\theta)\cos(m\theta)d\theta &= \frac{1}{2(n+m)}\left[\sin((n+m)\theta)\right]_0^\pi + \frac{1}{2(n-m)}\left[\sin((n-m)\theta)\right]_0^\pi, \\ &= 0.\end{aligned}$$

Finally, for the case $n = m \neq 0$,

$$\begin{aligned}\int_0^\pi \cos(n\theta)\cos(m\theta)d\theta &= \frac{1}{2}\int_0^\pi \left[\cos((n+m)\theta) + \cos((n-m)\theta)\right] d\theta, \\ &= \frac{1}{2}\int_0^\pi \left[\cos((n+m)\theta) + 1\right] d\theta, \\ &= \frac{1}{2(n+m)}\left[\sin((n+m)\theta)\right]_0^\pi + \frac{\pi}{2}, \\ &= \frac{\pi}{2}.\end{aligned}$$

Therefore, we have shown that the Chebyshev polynomials are orthogonal with respect to the weighted $L^2(-1,1)$ inner-product, according to

$$< T_n, T_m >= \int_{-1}^{1} \frac{T_n(x)T_m(x)}{\sqrt{1-x^2}}dx = \begin{cases} \pi & \text{if } m = n = 0, \\ \frac{1}{2}\pi & \text{if } m = n \neq 0, \\ 0 & \text{if } m \neq 0. \end{cases} \tag{A.1.4}$$

A.2 Chebyshev differentiation matrices

Suppose that for some function $f \in C^\infty(-1,1)$ there exists a uniformly convergent series of Chebyshev polynomials $T_n(x)$ such that

$$f(x) = \sum_{n=0}^{\infty} f_n T_n(x), \tag{A.2.5}$$

for coefficients f_0, f_1, f_2, ... Clearly, if f is a polynomial of order N then this series will be finite, truncating at the $n = N$th term. We assume similar forms for the derivatives $f'(x)$, $f''(x)$ and so on, i.e.

$$f^{(k)}(x) = \sum_{n=0}^{\infty} f_n^{(k)} T_n(x), \quad k = 0, 1, 2, ... \tag{A.2.6}$$

where $f^{(k)}$ is the kth derivative of f, and $f^{(0)} = f$. Our aim is to relate the coefficients in the series expansion of $f^{(k+1)}$ to those of $f^{(k)}$, and use this to develop a

method for approximating the solutions of linear ODEs.

We begin by differentiating $T_n(x)$ with respect to x

$$\begin{aligned}\frac{dT_n}{dx} &= \frac{dT_n}{d\theta}\cdot\frac{d\theta}{dx}, \\ &= \frac{n\sin(n\theta)}{\sin(\theta)},\end{aligned}$$

from which it follows that

$$\begin{aligned}\frac{1}{n+1}T'_{n+1}(x) - \frac{1}{n-1}T'_{n-1}(x) &= \frac{1}{\sin(\theta)}\left[\sin((n+1)\theta) - \sin((n-1)\theta)\right], \\ &= 2\cos(n\theta), \\ &= 2T_n(x), \qquad \text{for } n \geq 2.\end{aligned}$$

Considering the cases $n = 0$ and $n = 1$ individually, it is verified that

$$2T_n(x) = \frac{1}{n+1}T'_{n+1}(x) - \frac{1}{n-1}T'_{|n-1|}(x), \quad \text{for } n \geq 0. \tag{A.2.7}$$

Therefore

$$\begin{aligned}\frac{d}{dx}\sum_{n=0}^{\infty} f_n T_n(x) &= \sum_{n=0}^{\infty} f_n^{(1)} T_n(x), \\ &= \frac{1}{2}\sum_{n=0}^{\infty} f_n^{(1)}\left(\frac{1}{n+1}T'_{n+1}(x) - \frac{1}{n-1}T'_{|n-1|}(x)\right), \\ &= \frac{1}{2}\frac{d}{dx}\sum_{n=0}^{\infty} f_n^{(1)}\left(\frac{1}{n+1}T_{n+1}(x) - \frac{1}{n-1}T_{|n-1|}(x)\right),\end{aligned}$$

and so

$$2\frac{d}{dx}(f_0T_0+f_1T_1+\ldots) = \frac{d}{dx}\left((2f_0^{(1)} - f_2^{(1)})T_1 + \frac{(f_1^{(1)} - f_3^{(1)})}{2}T_2 + \frac{(f_2^{(1)} - f_4^{(1)})}{3}T_3 + \ldots\right).$$

Equating coefficients of T_i, $i \geq 1$ we have

$$2pf_p = c_{p-1}f_{p-1}^{(1)} - f_{p+1}^{(1)}, \quad p \geq 1, \tag{A.2.8}$$

where $c_0 = 2$ and $c_i = 1$ for $i \geq 1$. We sum both sides of equation (A.2.8) from

$p = n+1$ to $p = \infty$ over the terms $p + n \equiv 1 \pmod 2$, i.e.

$$\begin{aligned} 2 \sum_{\substack{p=n+1 \\ p+n\equiv 1 (\mathrm{mod}\ 2)}}^{\infty} p f_p &= \sum_{\substack{p=n+1 \\ p+n\equiv 1 (\mathrm{mod}\ 2)}}^{\infty} c_{p-1} f_{p-1}^{(1)} - f_{p+1}^{(1)}, \\ &= c_n f_n^{(1)} - f_{n+2}^{(1)} + c_{n+2} f_{n+2}^{(1)} - f_{n+4}^{(1)} + c_{n+4} f_{n+4}^{(1)} - f_{n+6}^{(1)} + \cdots, \\ &= c_n f_n^{(1)} - f_{n+2}^{(1)} + f_{n+2}^{(1)} - f_{n+4}^{(1)} + f_{n+4}^{(1)} - \cdots, \\ &= c_n f_n^{(1)}, \end{aligned}$$

since only c_0 is not equal to 1. Therefore we have cancellation of all terms on the right hand side except the first, leaving us with an expression for $f_n^{(1)}$ in terms of $\{f_p\}_{p=n+1}^{\infty}$. Moreover, it is easily seen that in general

$$f_n^{(k)} = \frac{2}{c_n} \sum_{\substack{p=n+1 \\ p+n\equiv 1 (\mathrm{mod}\ 2)}}^{\infty} p f_p^{(k-1)}, \quad n \geq 0. \tag{A.2.9}$$

Now, if we consider coefficients of $f^{(2)}(x)$,

$$\begin{aligned} f_n^{(2)} &= \frac{2}{c_n} \sum_{\substack{p=n+1 \\ p+n\equiv 1 (\mathrm{mod}\ 2)}}^{\infty} p f_p^{(1)}, \\ &= \frac{2}{c_n} \sum_{\substack{p=n+1 \\ p+n\equiv 1 (\mathrm{mod}\ 2)}}^{\infty} p \frac{2}{c_p} \sum_{\substack{q=p+1 \\ q+p\equiv 1 (\mathrm{mod}\ 2)}}^{\infty} q f_q, \\ &= \frac{4}{c_n} \sum_{\substack{p=n+1 \\ p+n\equiv 1 (\mathrm{mod}\ 2)}}^{\infty} p \sum_{\substack{q=p+1 \\ q+p\equiv 1 (\mathrm{mod}\ 2)}}^{\infty} q f_q \quad \text{since } c_{p\geq 1} = 1, \\ &= \frac{4}{c_n}(n+1)\left[(n+2)f_{n+2} + (n+4)f_{n+4} + (n+6)f_{n+6} + \ldots\right] \\ &\quad + \frac{4}{c_n}(n+3)\left[(n+4)f_{n+4} + (n+6)f_{n+6} + (n+8)f_{n+8} + \ldots\right] \\ &\quad + \frac{4}{c_n}(n+5)\left[(n+6)f_{n+6} + (n+8)f_{n+8} + (n+10)f_{n+10} + \ldots\right], \end{aligned}$$

$$
\begin{aligned}
&= \frac{4}{c_n}(n+1)(n+2)f_{n+2} \\
&\quad + \frac{4}{c_n}[(n+1)+(n+3)](n+4)f_{n+4} \\
&\quad + \frac{4}{c_n}[(n+1)+(n+3)+(n+5)](n+6)f_{n+6} \\
&\quad + \frac{4}{c_n}[(n+1)+(n+3)+(n+5)+(n+7)](n+8)f_{n+8}+\ldots, \\
&= \frac{4}{c_n}\sum_{\substack{p=n+2 \\ p\equiv n(\mathrm{mod}\ 2)}}^{\infty} p f_p \sum_{\substack{q=n+1 \\ q+n\equiv 1(\mathrm{mod}\ 2)}}^{p-1} q.
\end{aligned}
$$

This expression is greatly simplified by evaluating the finite sums

$$
\begin{aligned}
\sum_{\substack{q=n+1 \\ q+n\equiv 1(\mathrm{mod}\ 2)}}^{p-1} q &= \sum_{k=0}^{\frac{1}{2}(p-n)-1}(n+1+2k), \\
&= (n+1)\sum_{k=0}^{\frac{1}{2}(p-n)-1} 1 + 2\sum_{k=1}^{\frac{1}{2}(p-n)-1} k, \\
&= \frac{1}{2}(n+1)(p-n)+\frac{1}{2}(\frac{1}{2}(p-n)-1)(p-n), \\
&= \frac{1}{4}(p^2-n^2),
\end{aligned}
$$

where we have used the standard identities $\sum_{k=1}^{N} 1 = N$ and $\sum_{k=1}^{N} k = N(N+1)/2$. It follows that

$$
f_n^{(2)} = \frac{1}{c_n}\sum_{\substack{p=n+2 \\ p\equiv n(\mathrm{mod}\ 2)}}^{\infty} p(p^2-n^2)f_p, \quad n \geq 0, \tag{A.2.10}
$$

and similar expressions may be found for higher derivatives.

We now suppose that we can truncate the infinite series $f^{(k)}(x)$ at the $n = N$th term, so that

$$
\begin{aligned}
f^{(k)} &= \tilde{f}^{(k)}(x) + E_{N+1}(x), \\
&= \sum_{n=0}^{N} f_n^{(k)} T_n(x) + E_{N+1}(x),
\end{aligned}
$$

where $E_{N+1}(x)$ is the error term. If we define the vectors $\hat{\mathbf{f}}^{(k)} = (\hat{f}_0^{(k)}, \hat{f}_1^{(k)}, \hat{f}_2^{(k)}, \ldots, \hat{f}_N^{(k)})^T$, then upon substituting our approximation into equation (A.2.9) we derive an upper triangular $(N+1)\times(N+1)$ matrix $\bar{D}$ such that $\hat{\mathbf{f}}^{(k)} = D\hat{\mathbf{f}}^{(k-1)}$, where D is given

by

$$D = \begin{pmatrix} 0 & 1 & 0 & 3 & 0 & 5 & 0 & 7 & 0 & \dots \\ 0 & 0 & 4 & 0 & 8 & 0 & 12 & 0 & 16 & \dots \\ 0 & 0 & 0 & 6 & 0 & 10 & 0 & 14 & 0 & \dots \\ 0 & 0 & 0 & 0 & 8 & 0 & 12 & 0 & 16 & \dots \\ 0 & 0 & 0 & 0 & 0 & 10 & 0 & 14 & 0 & \dots \\ \dots & \dots & \dots & \dots & \dots & \dots & \dots & \dots & \dots & \dots \end{pmatrix}. \tag{A.2.11}$$

Equation (A.2.10) can be used in a similar way to obtain a matrix D^2 such that $\hat{\mathbf{f}}^{(k)} = D^2\hat{\mathbf{f}}^{(k-2)}$, where D^2 is given by

$$D^2 = \begin{pmatrix} 0 & 0 & 4 & 0 & 32 & 0 & 108 & \dots \\ 0 & 0 & 0 & 24 & 0 & 120 & 0 & \dots \\ 0 & 0 & 0 & 0 & 48 & 0 & 192 & \dots \\ \dots & \dots & \dots & \dots & \dots & \dots & \dots & \dots \end{pmatrix}. \tag{A.2.12}$$

It is easily seen that $\hat{\mathbf{f}}^{(k)} = D\hat{\mathbf{f}}^{(k-1)} = D(D\hat{\mathbf{f}}^{(k-2)}) = \dots = D^n\hat{\mathbf{f}}$, and so $D^2 = D \times D$ in the sense of matrix multiplication, thus the method is consistent. The coefficients of $\hat{\mathbf{f}}^{(k)}$ are then our approximation to the coefficients of the finite series $\tilde{f}(x)^{(k)}$, which is in turn our approximation to $f(x)^{(k)}$.

A.3 Curtis-Clenshaw quadrature

Often, we wish to approximate a given function $g(x)$ by a finite series of Chebyshev polynomials $\hat{g}(x)$

$$\hat{g}(x) = \sum_{n=0}^{N} \hat{g}_n T_n(x), \tag{A.3.13}$$

for coefficients $\hat{g}_0, \hat{g}_1, \hat{g}_2, \dots, \hat{g}_N$. To do this we use the standard discrete orthogonality result

$$\sum_{n=0}^{N} d_n \cos\left(\frac{in\pi}{N}\right) \cos\left(\frac{jn\pi}{N}\right) = \begin{cases} 0 & \text{if } i \neq j, \\ \frac{N}{2d_i} & \text{if } i = j, \end{cases} \tag{A.3.14}$$

where $d_0 = d_N = 1/2$ and $d_{0<n<N} = 1$. If we let $x_n = \cos(n\pi/N)$, then for some integer k

$$\begin{aligned}\sum_{n=0}^{N} d_n \hat{g}(x_n) \cos\left(\frac{kn\pi}{N}\right) &= \sum_{n=0}^{N}\sum_{m=0}^{N} d_n \hat{g}_m T_m(x_n) \cos\left(\frac{kn\pi}{N}\right), \\ &= \sum_{n=0}^{N}\sum_{m=0}^{N} d_n \hat{g}_m T_m\left(\cos\left(\frac{n\pi}{N}\right)\right) \cos\left(\frac{kn\pi}{N}\right), \\ &= \sum_{n=0}^{N}\sum_{m=0}^{N} d_n \hat{g}_m \cos\left(\frac{mn\pi}{N}\right) \cos\left(\frac{kn\pi}{N}\right), \\ &= \frac{N}{2d_k}\hat{g}_k.\end{aligned}$$

Therefore, we find our approximation $\hat{g}(x)$ by setting each coefficient according to

$$\hat{g}_k = \frac{2d_k}{N}\sum_{n=0}^{N} d_n \hat{g}\left(\cos\left(\frac{n\pi}{N}\right)\right) \cos\left(\frac{kn\pi}{N}\right). \tag{A.3.15}$$

A discussion of this method can be found in the book by Evans [19]

A.4 Chebyshev matrix representation of functions

Suppose we have two functions $f(x)$ and $g(x)$, for which we have Chebyshev polynomial approximations $\hat{f}(x)$ and $\hat{g}(x)$ respectively, with forms

$$\hat{f}(x) = \sum_{n=0}^{N} \hat{f}_n T_n(x), \quad \hat{g}(x) = \sum_{n=0}^{N} \hat{g}_n T_n(x), \tag{A.4.16}$$

for some N, and vectors of coefficients $\hat{\mathbf{f}} = (\hat{f}_0, ..., \hat{f}_N)^T$, $\hat{\mathbf{g}} = (\hat{g}_0, ..., \hat{g}_N)^T$. Now, we define the function $h(x) = f(x)g(x)$, and require to approximate $h(x)$ by $\hat{h}(x)$ which has the form

$$\hat{h}(x) = \sum_{n=0}^{N} \hat{h}_n T_n(x), \tag{A.4.17}$$

for the same N, and vector of coefficients $\hat{\mathbf{h}} = (\hat{h}_0, ..., \hat{h}_N)^T$. Then, we aim to construct a matrix F such that $\hat{\mathbf{h}} = F\hat{\mathbf{g}}$. We start with the simple example of $\hat{f}(x) = x$.

Referring to the weighted inner-product $< ., . >$ defined in (A.1.4) with associated norm $\|.\|$, we let $\hat{h}(x) = x\hat{g}(x)$, and take the inner product $\hat{h}(x)T_m(x)$ for some

$m \geq 0$, before normalizing by $\|T_m\|^2$.

$$\begin{aligned}
\frac{1}{\|T_m\|^2} < \hat{h}T_m > &= \frac{1}{\|T_m\|^2} < x\hat{g}T_m >, \\
&= \frac{1}{\|T_m\|^2} \sum_{n=0}^{N} \hat{g}_n < xT_nT_m >, \\
&= \frac{1}{\|T_m\|^2} \sum_{n=0}^{N} \hat{g}_n < T_1T_nT_m >, \\
&= \frac{1}{\|T_m\|^2} \frac{1}{2} \sum_{n=0}^{N} \hat{g}_n < T_1T_{n+m} > + \frac{1}{\|T_m\|^2} \frac{1}{2} \sum_{n=0}^{N} \hat{g}_n < T_1T_{|n-m|} >,
\end{aligned}$$

where we have used equation (A.1.2), and substituted $x = T_1(x)$. We now let m vary from 0 to N,

$$\begin{aligned}
\frac{1}{\|T_0\|^2} < \hat{h}T_0 > &= \frac{1}{\|T_0\|^2} \frac{1}{2} \sum_{n=0}^{N} \hat{g}_n < T_1T_n > + \frac{1}{\|T_0\|^2} \frac{1}{2} \sum_{n=0}^{N} \hat{g}_n < T_1T_{|n|} >, \\
&= \hat{g}_1 \frac{\|T_1\|^2}{\|T_0\|^2}, \\
&= \frac{1}{2}\hat{g}_1.
\end{aligned}$$

$$\begin{aligned}
\frac{1}{\|T_1\|^2} < \hat{h}T_1 > &= \frac{1}{\|T_1\|^2} \frac{1}{2} \sum_{n=0}^{N} \hat{g}_n < T_1T_{n+1} > + \frac{1}{\|T_1\|^2} \frac{1}{2} \sum_{n=1}^{N} \hat{g}_n < T_1T_{|n-1|} >, \\
&= \frac{1}{2}\hat{g}_0 + \frac{1}{2}\hat{g}_0 + \frac{1}{2}\hat{g}_2, \\
&= \hat{g}_0 + \frac{1}{2}\hat{g}_2.
\end{aligned}$$

Proceeding in this way, and noting that the inner product $< \hat{h}T_m > / \|T_m\|^2$ gives us the equality

$$\frac{1}{\|T_m\|^2} < \hat{h}T_m > = \frac{1}{\|T_m\|^2} \sum_{n=0}^{N} \hat{h}_n < T_nT_m > = \hat{h}_m, \tag{A.4.18}$$

we have found a linear relation between the coefficients of $\hat{\mathbf{h}}$ and the coefficients of $\hat{\mathbf{g}}$ such that we can write the matrix X, so that $\hat{\mathbf{h}} = X\hat{\mathbf{g}}$ contains the Chebyshev coefficients of the functions $\hat{h}(x) = x\hat{g}(x)$, where X is given by

$$X = \begin{pmatrix}
0 & \frac{1}{2} & 0 & 0 & 0 & \dots \\
1 & 0 & \frac{1}{2} & 0 & 0 & \dots \\
0 & \frac{1}{2} & 0 & \frac{1}{2} & 0 & \dots \\
0 & 0 & \frac{1}{2} & 0 & \frac{1}{2} & \dots \\
\dots & \dots & \dots & \dots & \dots & \dots
\end{pmatrix}. \tag{A.4.19}$$

In this way, by expressing x^n in terms of Chebyshev polynomials, we can construct the matrices X^n, $n \geq 0$. It follows that we can now easily find the coefficients of $\hat{h} = \hat{f}(x)\hat{g}(x)$ using the matrix multiplication method, when $\hat{f}$ is a low order polynomial, i.e. the function $f(x)$ it is approximating is a finite polynomial. In general, $f(x)$ is an arbitrary function of x, and so we now find a way to construct a matrix F for general $f \in C^\infty(-1,1)$.

The method is to construct the polynomial $\hat{f}(x)$ approximating $f(x)$ using the method of Curtis-Clenshaw quadrature (see above), so that $\hat{f}(x) = \sum_{n=0}^{N} \hat{f}_n T_n(x)$. We now take inner products of $\hat{h}T_K$ for some integer k, and normalize as before

$$\begin{aligned} \frac{1}{\|T_k\|^2} < hT_k > &= \frac{1}{2\|T_k\|^2} \sum_{n=0}^{N}\sum_{m=0}^{N} \hat{f}_n\hat{g}_m < T_{n+m}T_k > + \frac{1}{2\|T_k\|^2} \sum_{n=0}^{N}\sum_{m=0}^{N} \hat{f}_n\hat{g}_m < T_{|n-m|}T_k >, \\ &= \frac{1}{2}\left(\sum_{k=m}^{N+m} \hat{f}_{k-m} + \sum_{k=-m}^{N-m} \hat{f}_{k+m} + \sum_{k=m-N}^{m} \hat{f}_{m-k} \right) \sum_{m=0}^{N} \hat{g}_m. \end{aligned} \tag{A.4.20}$$

The above relation, then, provides us with a computational algorithm to calculate each element of the matrix F.

A.5 Example of the Chebyshev tau method

We now show how the method of approximation by Chebyshev polynomials can be used to solve linear eigenvalue problems. Consider the following eigenvalue problem,

$$u''(x) + \lambda f(x)u(x) = 0, \tag{A.5.21}$$

$$u'(1) + \alpha u(1) = 0, \tag{A.5.22}$$

$$u'(-1) + \beta u(-1) = 0, \tag{A.5.23}$$

for $x \in (-1,1)$, constants α and β, eigenvalue λ, and where $f(x)$ is a given function. We begin by assuming that u and f can be expanded as a Chebyshev polynomial series

$$u''(x) = \sum_{n=0}^{\infty} u_n^{(2)} T_n(x), \quad u(x) = \sum_{n=0}^{\infty} u_n T_n(x) \quad f = \sum_{n=0}^{\infty} f_n T_n(x), \tag{A.5.24}$$

for coefficients u_n and f_n. We now truncate the series expansions at the $n = N$th term, and denote $\tilde{u}(x) = \sum_{n=0}^{N} u_n T_n(x)$, with $\tilde{u}^{(2)}$ and $\tilde{f}$ defined similarly. Fox [22] shows us that the error resulting from this truncation can be expressed thusly

$$\tilde{u}^{(2)} + \lambda \tilde{f}\tilde{u} = \tau_1 T_{N-1} + \tau_2 T_N, \tag{A.5.25}$$

and so the τ's are a measure of the accuracy of our approximation. Taking the weighted Chebyshev inner product of equation (A.5.25) with the polynomial T_k, where $k = 0, 1, 2, ...N-2$, removes the τ's, and constructs the representation matrix F (as explained above). Finally, letting $\tilde{\mathbf{u}} = (u_0, u_1, ..., u_N)$ with $\tilde{\mathbf{u}}^{(2)}$ similarly defined, we can make the substitution $\tilde{\mathbf{u}}^{(2)} = D^2\tilde{\mathbf{u}}$, such that we arrive at the linear system

$$D^2\tilde{\mathbf{u}} + \lambda F\tilde{\mathbf{u}} = \mathbf{0}, \tag{A.5.26}$$

where we have added two rows of zeros to the bottom of matrices F and D^2 such that the matrices are square. We close the system by overwriting these two rows with the boundary conditions.

We deal with (A.5.22) and (A.5.23) by noting from (A.1.1) that

$$T_n(\pm 1) = (\pm 1)^n, \quad T_n'(\pm 1) = n^2(\pm 1)^{n+1}.$$

Therefore, the boundary conditions can be overwritten as

$$\sum_{n=0}^{N} n^2 u_n + \alpha \sum_{n=0}^{N} u_n = 0, \quad \sum_{n=0}^{N} n^2(-1)^{n+1} u_n + \beta \sum_{n=0}^{N} (-1)^n u_n = 0. \tag{A.5.27}$$

The system is now closed, and can be solved as a generalised eigenvalue problem $A\mathbf{x} = \sigma B\mathbf{x}$ using the QZ method of Moler & Stewart [42].

We refer the reader to the work of Orszag [48] for further details, as well as to Straughan [59] and Dongarra, Straughan & Walker [17] for more examples of implementing the Chebyshev tau method.

Appendix B

The compound matrix method

The compound matrix method is a modification of the standard shooting method. Consider the coupled system

$$u'' + \sigma v = 0, \tag{B.0.1}$$

$$v'' + \sigma u = 0, \tag{B.0.2}$$

$$u(1) = v(1) = u(-1) = v(-1) = 0, \tag{B.0.3}$$

for $u = u(x)$, $v = v(x)$ with $x \in (-1, 1)$, and eigenvalue σ. We assume that u and v can be decomposed as

$$u(x) = c_1 u_1(x) + c_2 u_2(x), \quad v(x) = c_1 v_1(x) + c_2 v_2(x), \tag{B.0.4}$$

and we transform the boundary value problem (B.0.1)-(B.0.3) in u, v into two initial value problems, in u_1, v_1 and u_2, v_2.

We must impose enough initial conditions at $x = -1$ for the problem to be well-posed. From (B.0.3), we already have $u_1(-1) = u_2(-1) = v_1(-1) = v_2(-1) = 0$. The conditions at $x = 1$ are then replaced with $u_1'(-1) = 1$, $u_2'(-1) = 0$ and $v_1'(-1) = 0$, $v_2'(-1) = 1$. These are then integrated forward. The correct boundary conditions at $x = 1$ are then imposed, and we note that this requires

$$\begin{vmatrix} u_1(1) & u_2(1) \\ v_1(1) & v_2(1) \end{vmatrix} = 0,$$

to hold at $x = 1$.

Therefore, we aim to iterate over σ producing a convergent sequence $\{\sigma_1, \sigma_2, ...\}$ by repeatedly integrating u_1, u_2, v_1, v_2, and calculating the above determinant. Though simple to implement, the shooting method suffers from one having to locate the zero of this determinant. The two quantities $u_1(1)v_2(1)$ and $u_2(1)v_1(1)$ must be very close to each other, although they need not be close to zero. Therefore, in general the method involves subtracting two nearly identical quantities, which may lead to significant round off errors.

The compound matrix method is to convert the problem into a system of ordinary differential equations in the determinants themselves. We let $\mathbf{x}_1 = (u_1, u_1', v_1, v_1')^T$, $\mathbf{x}_2 = (u_2, u_2', v_2, v_2')^T$, and the 4×2 matrix $X = (\mathbf{x}_1\mathbf{x}_2)$, i.e.

$$X = \begin{pmatrix} u_1 & u_2 \\ u_1' & u_2' \\ v_1 & v_2 \\ v_1' & v_2' \end{pmatrix}. \tag{B.0.5}$$

We then let y_1 be the first minor of X, with y_2 to y_6 similarly defined,

$$\begin{aligned} y_1 &= u_1u_2' - u_2u_1', \\ y_2 &= u_1v_2 - u_2v_1, \\ y_3 &= u_1v_2' - u_2v_1', \\ y_4 &= u_1'v_2 - u_2'v_1 \\ y_5 &= u_1'v_2' - u_2'v_1', \\ y_6 &= v_1v_2' - v_2v_1', \end{aligned}$$

before differentiating each y_i with respect to x. For example

$$\begin{aligned} y_1' &= u_1'u_2' + u_1u_2'' - u_2'u_1' - u_2u_1'', \\ &= u_1u_2'' - u_2u_1'', \\ &= u_1(-\sigma v_2) - u_2(-\sigma v_1), \\ &= -\sigma(u_1v_2 - u_2v_1), \\ &= -\sigma y_2. \end{aligned}$$

Proceeding in this way results in a system of six ordinary differential equations in six unknowns.

$$\begin{aligned} y_1' &= -\sigma y_2, \\ y_2' &= y_4 + y_3, \\ y_3' &= 0, \\ y_4' &= y_5, \\ y_5' &= \sigma(y_2 - y_6), \\ y_6' &= \sigma y_2, \end{aligned}$$

i.e. we arrive at the system $\mathbf{y}' = A\mathbf{y}$ where A is a 6×6 matrix with constant coefficients, and $\mathbf{y} = (y_1, ..., y_6)^T$. We therefore pick a starting value of σ, integrate our ODE in $\mathbf{y}$ from the initial condition $\mathbf{y} = (0, 0, 0, 0, 1, 0)^T$ (having substituted our assumed initial conditions), and then test our boundary conditions at $x = 1$, which translate as $y_2 = 0$. We then proceed to iterate over σ until y_2 is zero to some predefined tolerance.

A thorough discussion of the compound matrix method can be found in the books by Straughan [59] and Drazin & Reid [18], or the work of Ivansson [28].